NASA Technical Memorandum 102816

Forces and Pressures Induced on Circular Plates by a Single Lifting Jet in Ground Effect

David C. Bellavia, Douglas A. Wardwell,
Victor R. Corsiglia, and Richard E. Kuhn

March 1991

National Aeronautics and
Space Administration

NASA Technical Memorandum 102816

Forces and Pressures Induced on Circular Plates by a Single Lifting Jet in Ground Effect

David C. Bellavia, Douglas A. Wardwell, Victor R. Corsiglia,
Ames Research Center, Moffett Field, California

Richard E. Kuhn
STO-VL Technology, San Diego, California

March 1991

National Aeronautics and
Space Administration

Ames Research Center
Moffett Field, California 94035-1000

FORCES AND PRESSURES INDUCED ON CIRCULAR PLATES BY A SINGLE LIFTING JET IN GROUND EFFECT

David C. Bellavia, Douglas A. Wardwell, Victor R. Corsiglia, and Richard E. Kuhn*

Ames Research Center

SUMMARY

NASA Ames is conducting a program to develop improved methods for predicting suckdown and hot-gas ingestion on jet V/STOL aircraft when they are in ground effect. As part of that program a data base is being created that provides a systematic variation of parameters so that current empirical prediction procedures can be modified. The first series of tests in this program is complete. This report is one of three that presents the data obtained from tests conducted at Lockheed Aeronautical Systems – Rye Canyon Facility and the High Bay area of the 40- by 80-Foot Wind Tunnel at Ames Research Center. This report specifically deals with suckdown on two circular plates.

SYMBOLS

A_{jet}	jet area; 1.188 in^2
C_p	pressure coefficient; $C_p = 2\ \Delta P\ (A_{jet})/T$
d_e	equivalent nozzle diameter, in.; $d_e = 1.23$ in.
h	model height, in.
NPR	nozzle pressure ratio; $NPR = P_{jet}/P_{amb}$
P	local total pressure, psig
P_{amb}	ambient pressure, psia
P_i	local static absolute pressure, psia
P_{jet}	total absolute pressure at the jet exit, psia
r	radial distance from disk center, in.
R	disk radius, in.

*STO-VL Technology, 16527 Sambroso Place, San Diego, CA 92128.

T	thrust, lb
ΔL	jet-induced lift, lb
ΔP	local pressure difference, $\Delta P = P_i - P_{amb}$

INTRODUCTION

The propulsion-induced aerodynamics experienced by jet V/STOL aircraft when hovering close to the ground is being investigated at Ames Research Center. For a multiple-jet configuration in ground effect, a flow field is generated as shown in figure 1. The hot jets impinge on the ground and form a wall jet that entrains surrounding air. This entrainment induces a low-pressure area on the lower surface of the aircraft which causes a lift loss, or suckdown. Meanwhile, a fountain upwash is generated in the area between the jets, thereby inducing a high-pressure area called fountain lift. The net jet-induced lift in hover is the combination of suckdown and fountain lifts. Hot-gas ingestion (HGI) is caused by the hot-wall jet being drawn into the engine inlet. This temperature increase can cause inlet distortion resulting in compressor stall and reduced thrust.

Throughout the 1950s and 1960s there were efforts to evaluate the effects of propulsion-induced aerodynamics on a diverse set of V/STOL aircraft configurations. However, what has been needed is a systematic variation of parameters in order to create a larger data base for predicting the jet-induced lift and hot-gas ingestion on potential V/STOL designs in hover. The first of these efforts to predict the jet-induced lift in hover was reported by Wyatt (ref. 1). Pressure distribution data would help in the understanding of the aerodynamics of jet-induced flow and for prediction method development. However, pressure data are rarely available. Wyatt's study did not contain any pressure data and most of the other studies in the literature include only total force and moment data on complete V/STOL configurations.

A program has been under way at Ames Research Center that is attempting to improve methods for predicting the jet-induced lift and hot-gas ingestion on jet V/STOL aircraft when they are hovering in ground effect. As part of that program a data base is being created that provides a systematic variation of parameters so that new empirical prediction procedures can be developed. The data will also be useful for the validation of computational fluid dynamics codes.

The first series of tests in this program has been completed. This report is one of three that is presenting the data obtained from tests conducted at Lockheed Aeronautical Systems – Rye Canyon Facility and the High Bay area of the 40- by 80-Foot Wind Tunnel at Ames Research Center. The tests were conducted at Ames to check out the instrumentation and to evaluate the effect of room size on the data. The force and pressure data for a tandem jet V/STOL arrangement are presented in reference 2. Hot-gas ingestion data for the configurations of reference 2 will be presented at a later date.

AMES HIGH BAY TEST

Hover Test Rig

The hover test rig at the Ames High Bay area (figs. 2,3) consisted of a jet issuing through a hole in the center of a circular plate. The nozzle was pointed vertically upward and was mounted to a rectangular plenum. High-pressure air was plumbed to the plenum. The plenums had a maximum weight flow of 2.5 lb/sec at a nozzle pressure ratio of 6.0. The circular disk was mounted to a six-component strain-gage balance (TASK balance 1.5 MK IIC). The nozzle and plenum were non-metric, that is, the strain-gage balance measured only induced aerodynamic forces on the circular plate.

For in-ground-effect (IGE) studies an 8- by 8-ft plywood ground plane was used (figs. 3,4). This ground plane was supported by two 16-ft by 2-in. wooden beams. For additional stiffness, seven 2- by 4-in wooden beams were provided along with two ground-plane supports. This ground plane was mounted to an apparatus (two axis survey rig) that moved the ground plane in a vertical direction, thereby changing the "height" (h) of the model. The height ranged from a minimum of 2 in. between the disk's bottom surface and the ground plane to a maximum of 40 in. ($1.6 \leq h/d_e \leq 32$). The entire rig was set up in the Ames 40- by 80-Foot Wind Tunnel High Bay, which is shown in figures 4 and 5. This large room enclosure ensured that there would be no interference from the walls or ceiling.

Details of Nozzle and Plenum

The ASME nozzle, made of 321 stainless steel, was attached to a rectangular plenum made of 304 stainless steel. As shown in figure 6, the nozzle has three porous plates to improve flow quality. Steel rods (3/8 in.-diam) were welded into place to stiffen the plenum wall. The inner portion of the nozzle exit is contoured to ASME specifications (fig. 7).

A Kiel probe assembly (shield diameter = 0.095 in.) to sense the nozzle total pressure and temperature was mounted in the nozzle 3.5 in. from the exit of the nozzle and 2.0 in. (26 hole diameters) downstream of the last porous plate (figs. 7,8).

Model Hardware

The 20-in.-diam disk and 10-in.-diam disk are schematically shown in figure 7. The top edge of each disk is chamfered to an angle as shown. The edge on each disk is blunt (0.050 in. wide) and each disk is 0.25 in. thick. The nozzle exit hole is chamfered to an angle as shown. There was a 0.050-in. annular gap between the disks and the nozzle. Before and after each daily run the gap was visually inspected to ensure that there was no fouling between the disks and the nozzle. However, some data were taken with the gap sealed to see what effect this had on the induced pressures.

Pressure taps were provided along both sides of the 10- and 20-in. disks in two radial rows (figs. 9,10). One row on both the top and bottom of each disk has a fine grid of pressure taps. A close-up photo of the 20-in. disk installed on the balance is shown in figure 11.

Instrumentation and Data Acquisition System

The instrumentation used consisted of a six-component strain-gage balance, two thermocouples, three pressure transducers, and one scanivalve module. Figure 12 shows a simple schematic of the data acquisition system, and figure 13 shows a picture of the setup.

The strain-gage balance was used to measure the lift-loss ($\Delta L/T$) on the plates. Only the axial force component (100 lb max.) of the balance was used; therefore, no gage interactions were used in calculating the lift-loss.

The balance and pressure transducers were supplied an excitation voltage by a group of signal conditioners; each instrument had its own signal conditioner. The output of each instrument was fed back to its signal conditioner and could be monitored in real time on a digital panel meter. The cables that connected the signal conditioners to the transducers and strain-gage balance were 50 ft long, as were the wires from the thermocouples to the hot-box reference junction.

One nozzle transducer (100-psig), was used to monitor the nozzle pressure ratio (NPR). Two scanivalve pressure transducers (1-psig and 0.09-psig (SETRA)) were used separately on a 48-port scanivalve module. The SETRA transducer was used to measure extremely small pressures on the 20-in. disk when it was out of ground effect (OGE) and served as a check on the accuracy of the 1-psig transducer. The 1-psig transducer was used both IGE and OGE. There was also a 25-psia pressure transducer to monitor ambient pressure.

Only two thermocouples were used; one to monitor the ambient temperature (Copper-Constantan) and the other to monitor the nozzle exit air temperature (Chromel-Alumel). Both thermocouples were wired to a 150 °F hot-box reference junction.

All instrumentation signals were sent to a set of amplifiers (gain 128). The amplified signals were input to a 64-channel scanner card in an HP 6942A multiprogrammer. During the data acquisition sequence (fig. 14) the raw voltages were stored in a 64-K word memory buffer in the multiprogrammer. After the data acquisition sequence was completed the voltages were downloaded into the HP 9000/200 computer system where they were averaged. The averaged raw data was then converted to engineering units, then stored on a Bering 20-mB Bernoulli cartridge, and output to an HP 2671G thermal printer.

Nozzle Surveys

Nozzle surveys were conducted in the Ames 40 x 80 Wind Tunnel High Bay area. A Kiel probe assembly was attached to the two-axis survey rig (fig. 15). Motion was axially and radially relative

to the jet. The survey rig's motor controller was capable of positioning the Kiel probe assembly in 0.001-in. increments in both the axial and radial directions.

The Kiel probe extending inside the nozzle monitored the total jet pressure (P_{jet}). The scanning Kiel probe (P) was mounted on the survey rig to survey the total pressures of the nozzle exhaust at various axial and radial stations. Both pressures were monitored by the data acquisition system and were used to define the nozzle total pressure ratio (P/P_{jet}). The computer averaged 20 samples per data point before displaying the ratio to the screen.

For the radial surveys (fig. 16) the scanning Kiel probe (P) was positioned at a single axial station (0.1 in. from the exit of the nozzle) and moved radially across the exit of the nozzle in 0.05-in. increments.

For the axial surveys (fig. 17) the scanning Kiel probe (P) was positioned on the nozzle centerline about 0.1 in. from the exit and the Kiel probe was moved along the nozzle axis away from the nozzle exit in 2-in. increments to a maximum distance of 24 in. (19 nozzle diameters).

DESCRIPTION OF RYE CANYON TEST

The IGE and OGE tests on the 20-in. circular disk were conducted using the Hover Test Rig set up at Rye Canyon (figs. 18-21). At this facility, the same plenum, nozzle, and strain-gage balance were used as in the Ames High Bay test, but they were mounted to an A-frame such that the nozzle was pointed downward.

The A-frame is constructed of 4- by 4-in^2 steel tubing. Flanges were welded to the attachment points and 1/2-in. bolts were used to clamp them together. The A-frame is 10 ft high and is 7 ft wide at the base. The aluminum ground plane is 8- by 8-ft. The ground plane was moved vertically by a hydraulically operated scissors lift with a range of motion of 50 in.

The entire test rig and model were enclosed in a test cell that was 20 ft wide, 28.5 ft deep, and 15 ft high. At one end of the room there was a roll-up door that was 16 ft wide and 11 ft high (fig. 20). Tests were performed with the roll-up door in both the open and closed positions to observe the effect on the flow field of removing one wall of the room.

With the exception of the test setup arrangements for the Ames High Bay test (fig. 2) and the Rye Canyon test (fig. 18) and the test cell, all instrumentation, software, and hardware were exactly the same for the Ames High Bay test and the Rye Canyon test.

PRESENTATION OF DATA

The data are presented without analysis. Groups 1 through 4 (figs. 22-42) are plots of pressure coefficient as a function of its radial location on both the 10-in. and 20-in. disks (table 1). Group 5

(figs. 43-47) presents the strain-gage balance lift-loss data obtained for both disks (10-in. and 20-in.) as a function of height, nondimensionalized by the jet diameter (d_e) (table 2).

REFERENCES

1. Wyatt, L. A.: Static Test of Ground Effect on Planforms Fitted with a Centrally Located Round Lifting Jet. Ministry of Aviation, London, England, CP 749, June 1962.

2. Bellavia, D. C.; Wardwell, D. A.; Corsiglia, V. R.; and Kuhn, R. E.: Suckdown, Fountain Lift, and Pressures Induced on Two Tandem Jet V/STOL Configurations. NASA TM-102817, 1991.

Table 1. Figure index: c_p vs. r/R (groups 1-4)

h/d_e	NPR	Figure no.
Group 1. 20-in. disk (Ames)		
OGE (SETRA)	1.7, 1.7, 2.3, 2.3, 2.9	22(a)-22(e)
	4.0, 5.0, 6.1, 3.8	22(f)-22(i)
OGE	1.7, 2.3, 3.0, 4.1	23(a)-23(d)
	5.2, 5.8	23(e),23(f)
Group 2. 20-in. disk (Ames)		
1.6, 2.4, 3.3, 4.9, 8.1	1.5	24(a)-24(e)
8.1, 12.2, 16.3, 24.4		24(f)-24(i)
1.6, 2.4, 3.3, 4.9, 8.1	2	25(a)-25(e)
8.1, 12.2, 16.3, 24.4		25(f)-25(i)
1.6	2.6	26
2.4, 3.3, 4.9, 8.1	4	27(a)-27(d)
8.1, 12.2, 16.3, 24.4		27(e)-27(h)
3.3, 4.9, 8.1, 8.1	6	28(a)-28(d)
12.2, 16.3, 24.4		28(e)-28(g)
Group 3. 10-in. disk (Ames)		
1.6, 2.4, 3.3, 4.9	1.5	29(a)-29(d)
8.1, 12.2, 16.3		29(e)-29(g)
1.6, 2.4, 3.3, 4.9	2	30(a)-30(d)
8.1, 12.2, 16.3		30(e)-30(g)
1.6, 2.4, 3.3, 4.9	3	31(a)-31(d)
8.1, 12.2, 16.3		31(e)-31(g)
1.6, 2.4, 3.3, 4.9	4	32(a)-32(d)
8.1, 12.2, 16.3		32(e)-32(g)
8.1	5	33
1.6, 2.4, 3.3, 4.9	6	34(a)-34(d)
8.1, 12.2, 16.3		34(e)-34(g)
Group 4. 20-in. disk (Rye)		
OGE	1.5, 2, 2.5	35(a)-35(c)
	3, 4, 5, 6	35(d)-35(g)
4.1, 8.1, 16.3	1.5	36(a)-36(c)
4.1, 4.9, 8.1, 8.1	2	37(a)-37(d)
9.8, 12.2, 16.3, 16.3		37(e)-37(h)
20.4, 24.4, 32.5		37(i)-37(k)
4.1, 8.1, 16.3	2.5	38(a)-38(c)
4.1, 8.1, 8.1, 16.3	3	39(a)-39(d)
8.1, 16.3	4	40(a),40(b)
8.1, 16.3	5	41(a),41(b)
4.9, 8.1, 8.1, 9.8, 12.2	6	42(a)-42(e)
16.3, 16.3, 20.4, 32.5		42(f)-42(i)

Table 2. Figure index: ΔL/T (group 5)

Configuration	h/d_e	NPR	Figure no.
20-in. disk (Ames)	Range	1.5, 2, 4, 6	43
10-in. disk (Ames)	Range	1.5, 2, 3, 4, 6	44
20-in. disk (Rye)			
Door half open	Range	1.5, 2, 2.5, 3, 4, 5, 6	45
Door full open	Range	1.5, 2, 2.5, 3, 4, 5, 6	46
20-in. disk (Rye)	OGE	Range	47

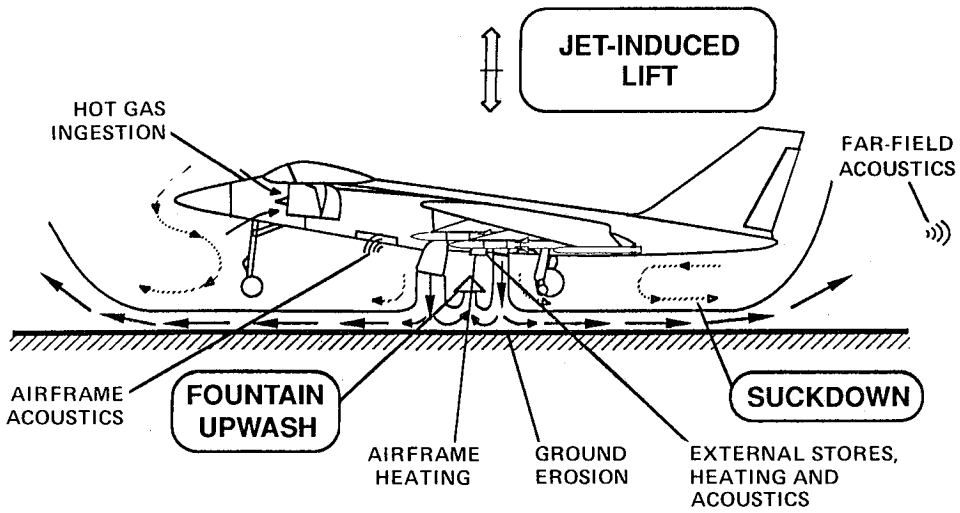

Figure 1. Research topics associated with the flow field of a STOVL aircraft hovering in ground effect.

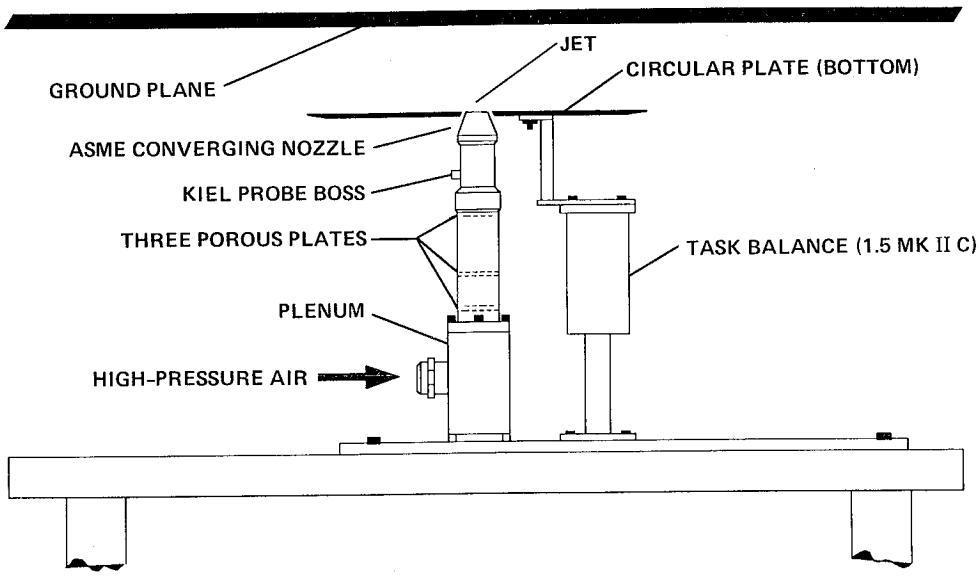

Figure 2. Schematic of test setup, large room, located in High-Bay Area of 40- by 80-Foot Wind Tunnel at Ames Research Center.

ORIGINAL PAGE
BLACK AND WHITE PHOTOGRAPH

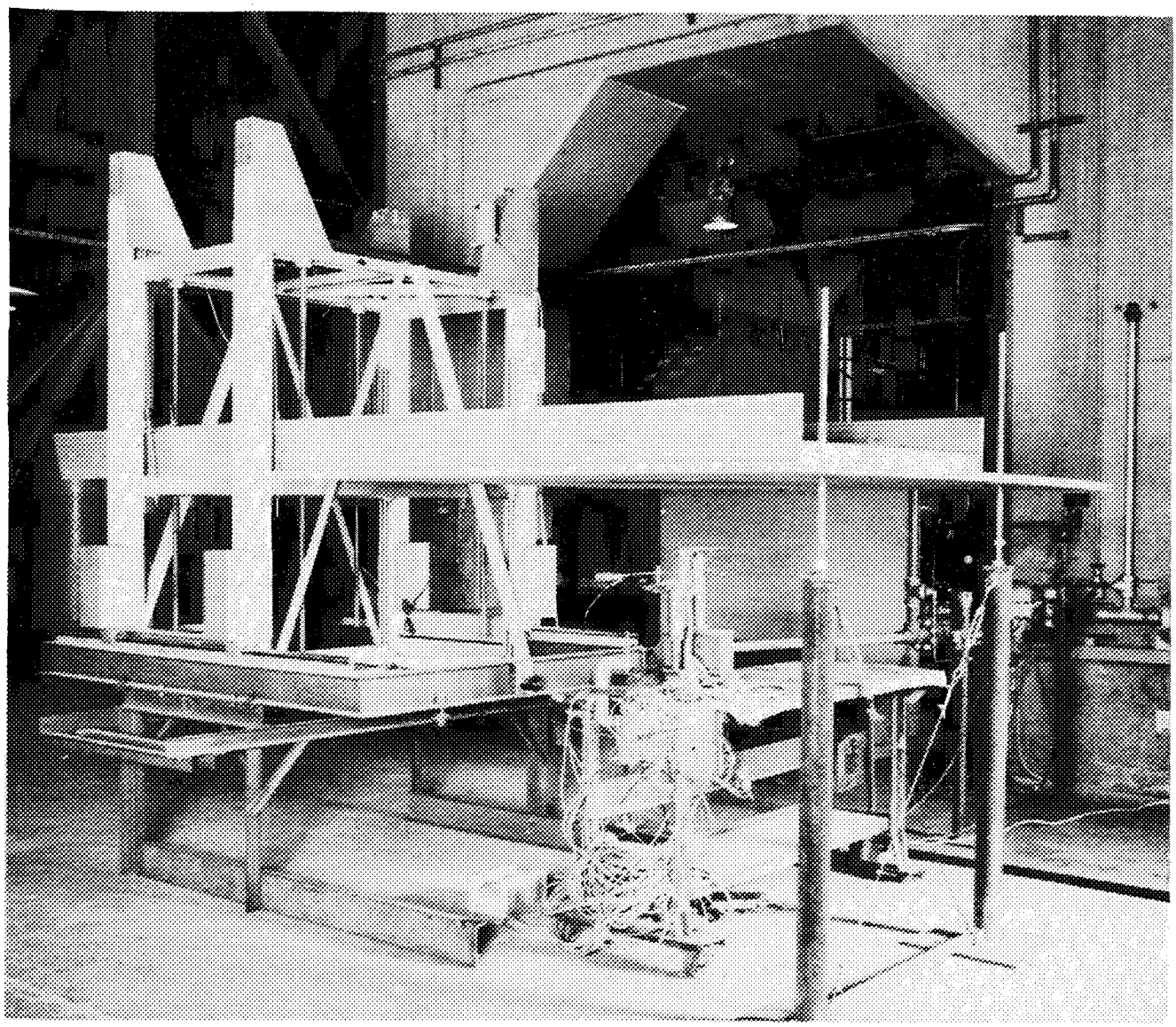

Figure 3. Test setup, large room, located in High-Bay Area of 40- by 80-Foot Wind Tunnel at Ames Research Center.

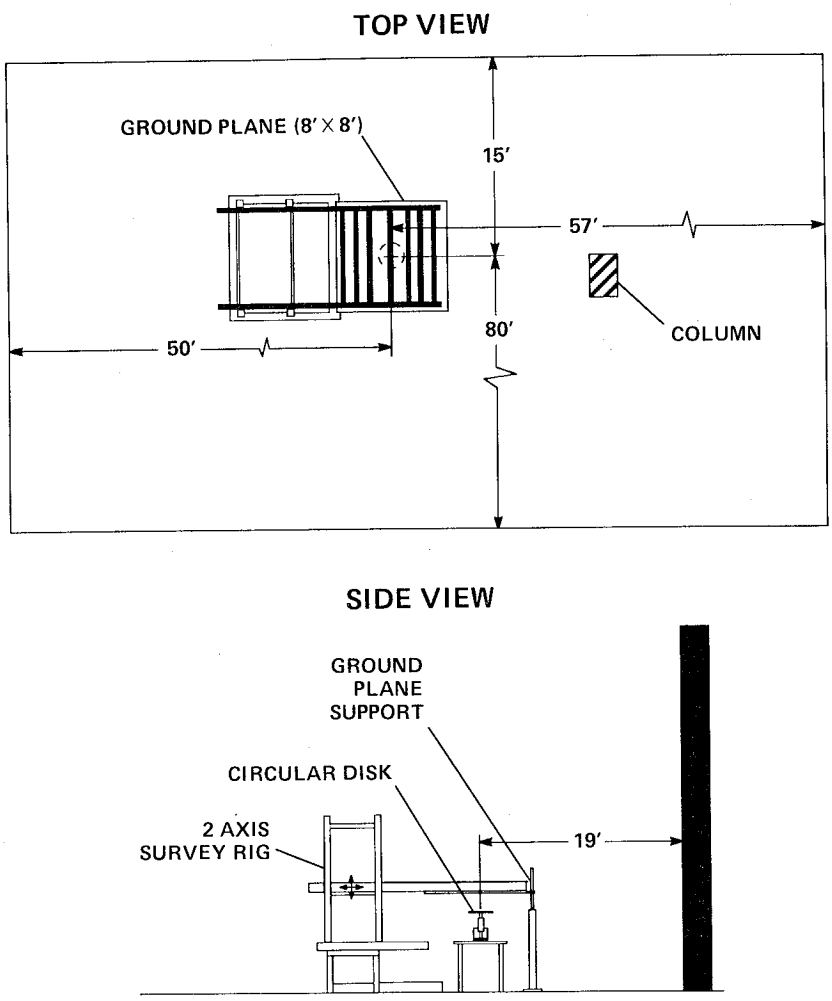

Figure 4. Survey rig and ground board, large room.

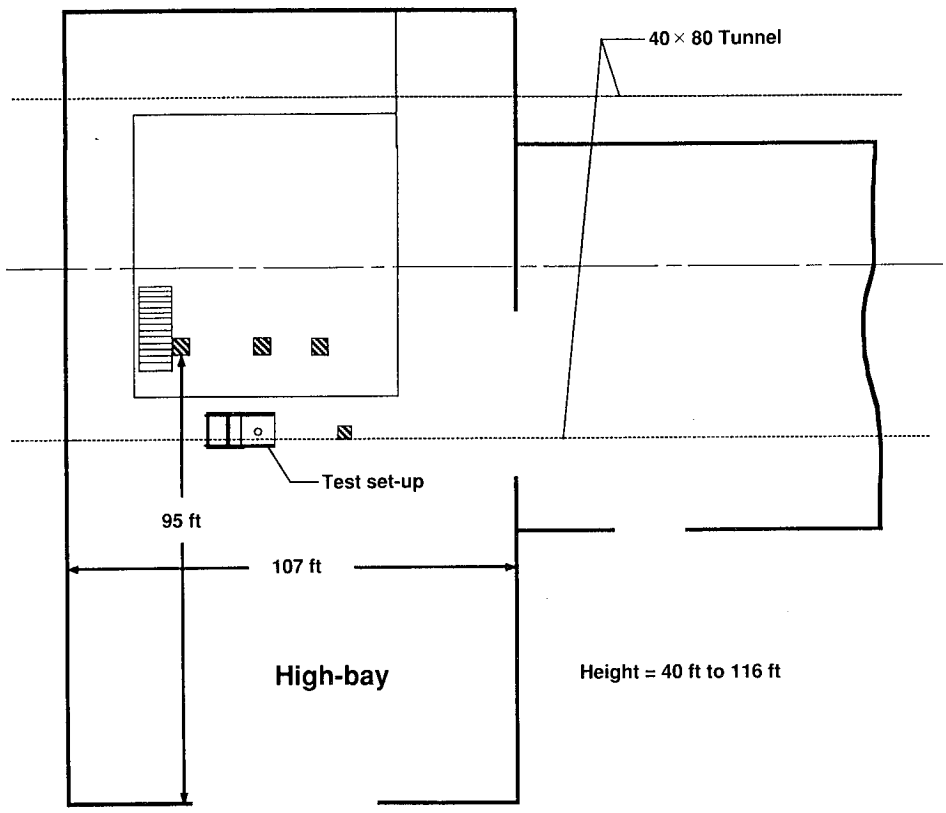

Figure 5. Location of test setup (large room) relative to walls and ceiling.

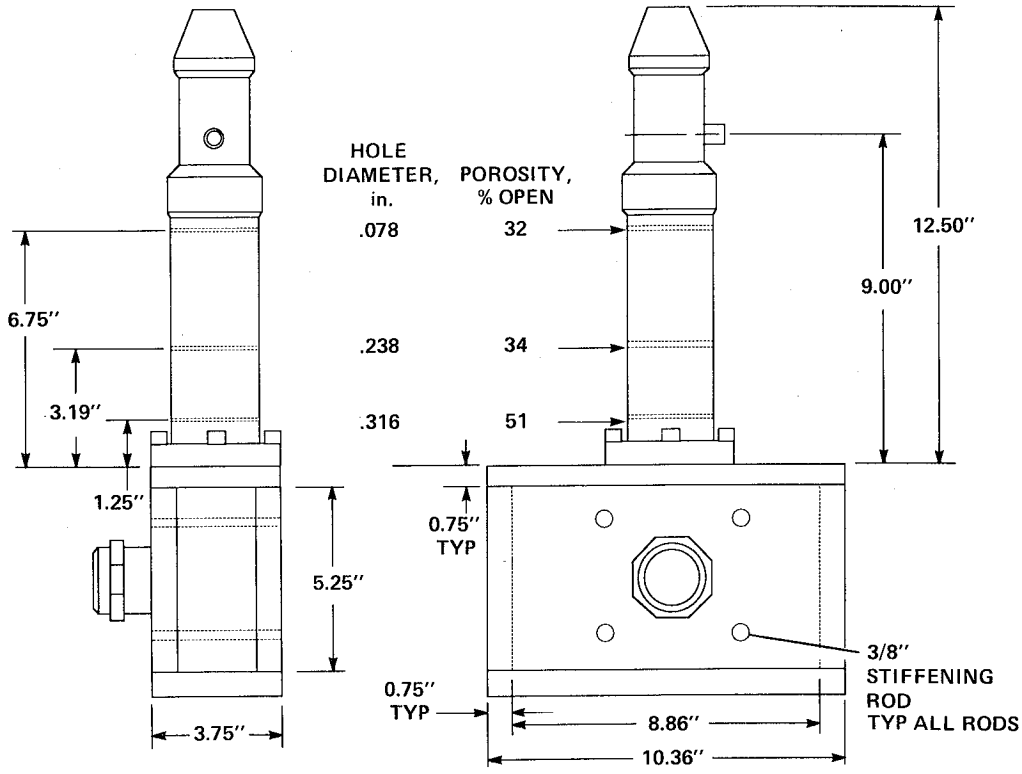

Figure 6. Details of nozzle and plenum assembly.

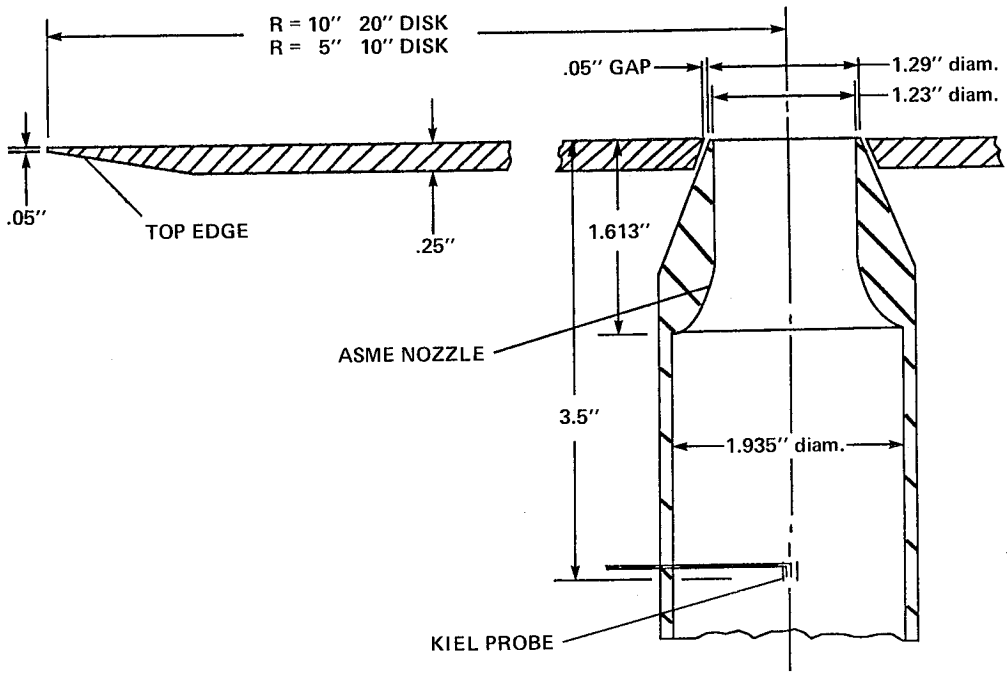

Figure 7. Details of nozzle exit and circular plate.

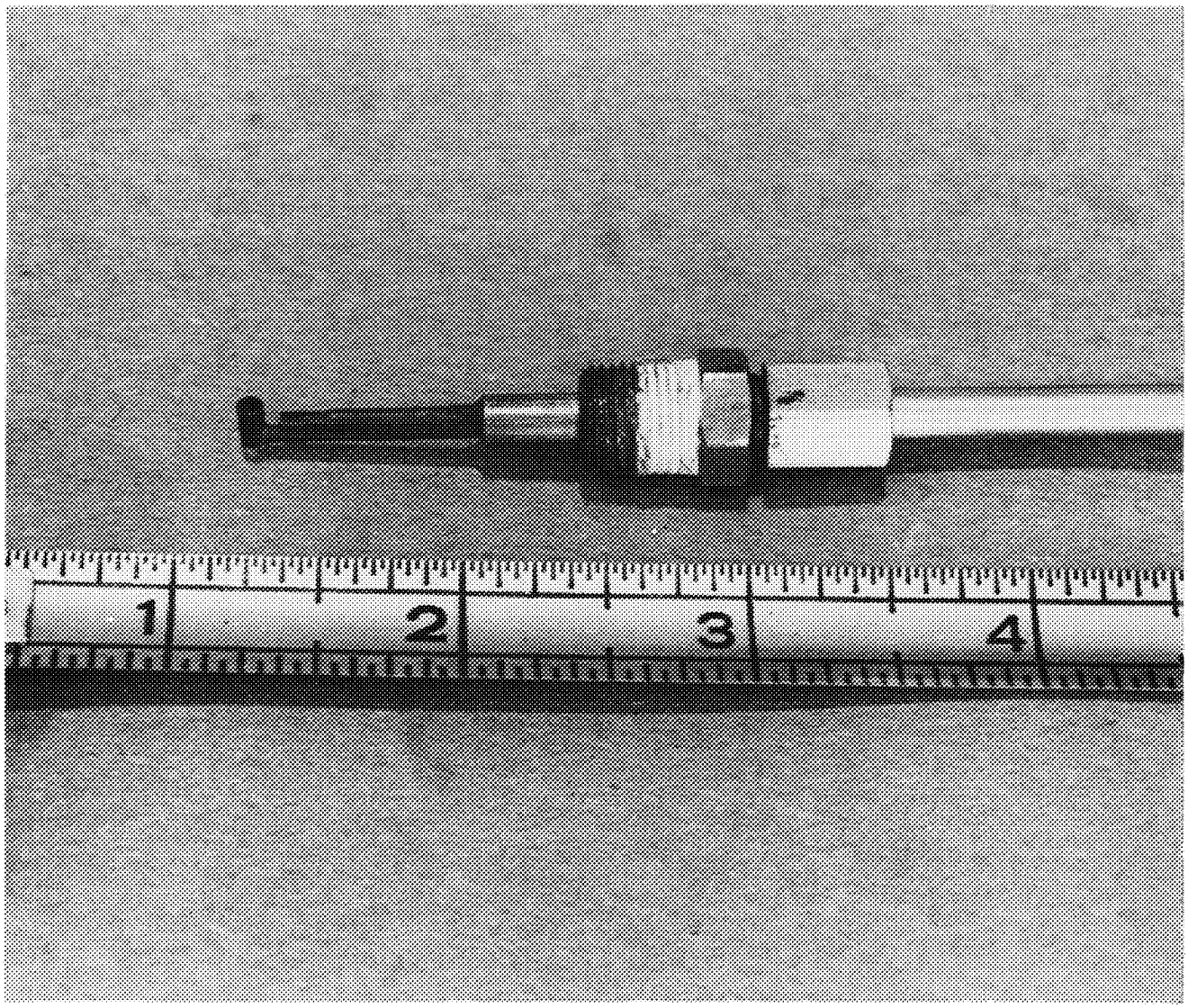

Figure 8. Kiel probe used in nozzle.

RADIUS, in.	1	1.13	1.25	1.5	2	2.5	3	3.5	4	4.5	4.75	4.94
TOP	X	X		X					X	X	X	X
BOTTOM	X	X	X	X	X	X	X	X	X	X	X	X

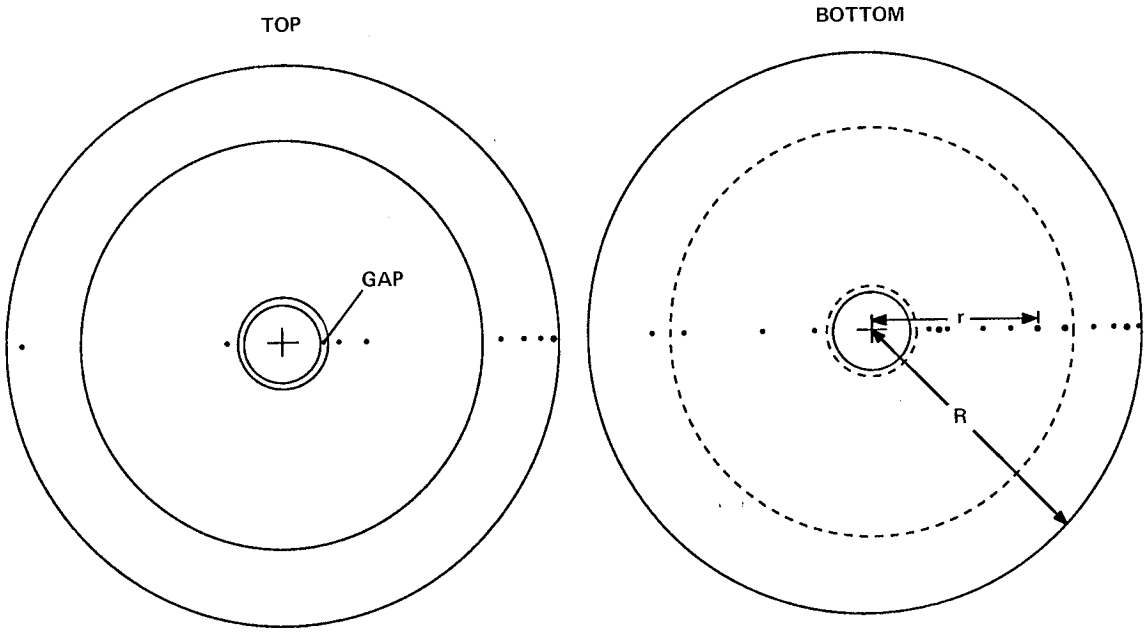

Figure 9. Pressure taps on 10-in. circular plate.

RADIUS, in.	0.75	1	1.31	1.5	1.56	1.88	2	2.19	2.5	3	4	5	6	7	8	8.5	9	9.5	9.94
TOP				X		X				X					X		X	X	X
BOTTOM	X	X	X	X	X	X	X	X	X	X	X	X	X	X	X	X	X	X	X

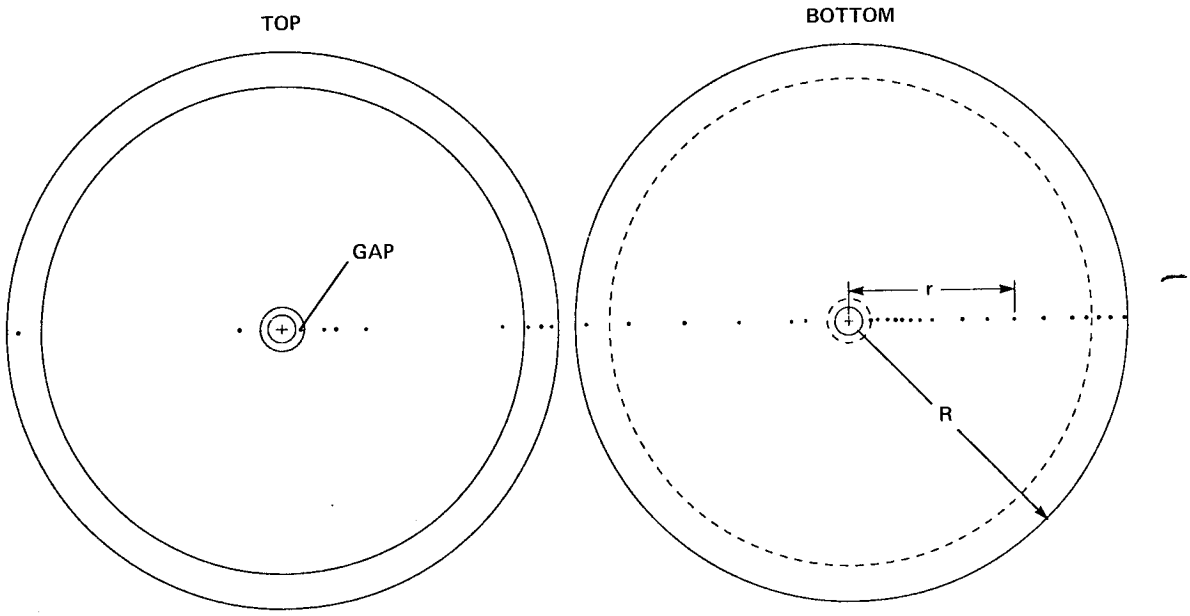

Figure 10. Pressure taps on 20-in. circular plate.

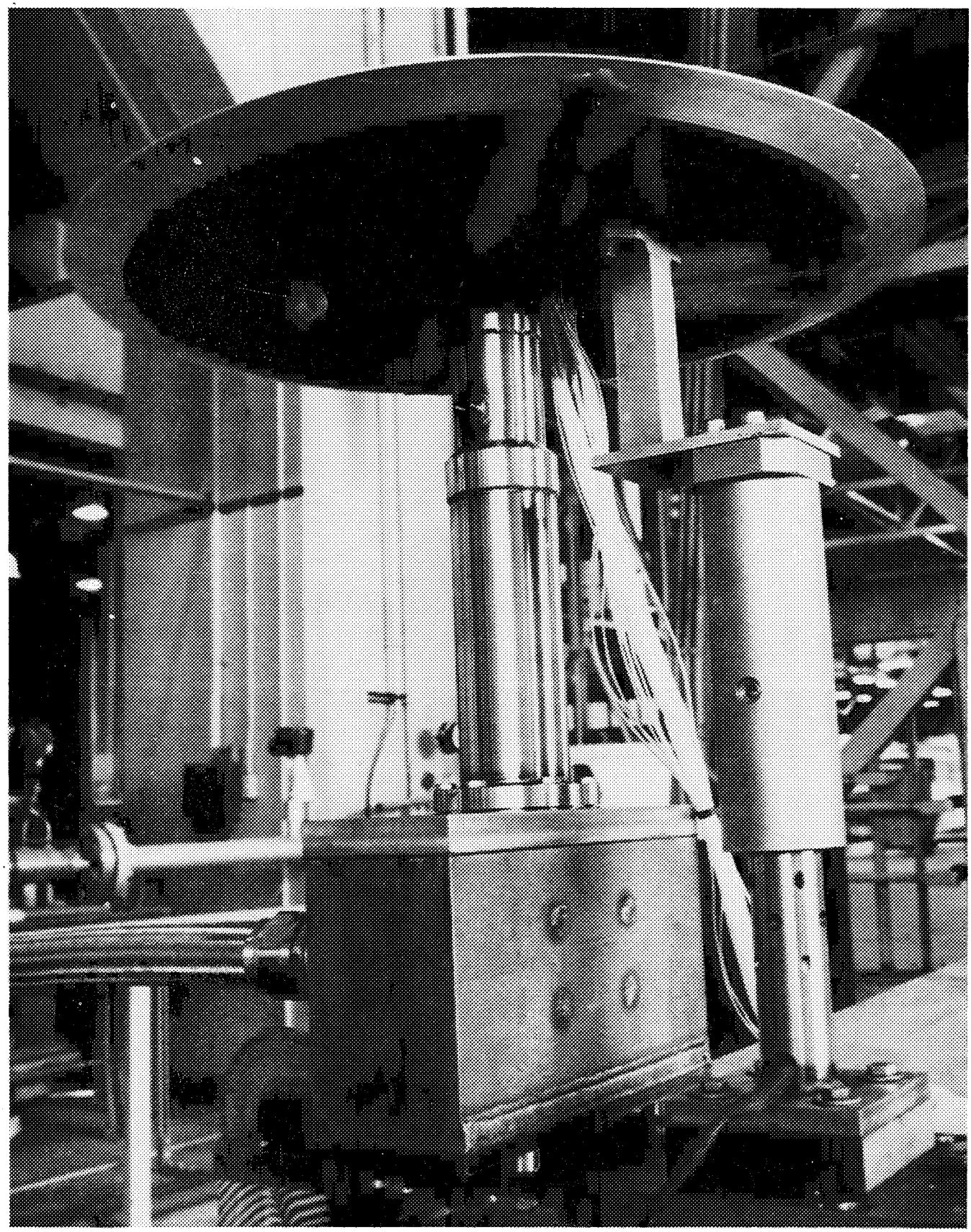

Figure 11. Installation of 20-in. circular plate.

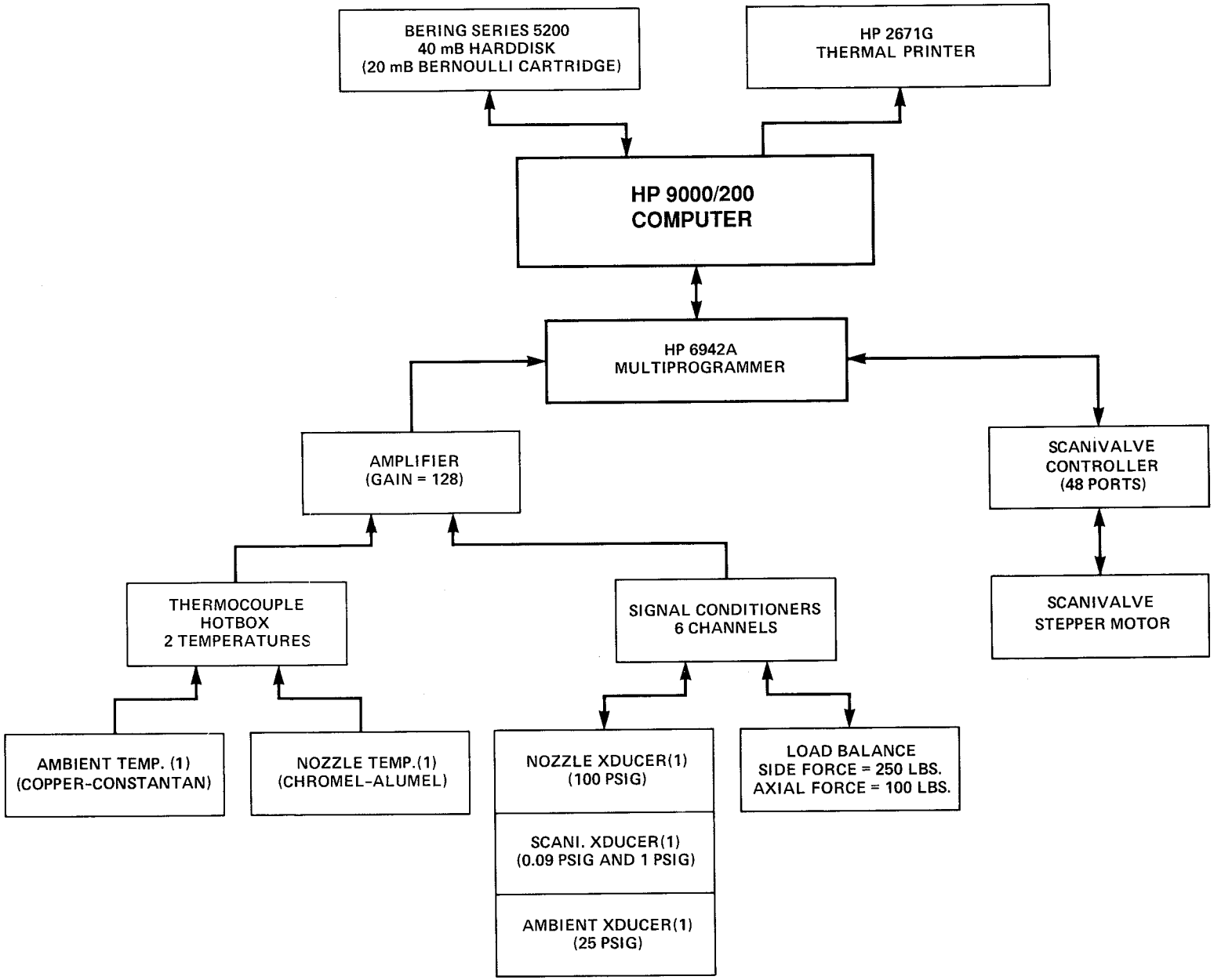

Figure 12. Instrumentation and data acquisition system.

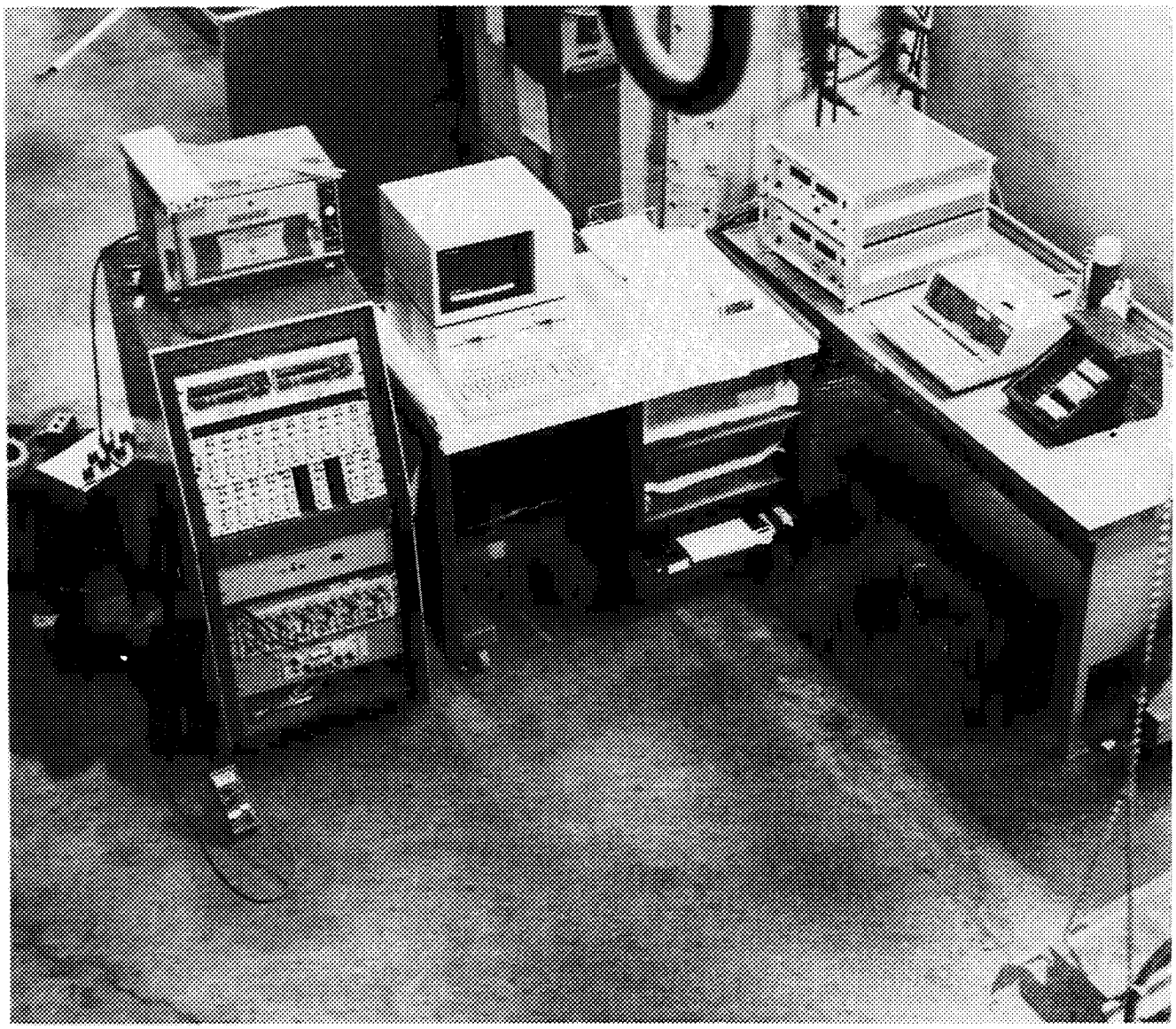

Figure 13. Data acquisition system setup.

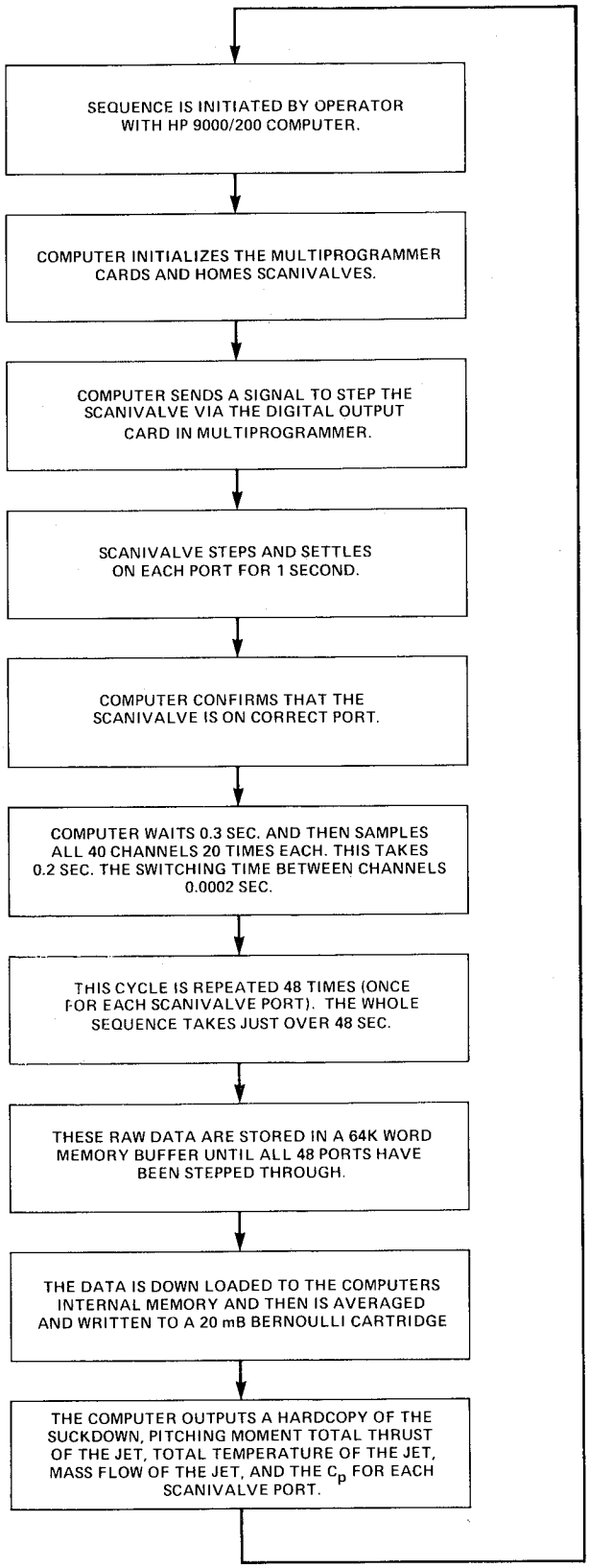

Figure 14. Data acquisition sequence.

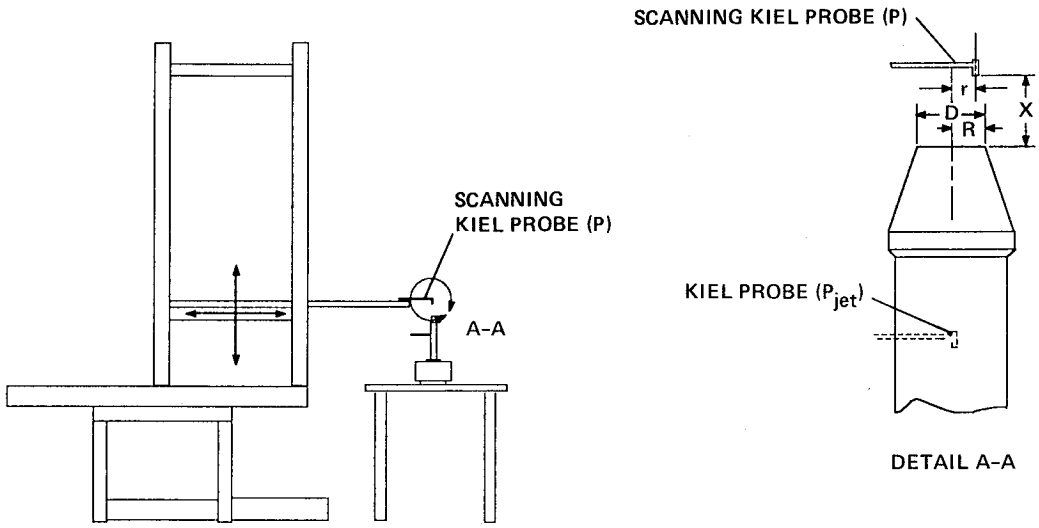

Figure 15. Nozzle survey setup.

Figure 16. Nozzle radial total pressure surveys.

Figure 17. Nozzle axial total pressure surveys.

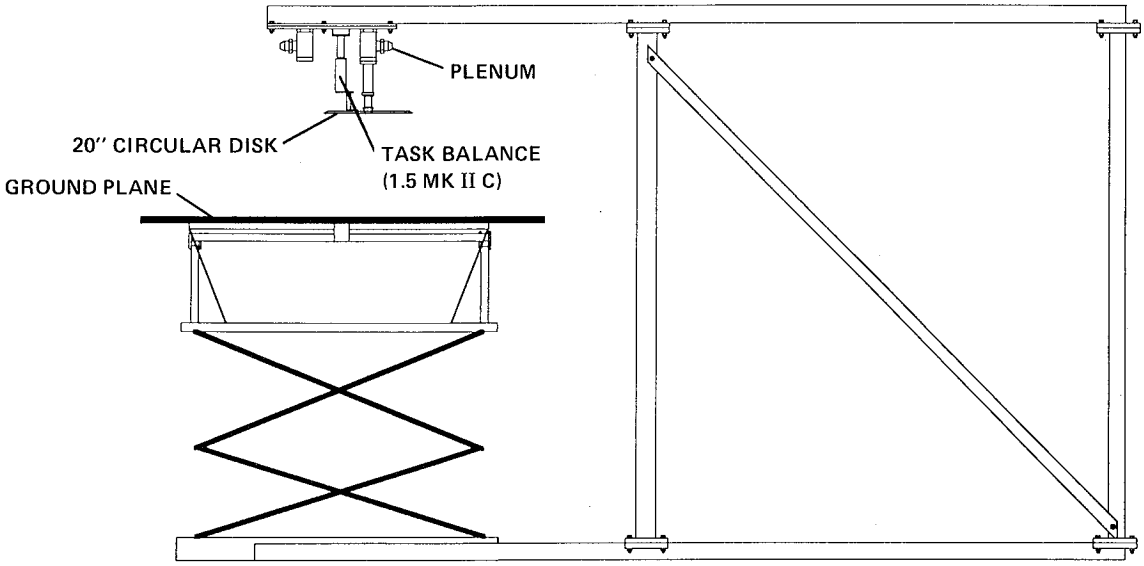

Figure 18. Hover test rig, test cell, located at Lockheed Aeronautical Systems-Rye Canyon Facility.

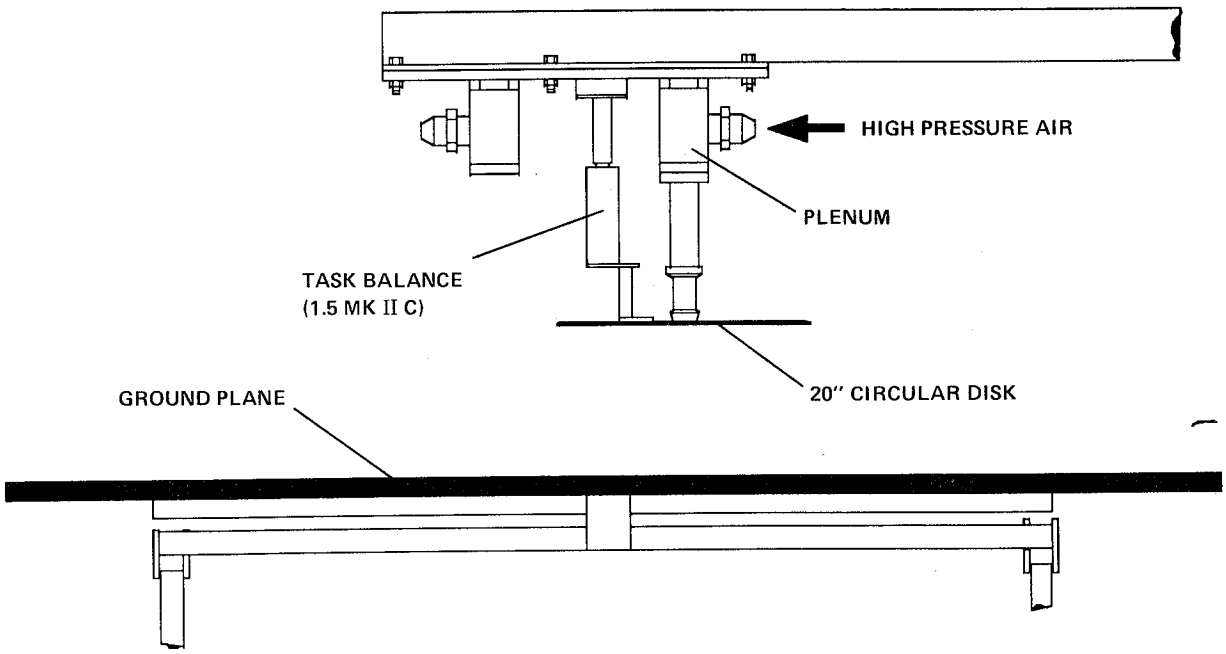

Figure 19. Hover test rig details (test cell).

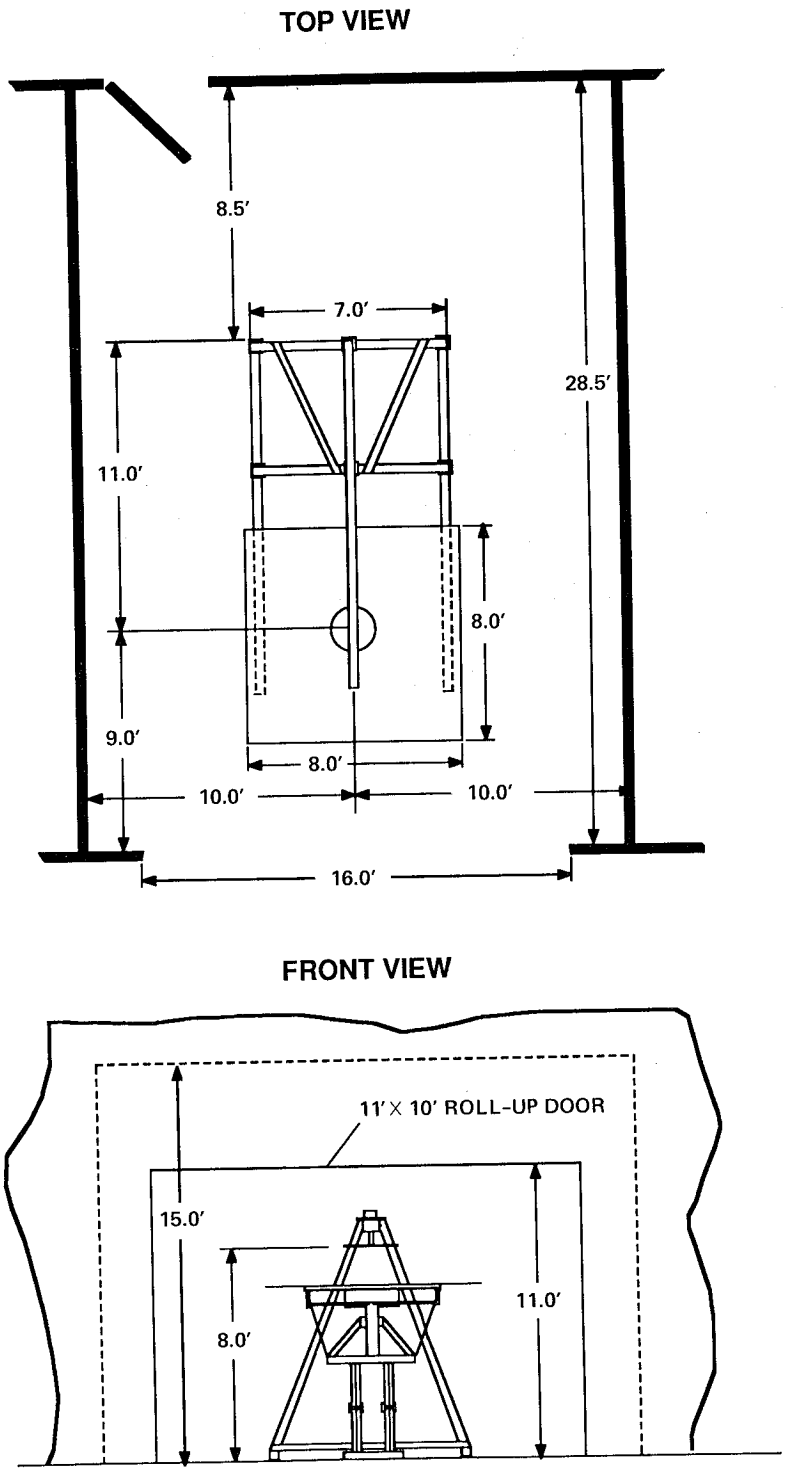

Figure 20. Location of test setup (test cell) relative to walls and ceiling.

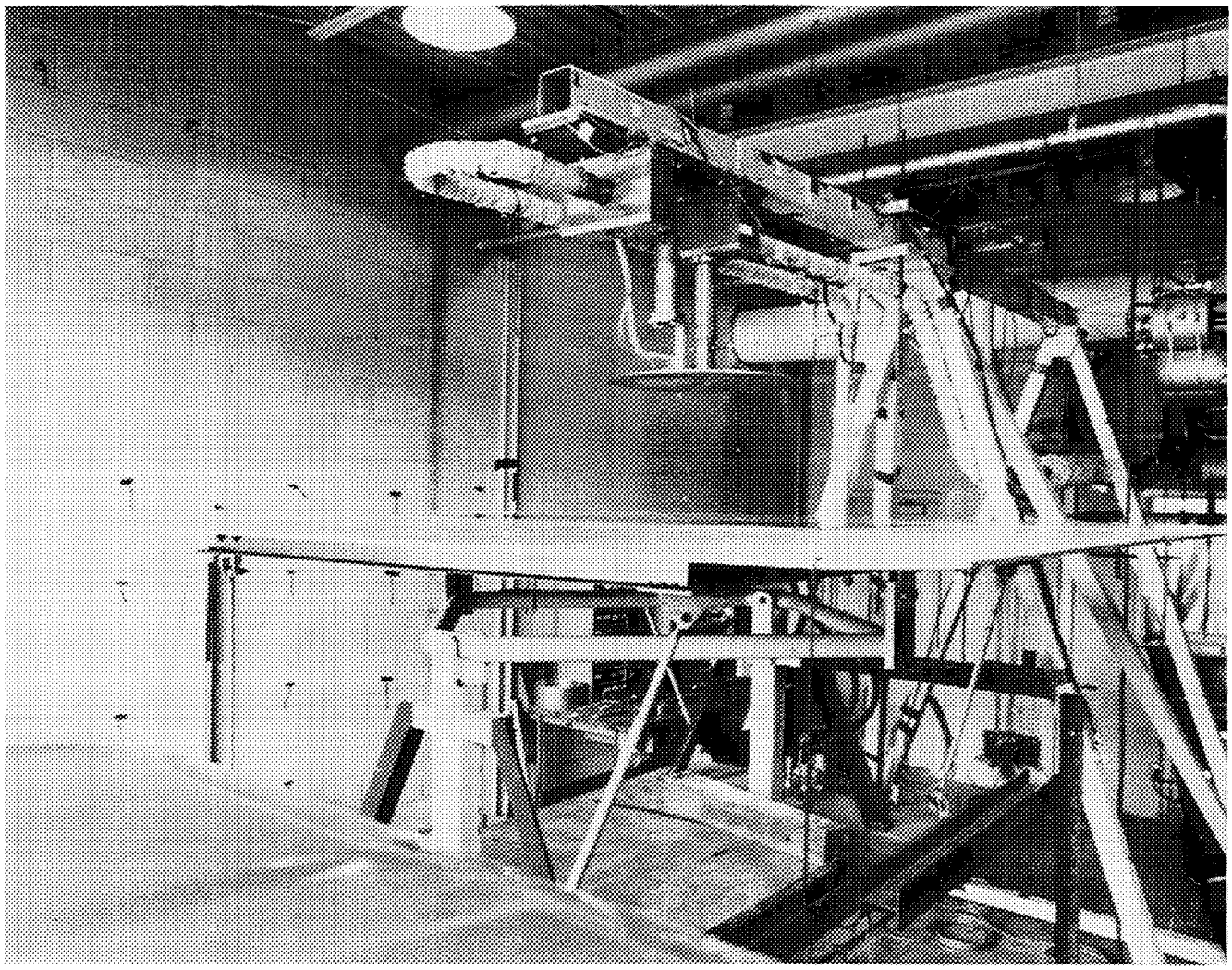

Figure 21. Hover test rig installation, test cell, 20-in. circular plate installed.

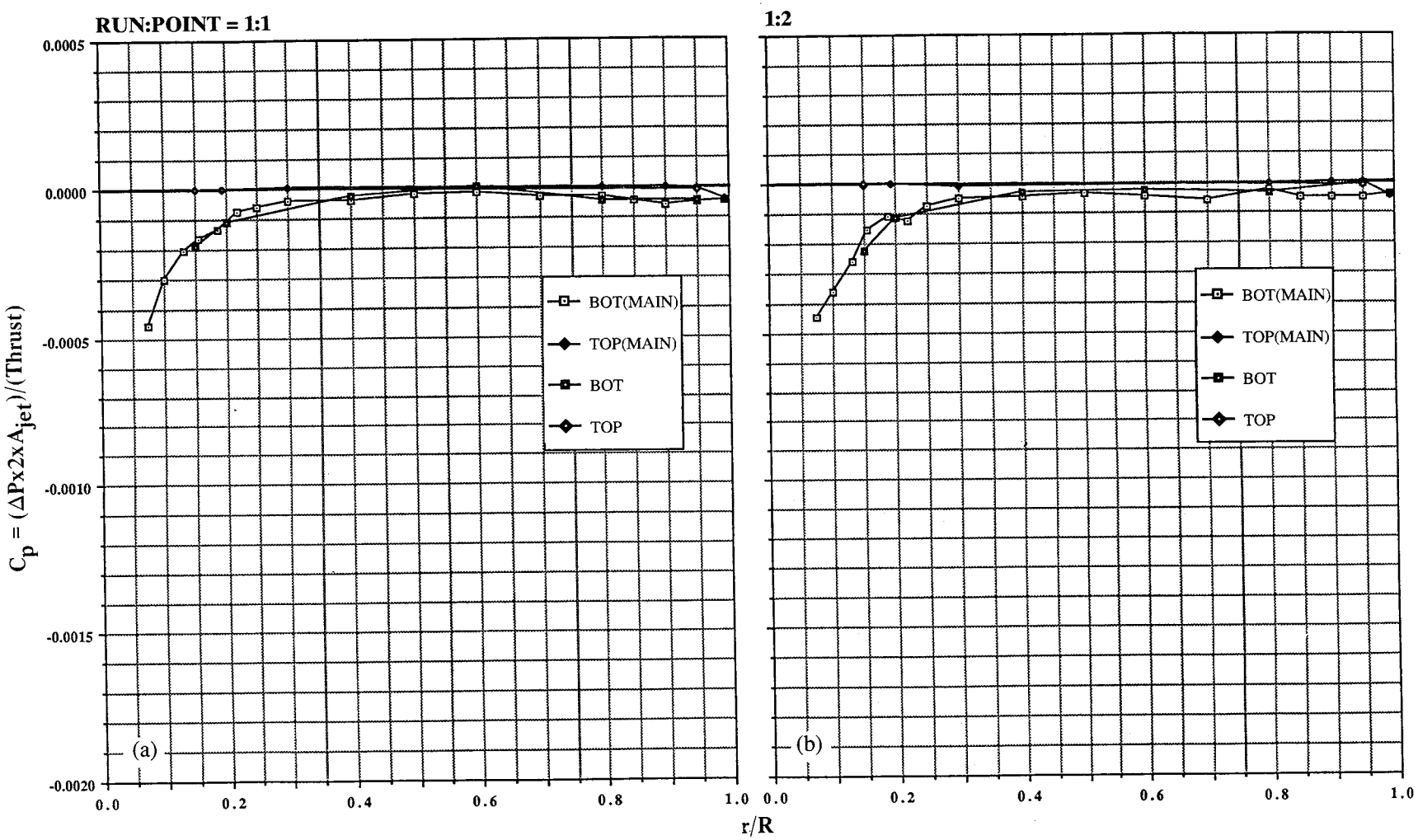

Figure 22. Pressures induced on 20-in. circular plate out of ground effect, SETRA pressure transducer, large room. (a) NPR = 1.66, T = 19 lb, (b) NPR = 1.66, T = 19 lb (repeat).

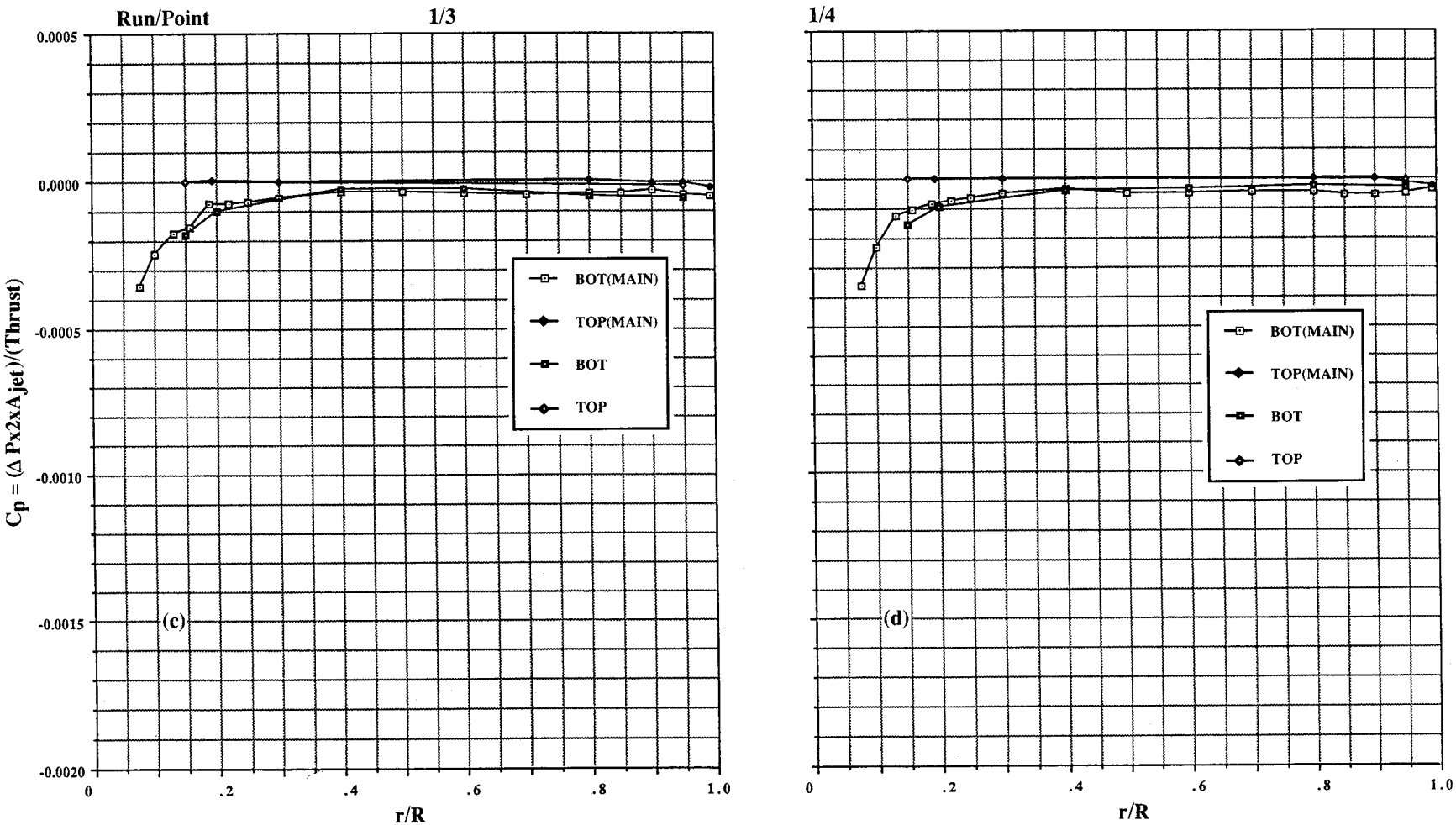

Figure 22. Continued. (c) NPR = 2.28, T = 33 lb, (d) NPR = 2.28, T = 33 lb (repeat).

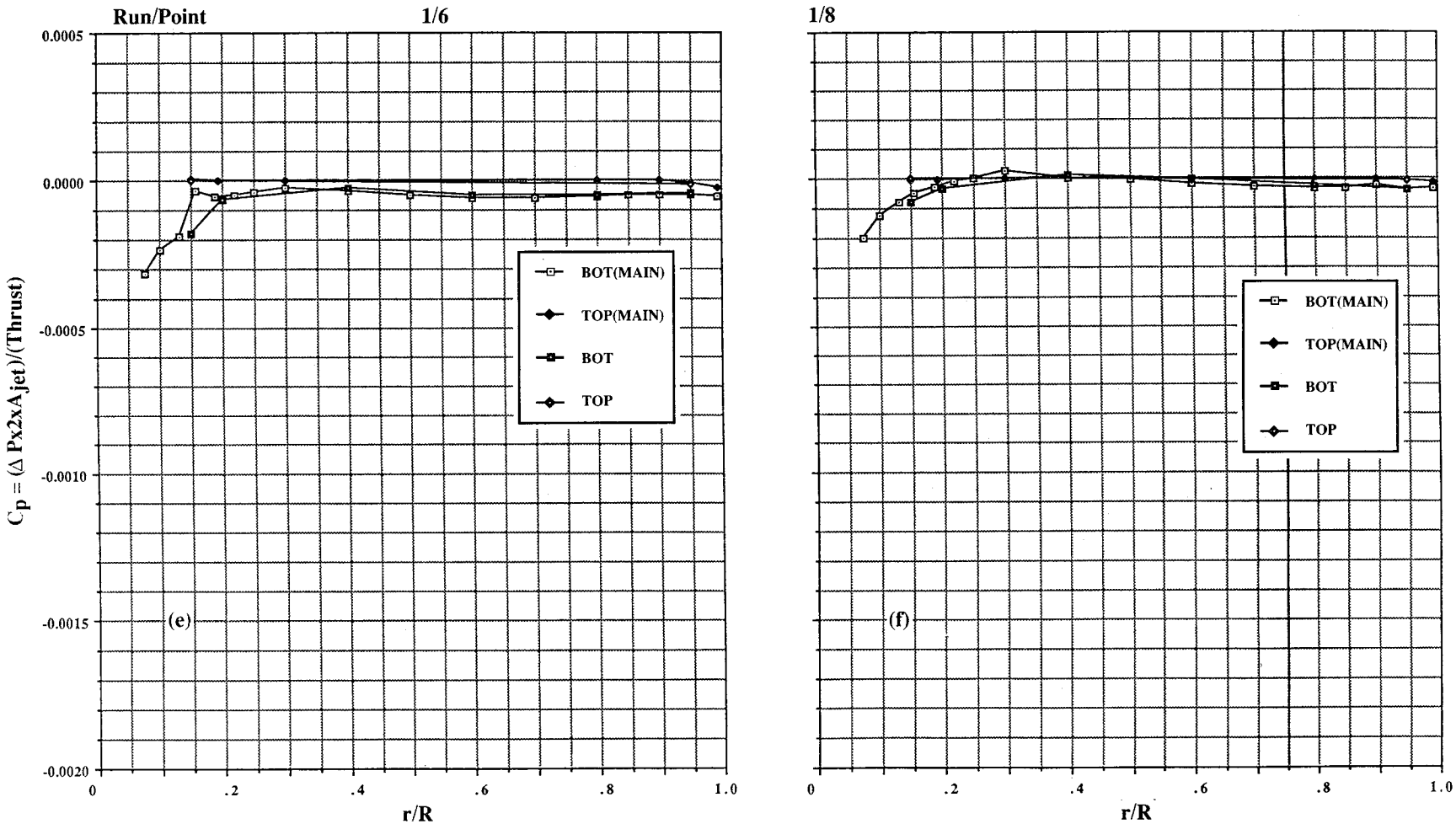

Figure 22. Continued. (e) NPR = 2.9, T = 48 lb, (f) NPR = 4.0, T = 71 lb.

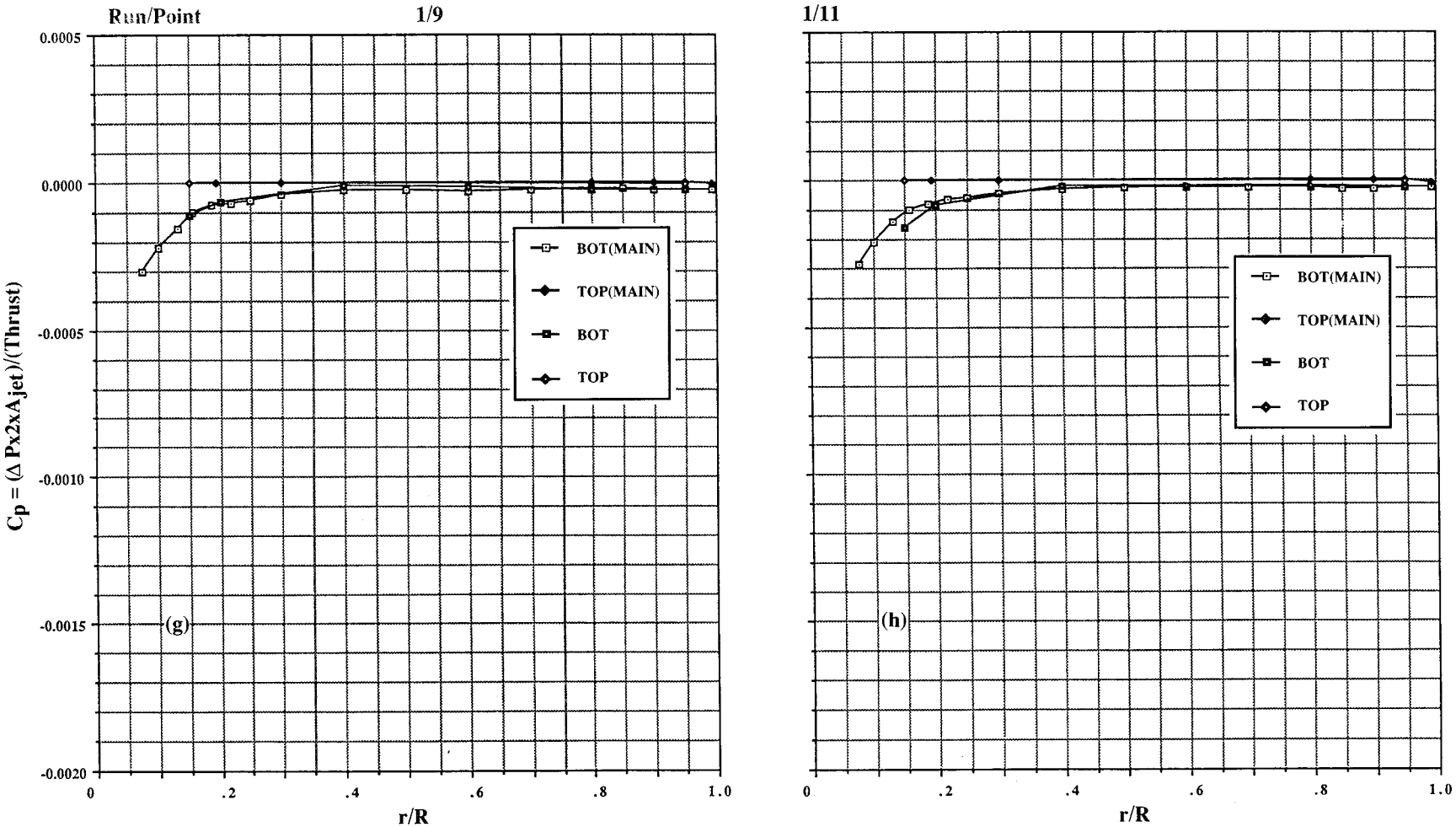

Figure 22. Continued. (g) NPR = 5.0, T = 94 lb, (h) NPR = 6.1, T = 118 lb.

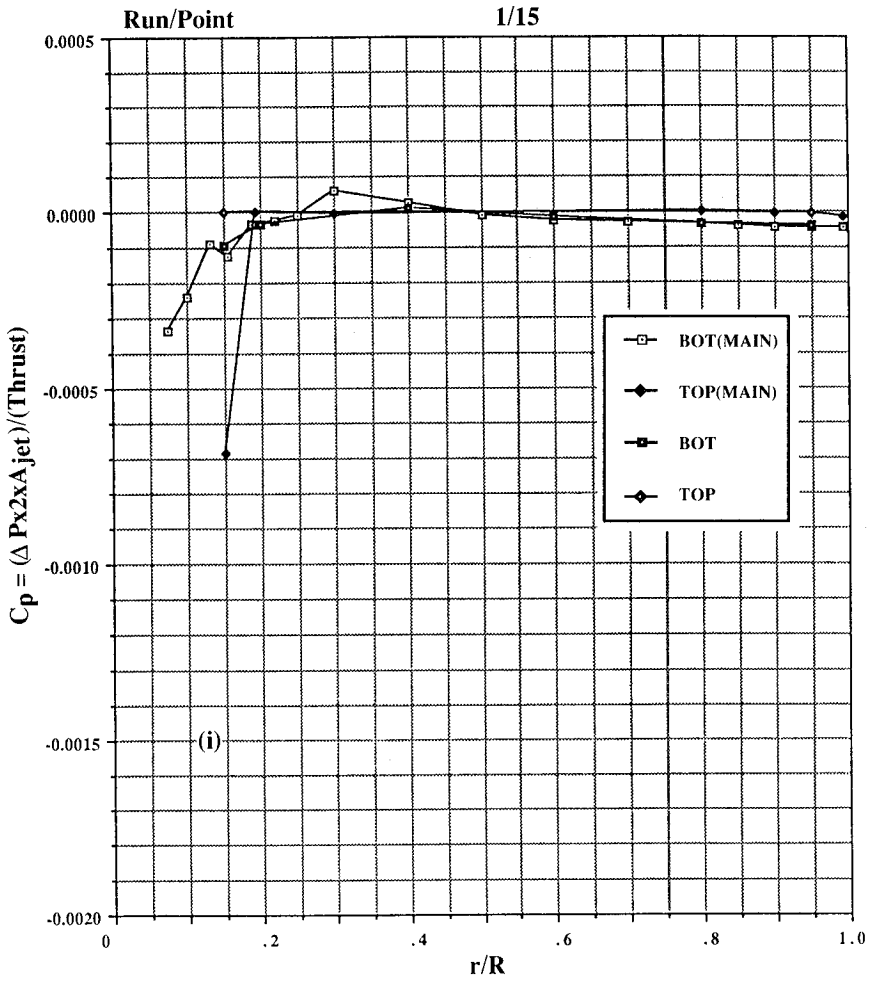

Figure 22. Concluded. (i) NPR = 3.8, T = 68 lb.

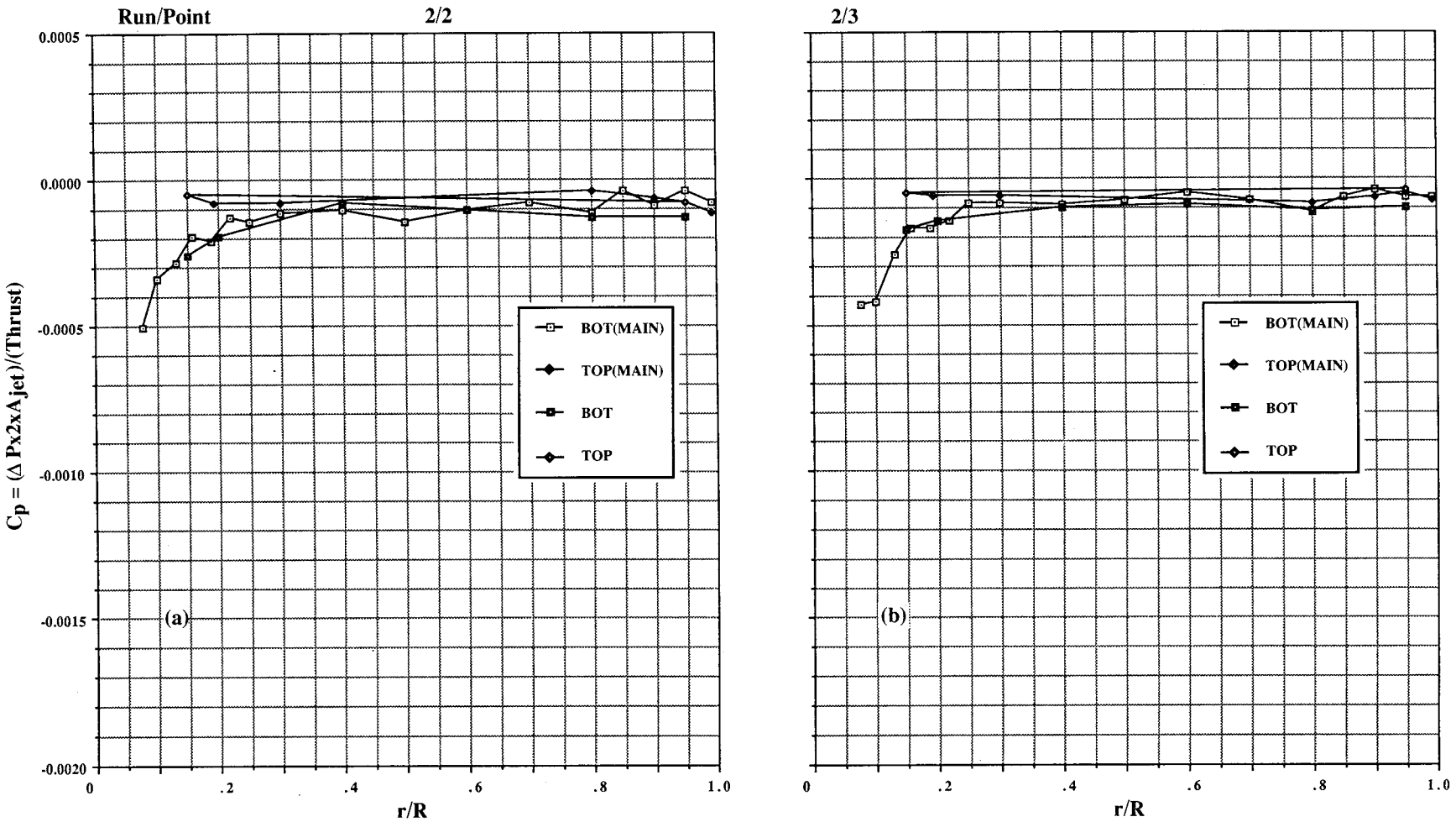

Figure 23. Pressures induced on 20-in. circular plate out of ground effect, large room. (a) NPR = 1.74, T = 21 lb, (b) NPR = 2.26, T = 33 lb.

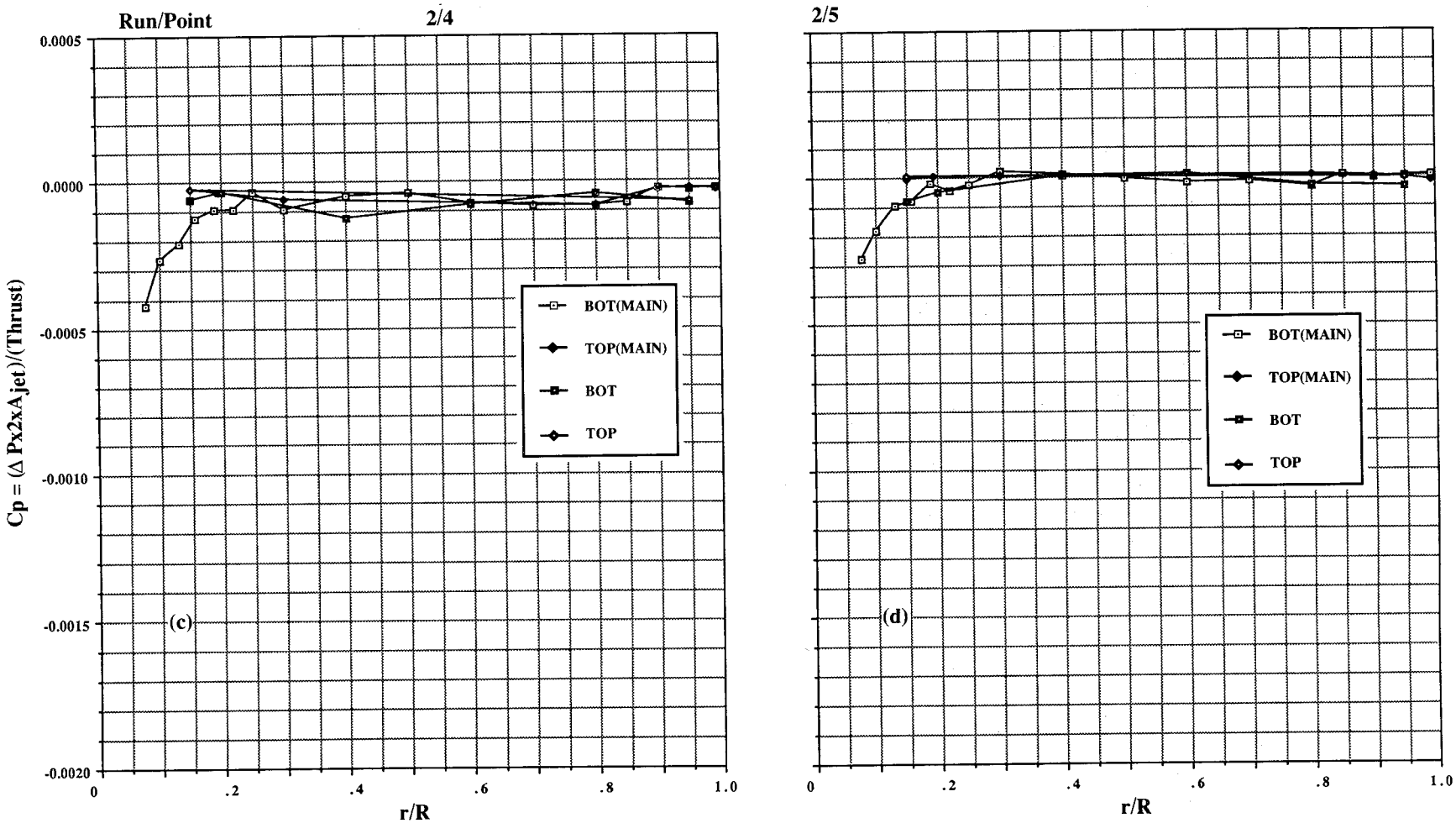

Figure 23. Continued. (c) NPR = 3.0, T = 48 lb, (d) NPR = 4.1, T = 74 lb.

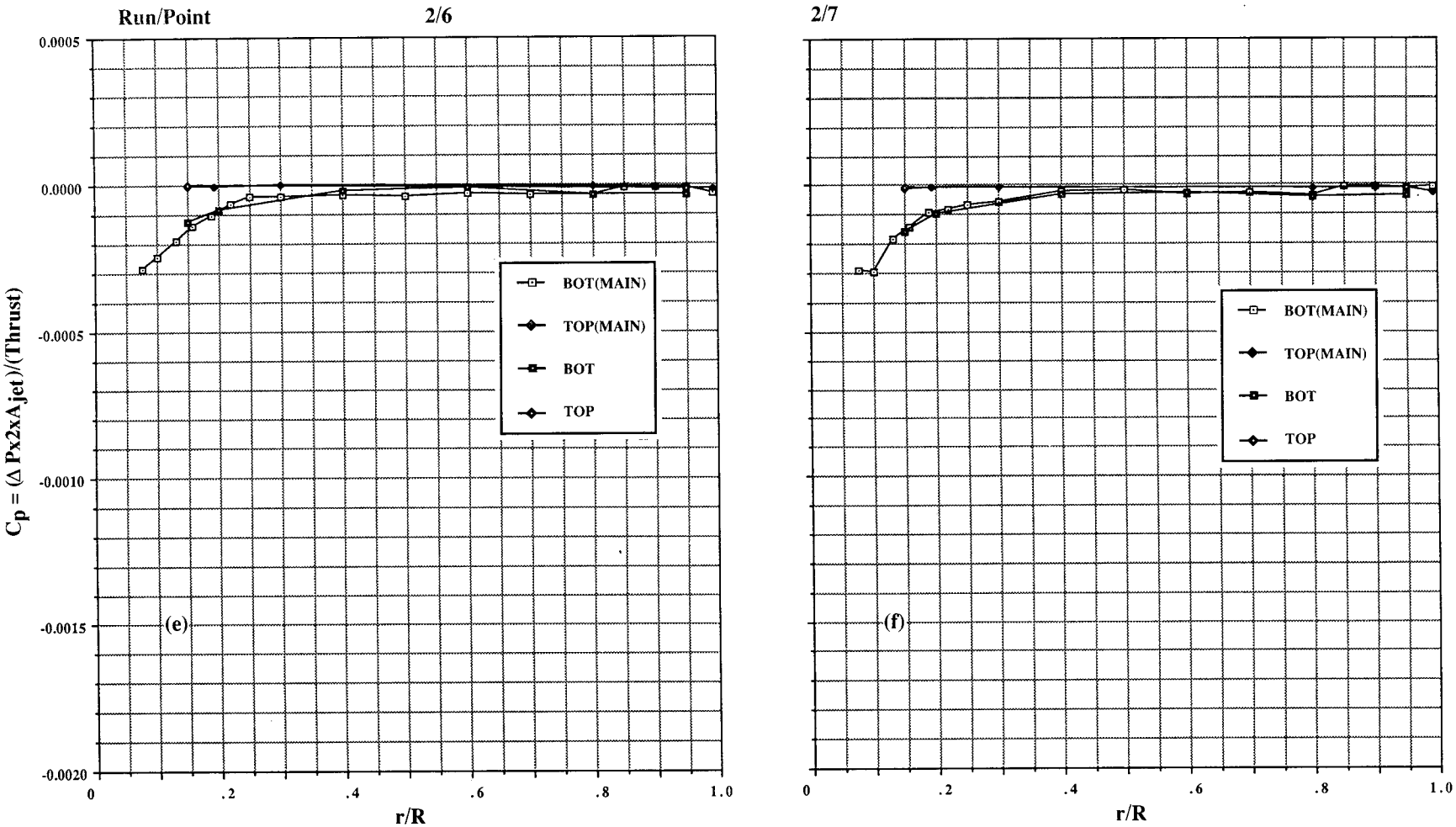

Figure 23. Concluded. (e) NPR = 5.2, T = 97 lb, (f) NPR = 5.8, T = 112 lb.

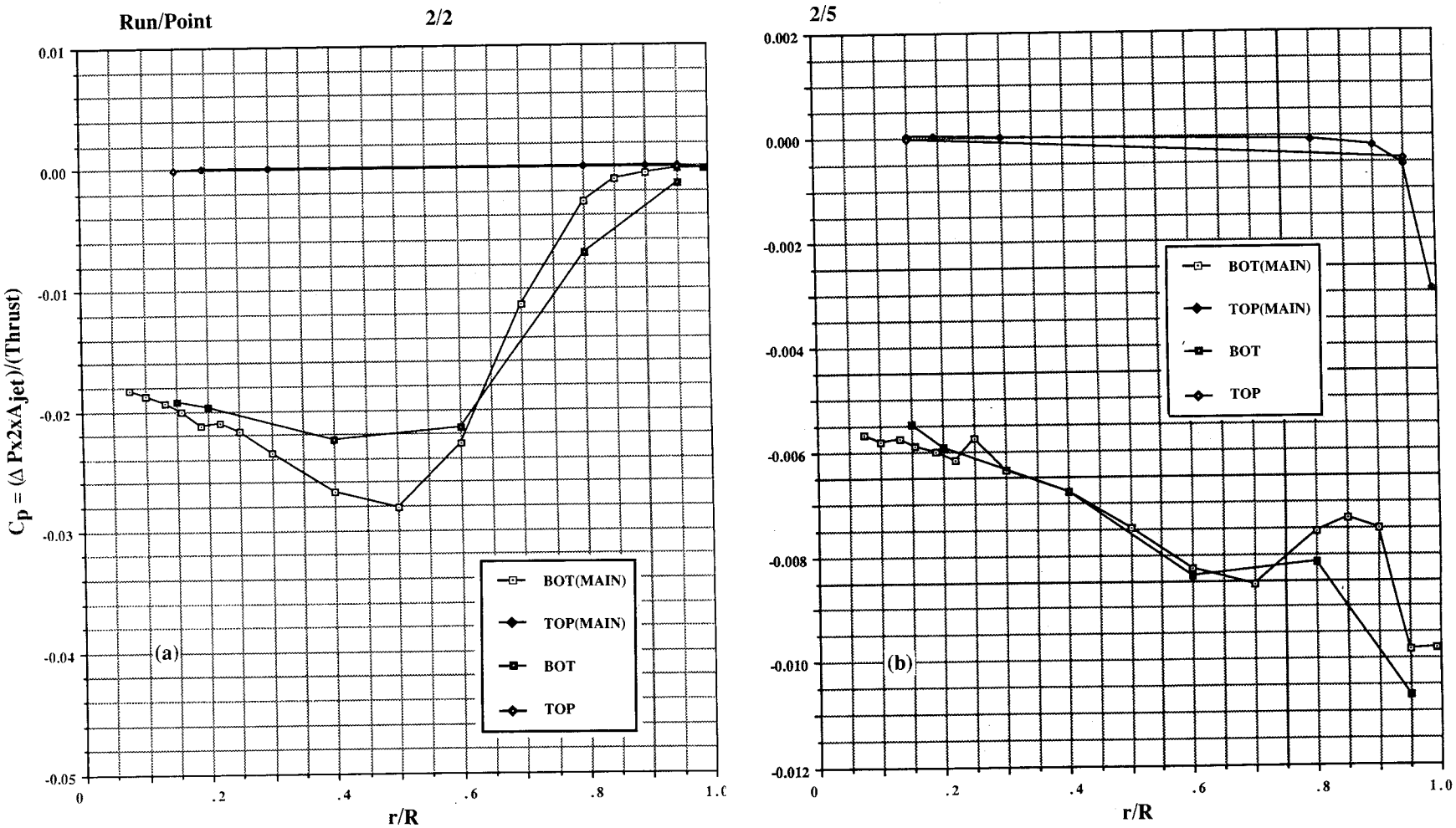

Figure 24. Pressures induced on 20-in. circular plate in ground effect, NPR = 1.5, T = 16 lb, large room. (a) $h/d_e = 1.6$, (b) $h/d_e = 2.4$.

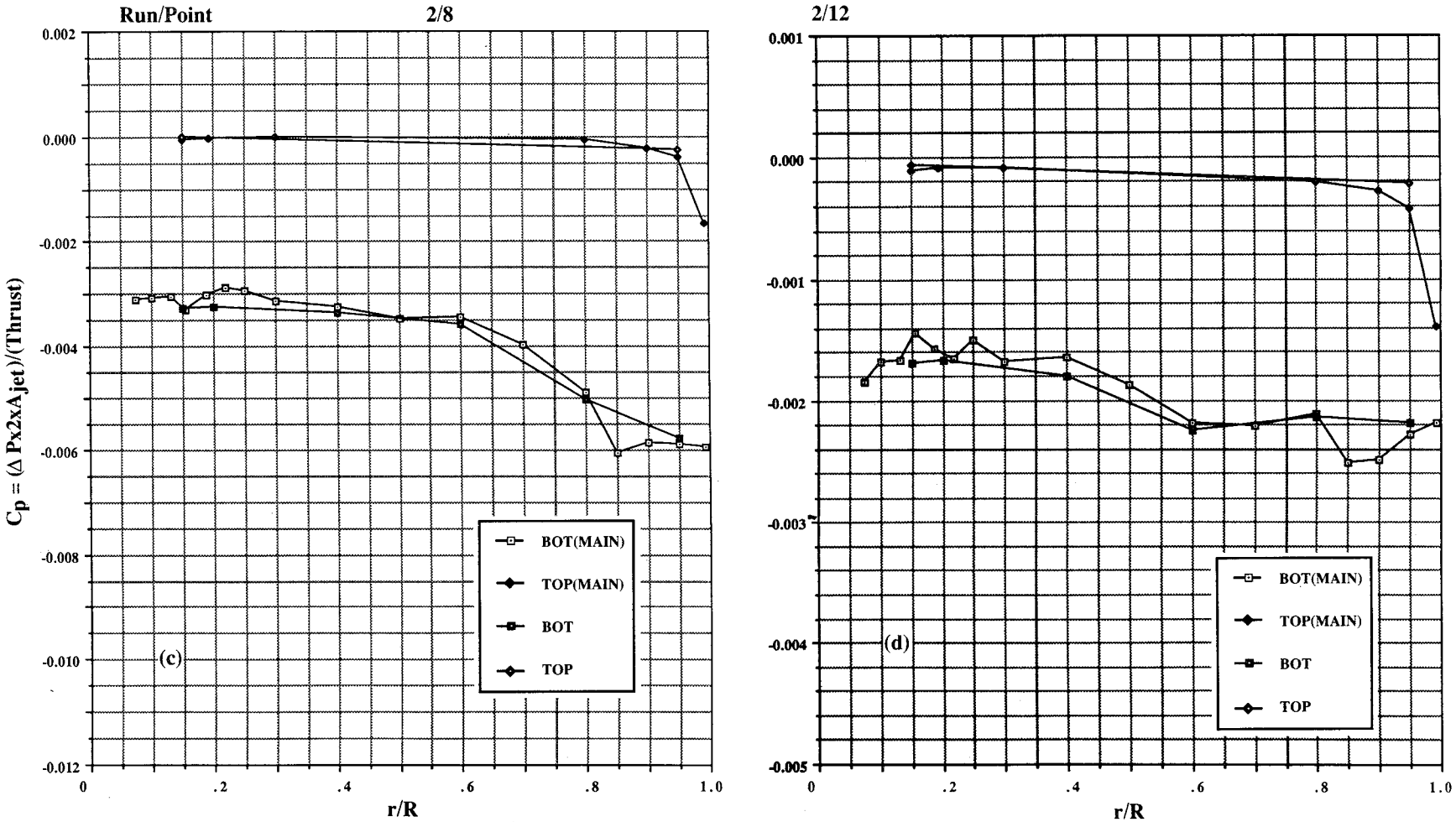

Figure 24. Continued. (c) $h/d_e = 3.3$, (d) $h/d_e = 4.9$.

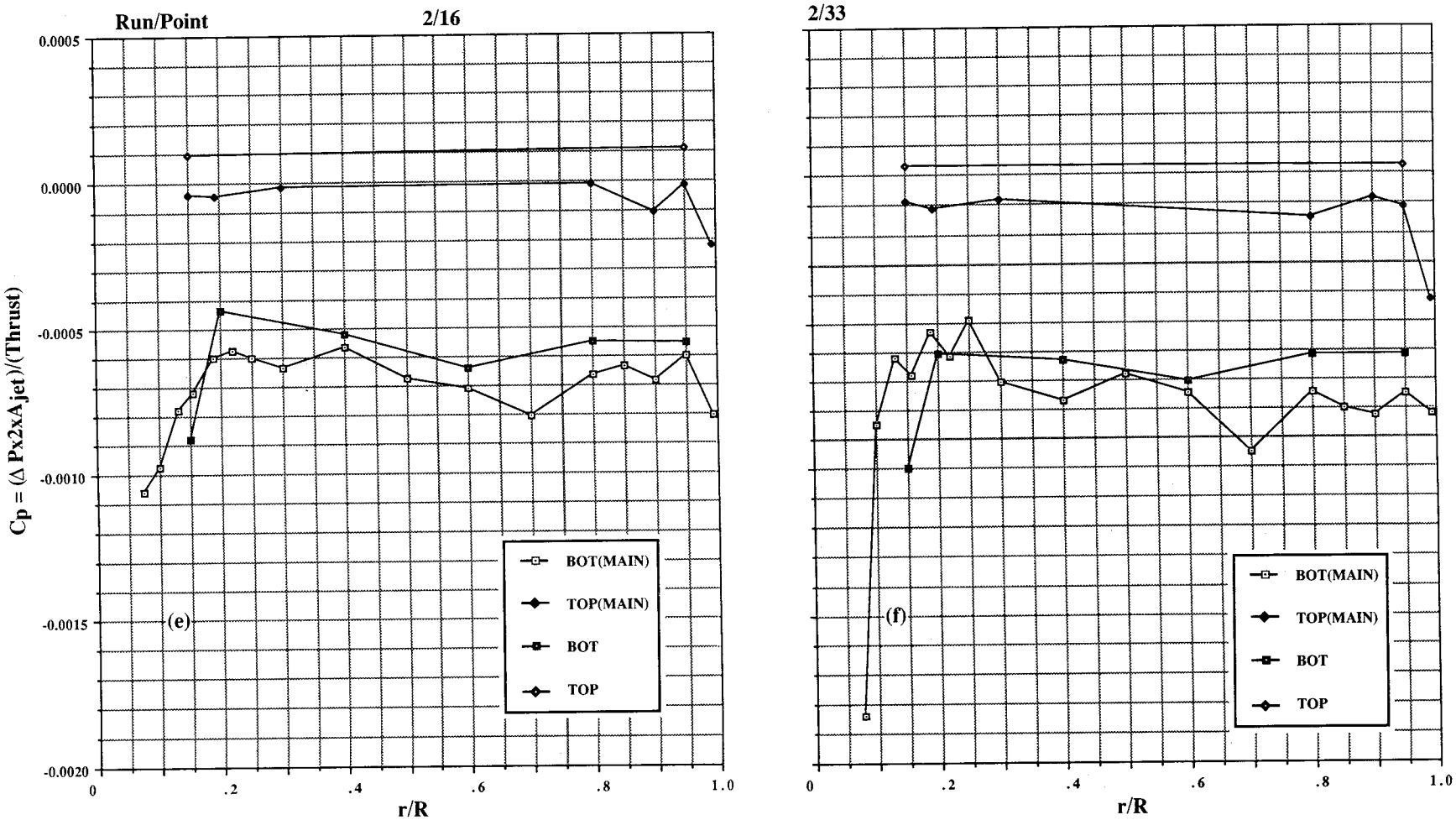

Figure 24. Continued. (e) $h/d_e = 8.1$, (f) $h/d_e = 8.1$ (gap sealed).

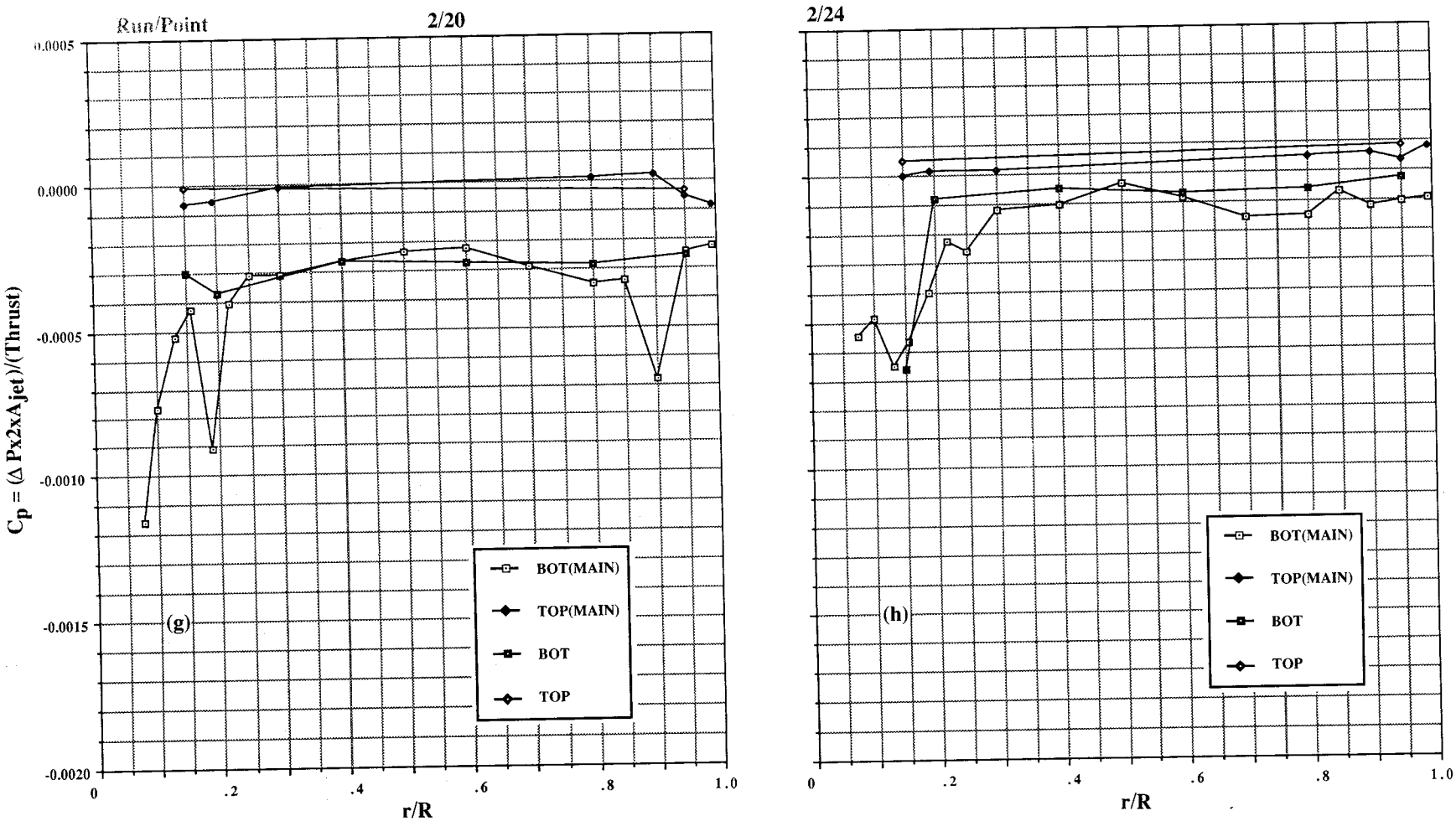

Figure 24. Continued. (g) $h/d_e = 12.2$, (h) $h/d_e = 16.3$.

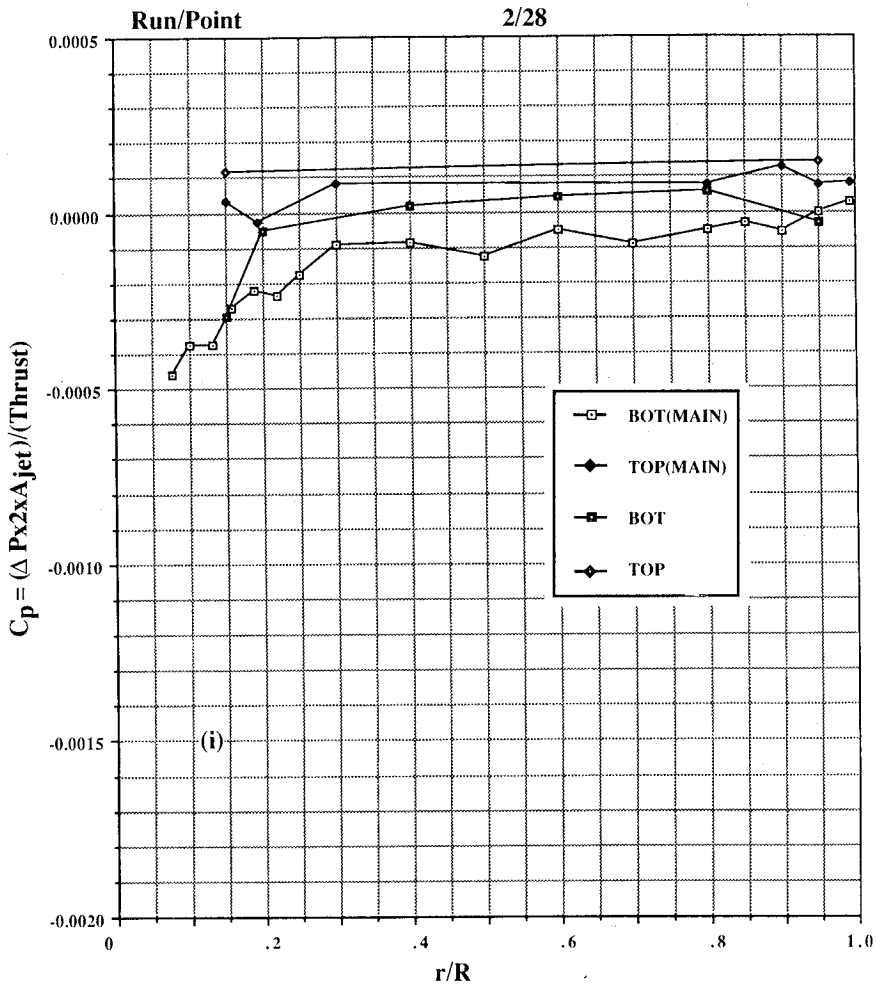

Figure 24. Concluded. (i) $h/d_e = 24.4$.

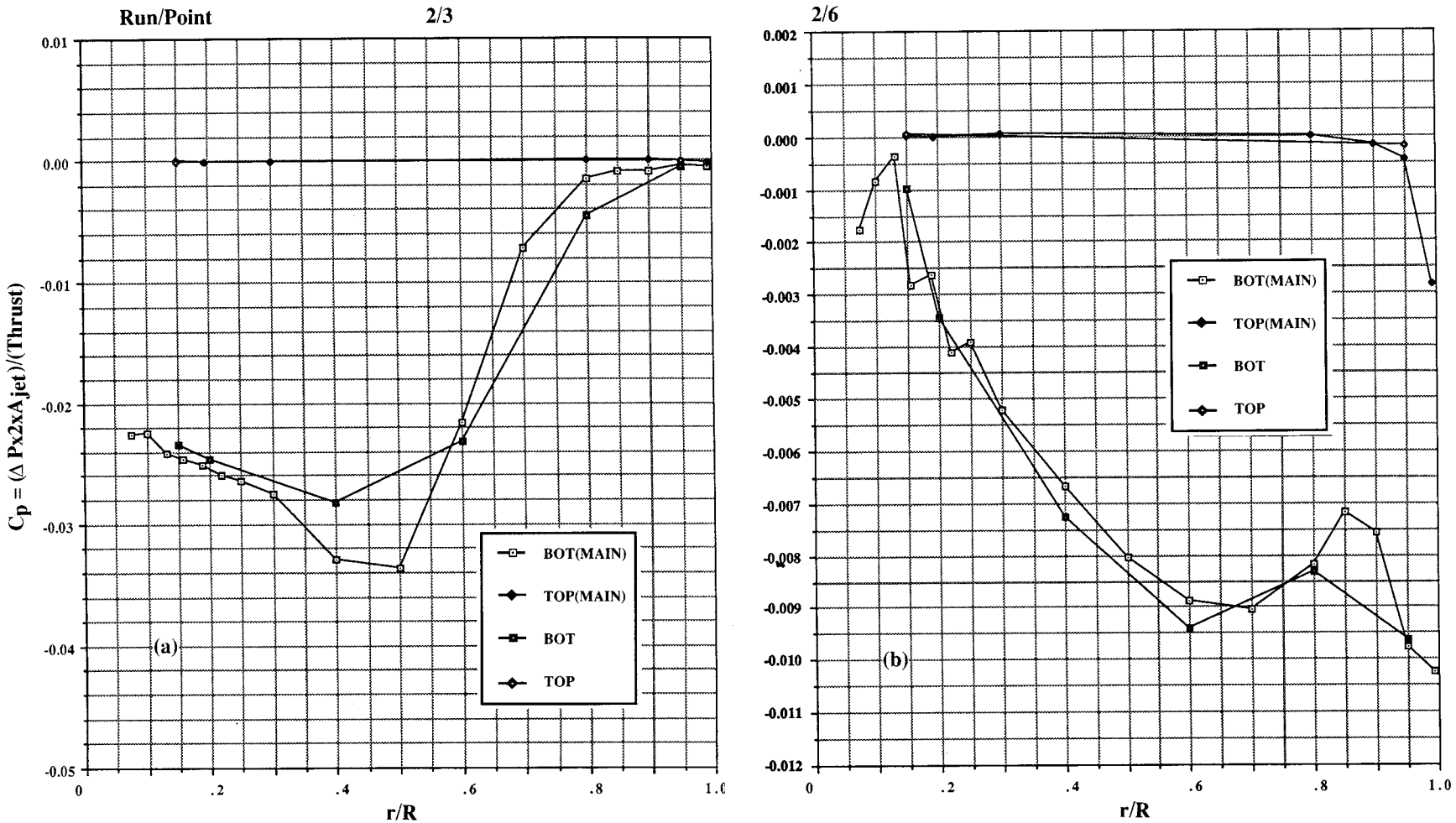

Figure 25. Pressures induced on 20-in. circular plate in ground effect, NPR = 2.0, T = 29 lb, large room. (a) $h/d_e = 1.6$, (b) $h/d_e = 2.4$.

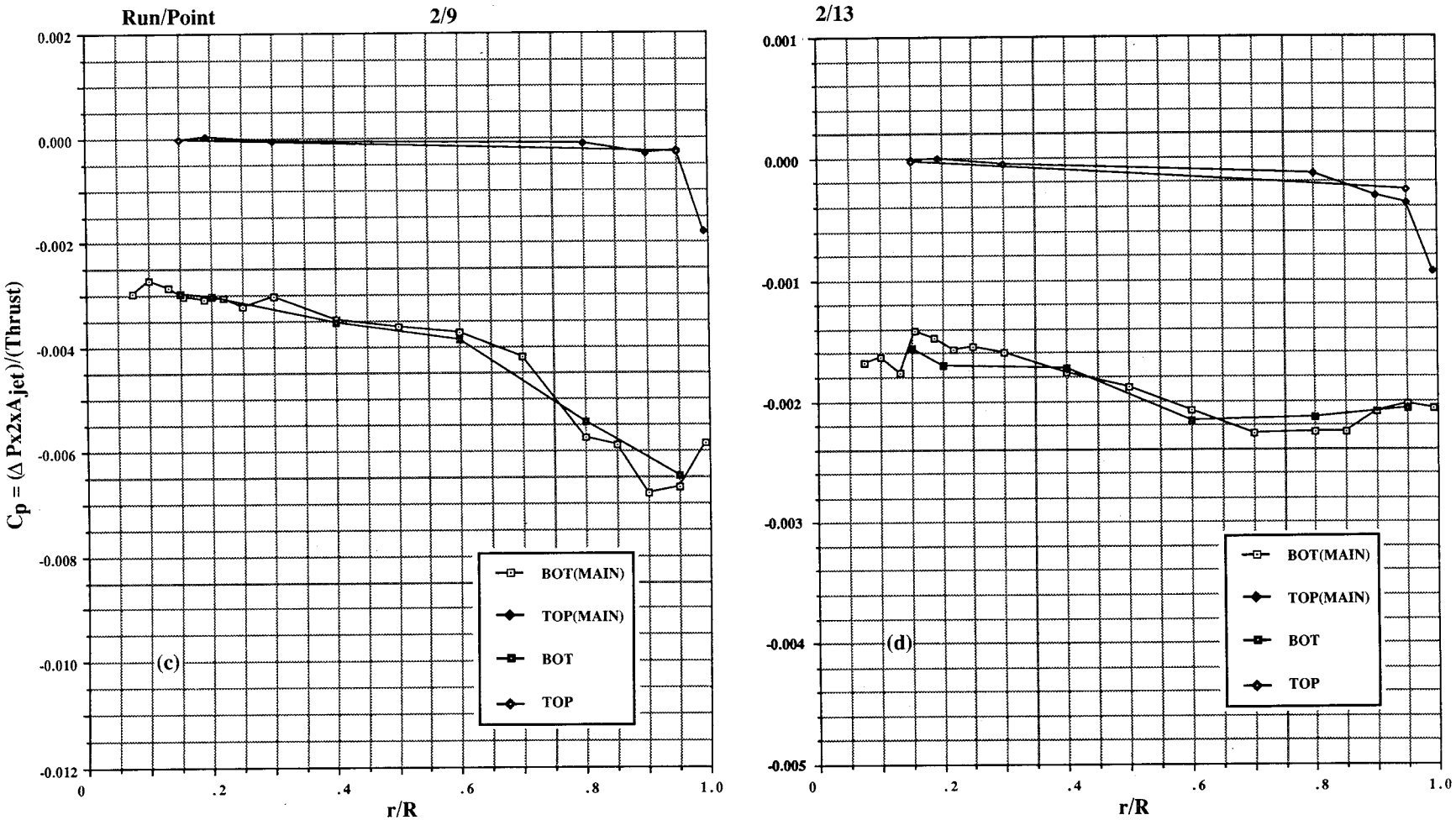

Figure 25. Continued. (c) $h/d_e = 3.3$, (d) $h/d_e = 4.9$.

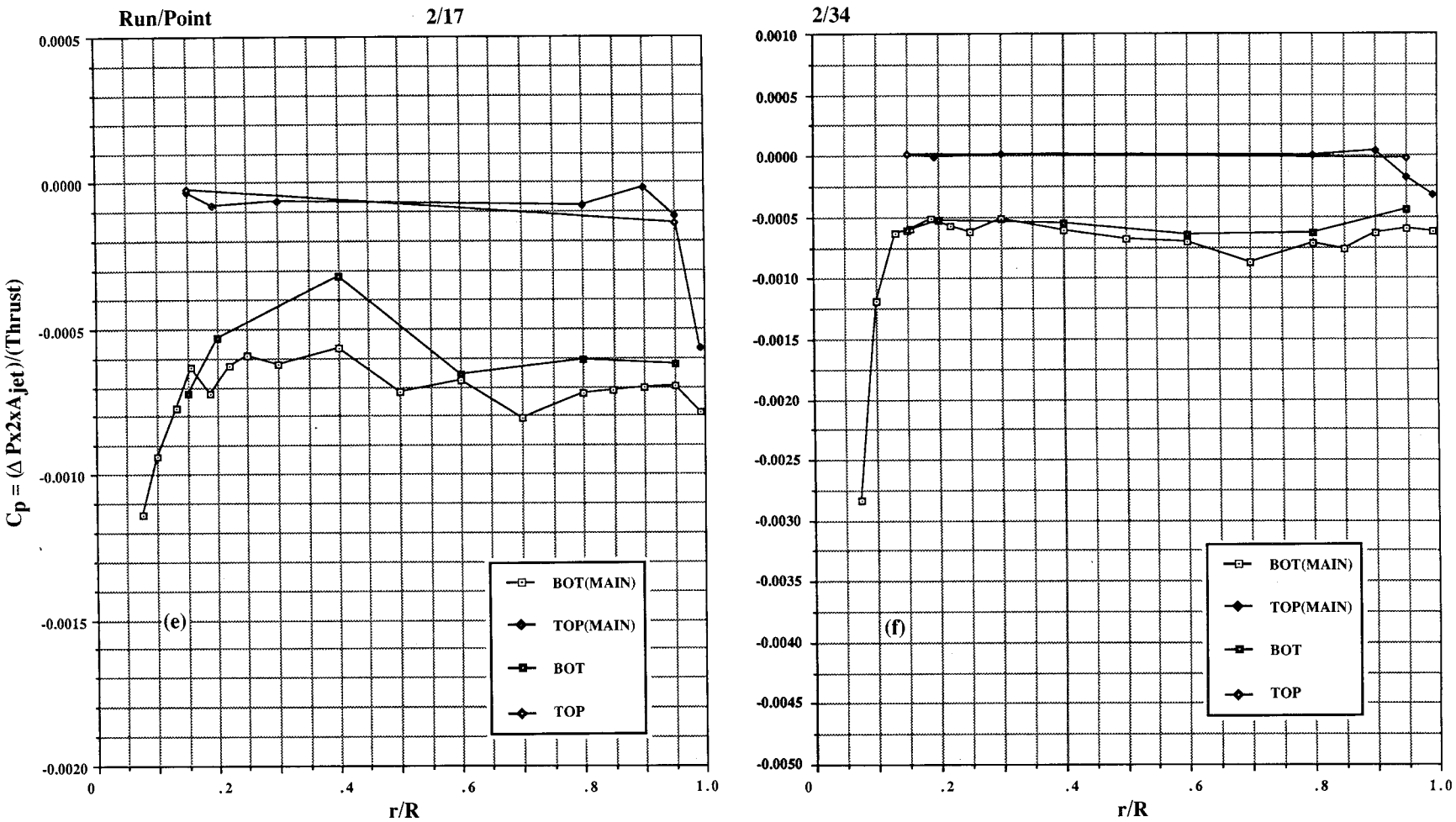

Figure 25. Continued. (e) $h/d_e = 8.1$, (f) $h/d_e = 8.1$ (gap sealed).

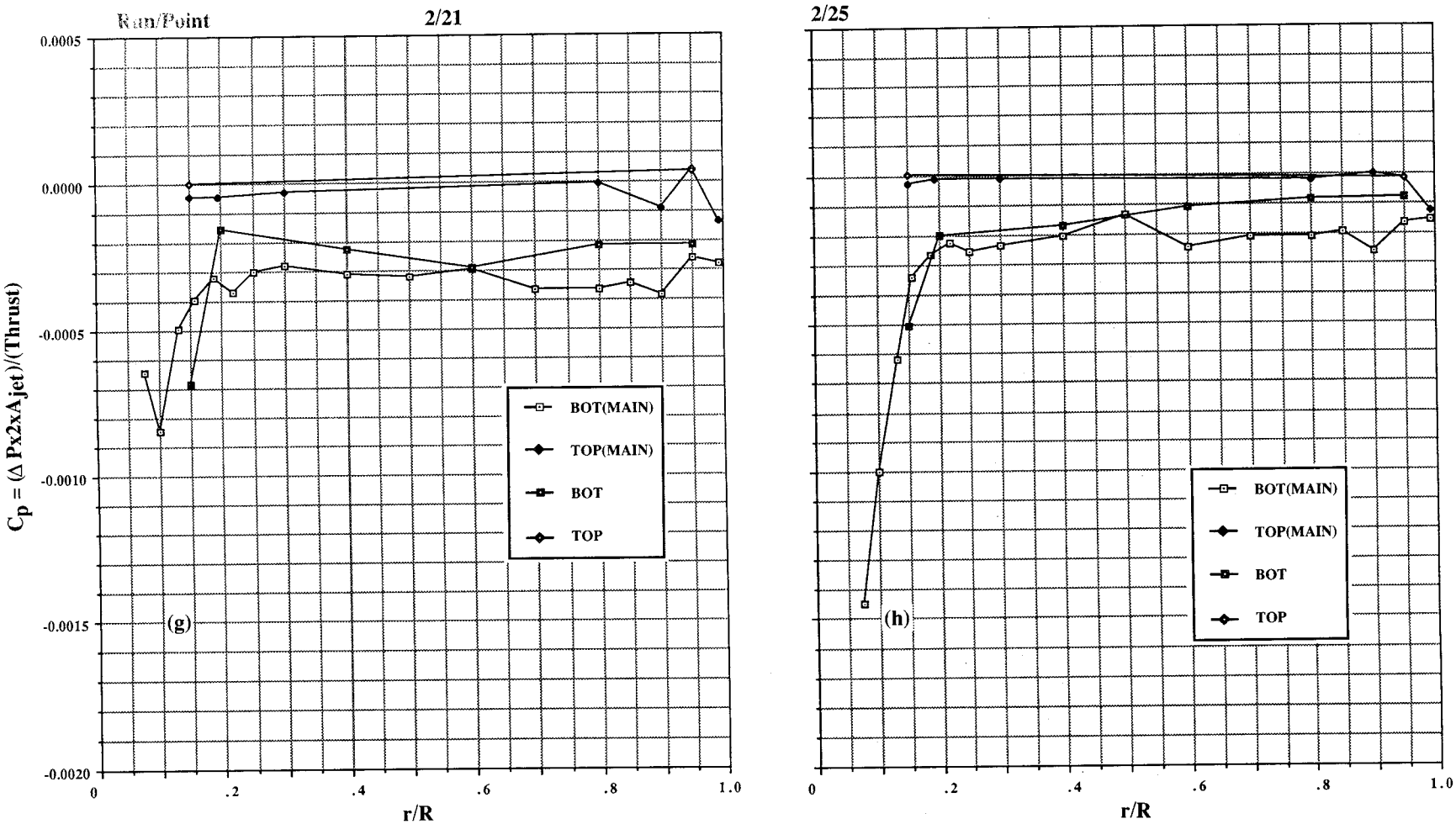

Figure 25. Continued. (g) $h/d_e = 12.2$, (h) $h/d_e = 16.3$.

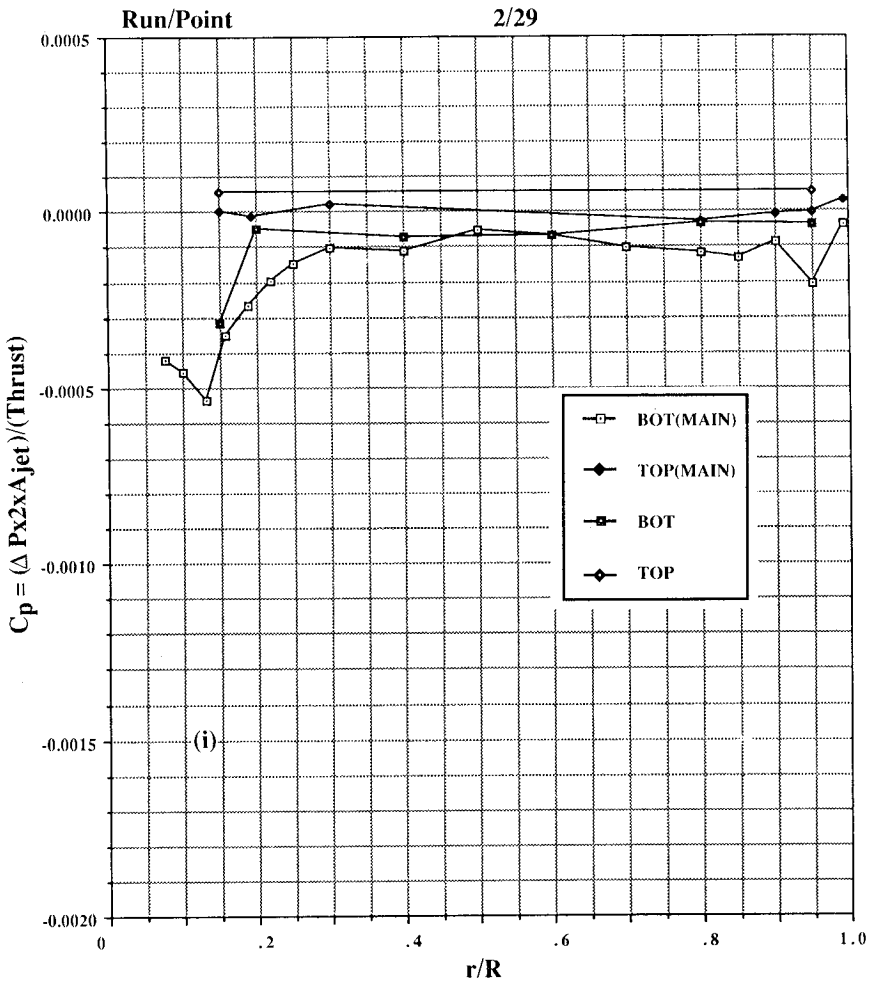

Figure 25. Concluded. (i) $h/d_e = 24.4$.

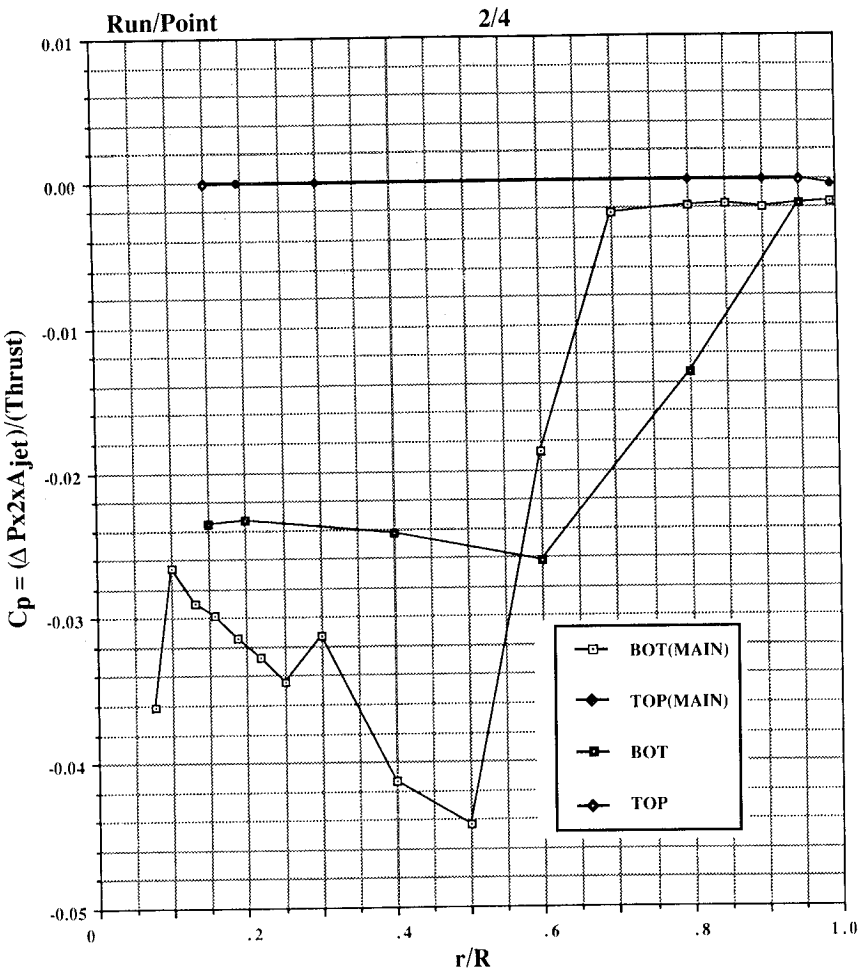

Figure 26. Pressures induced on 20-in. circular plate in ground effect, NPR = 2.6, T = 40 lb, h/d_e = 1.6, large room.

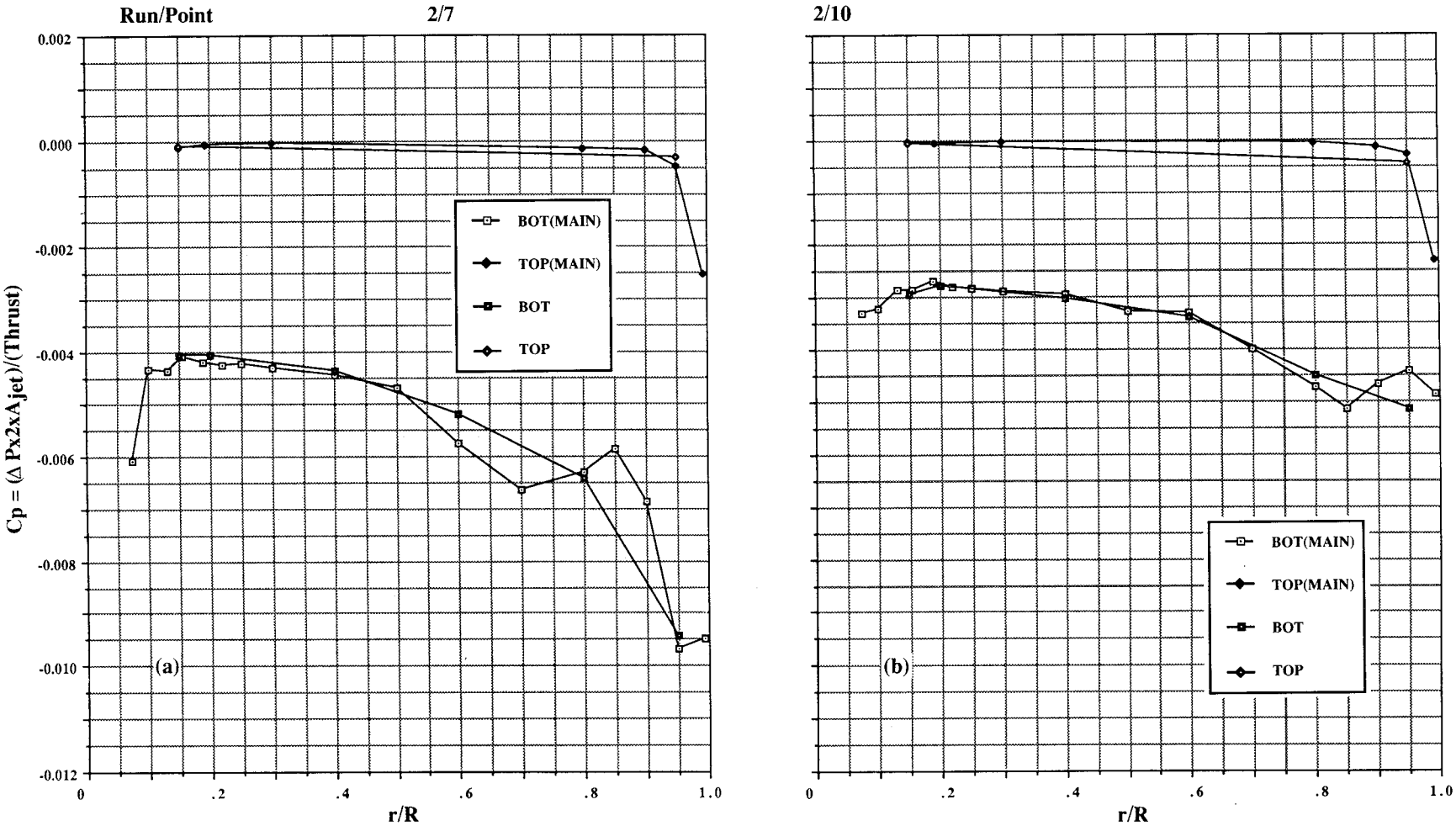

Figure 27. Pressures induced on 20-in. circular plate in ground effect, NPR = 4.0, T = 72 lb, large room. (a) $h/d_e = 2.4$, (b) $h/d_e = 3.3$.

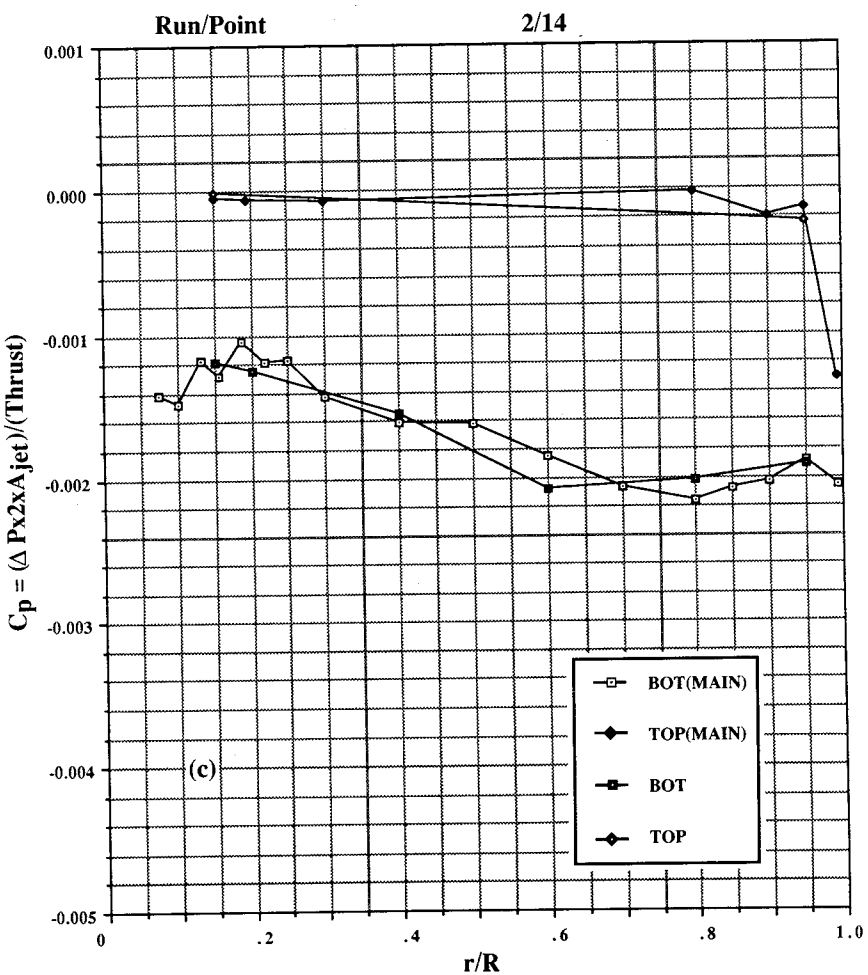

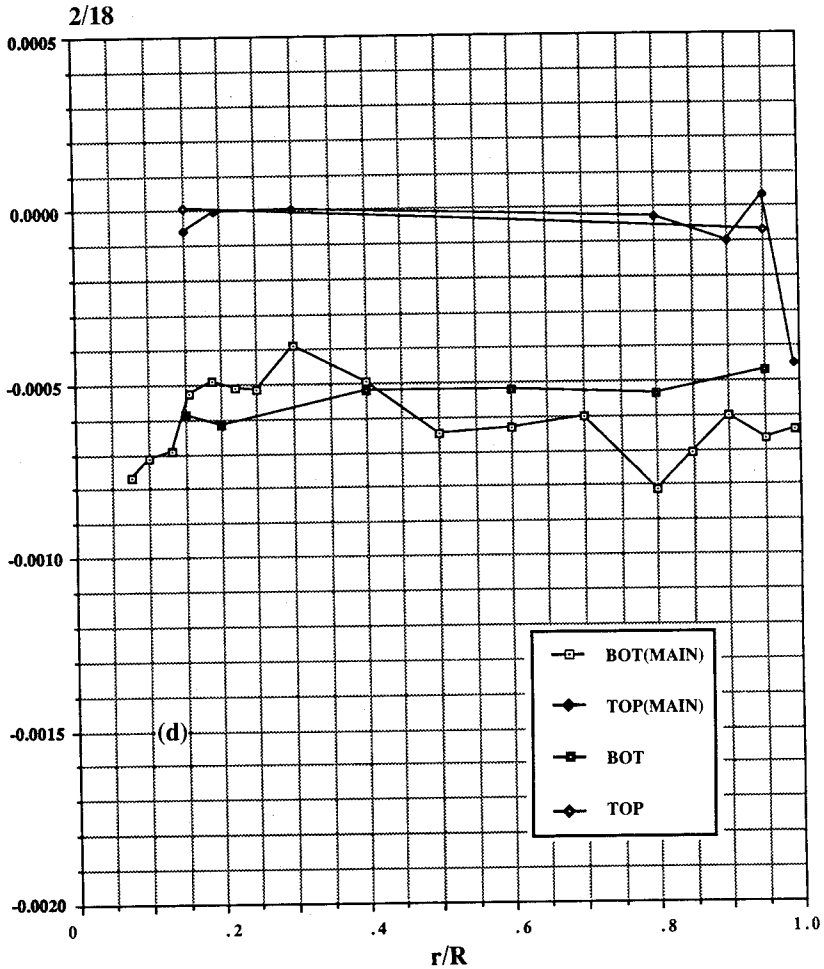

Figure 27. Continued. (c) $h/d_e = 4.9$, (d) $h/d_e = 8.1$.

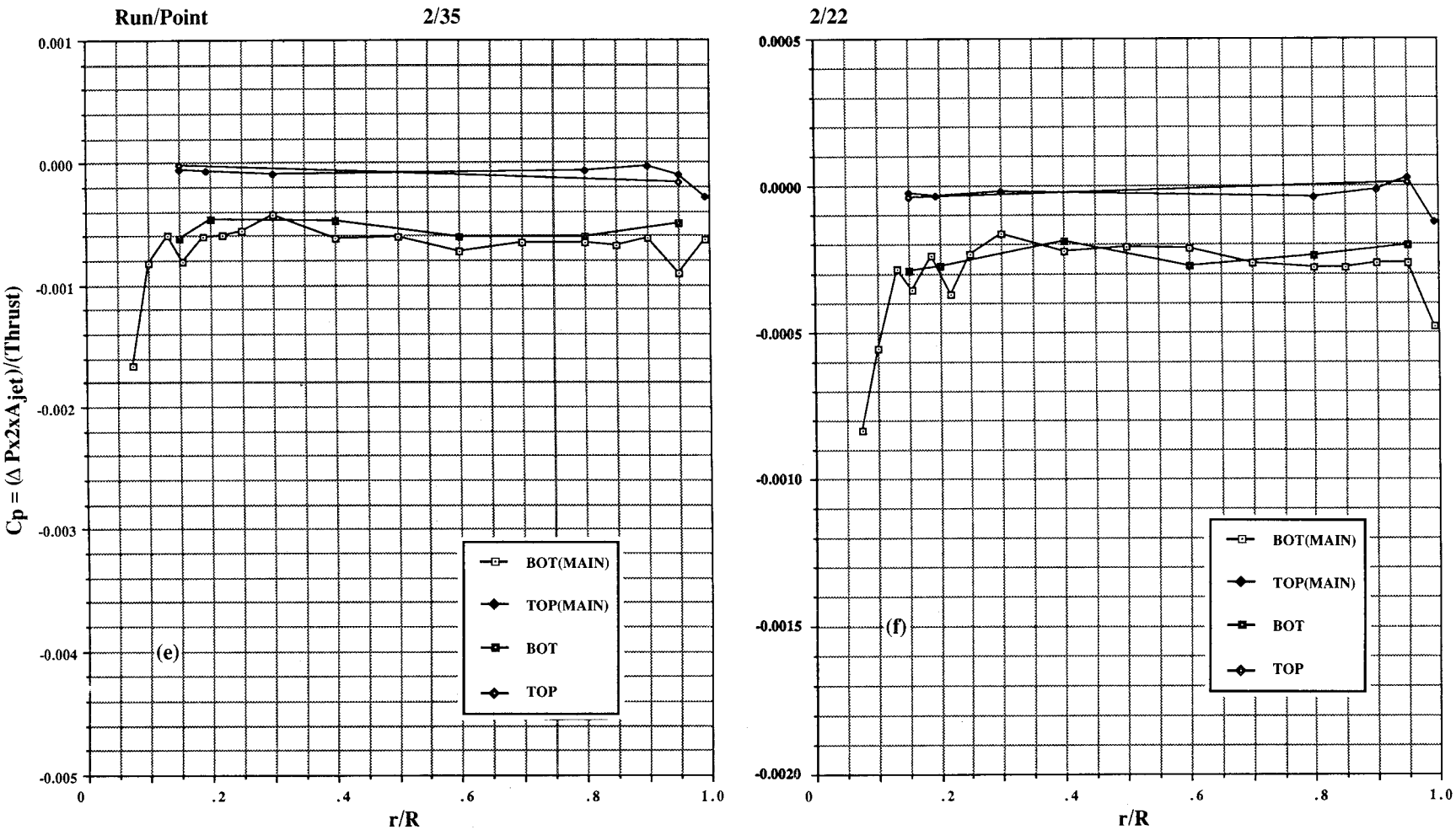

Figure 27. Continued. (e) $h/d_e = 8.1$ (gap sealed), (f) $h/d_e = 12.2$.

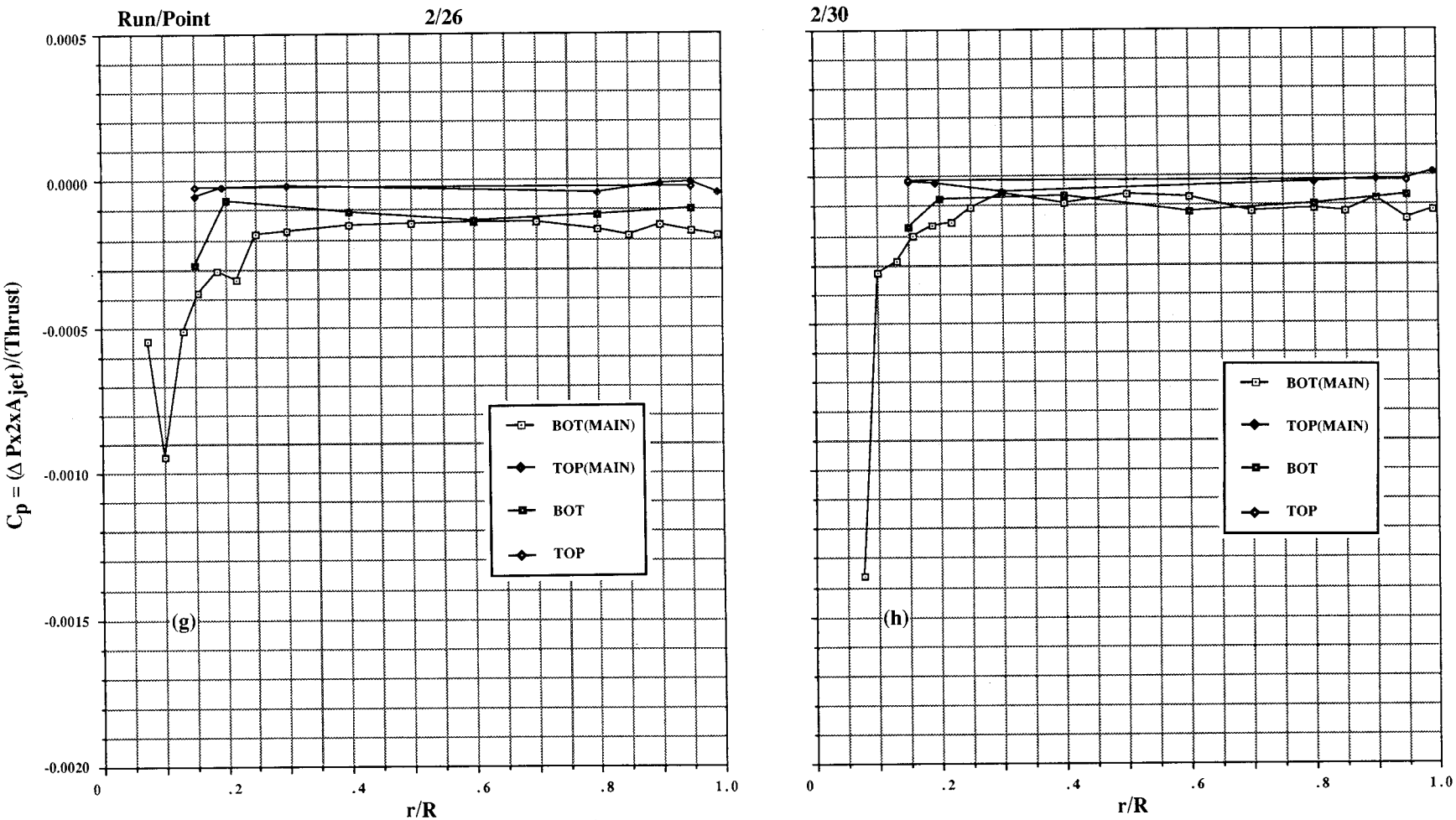

Figure 27. Concluded. (g) $h/d_e = 16.3$, (h) $h/d_e = 24.4$.

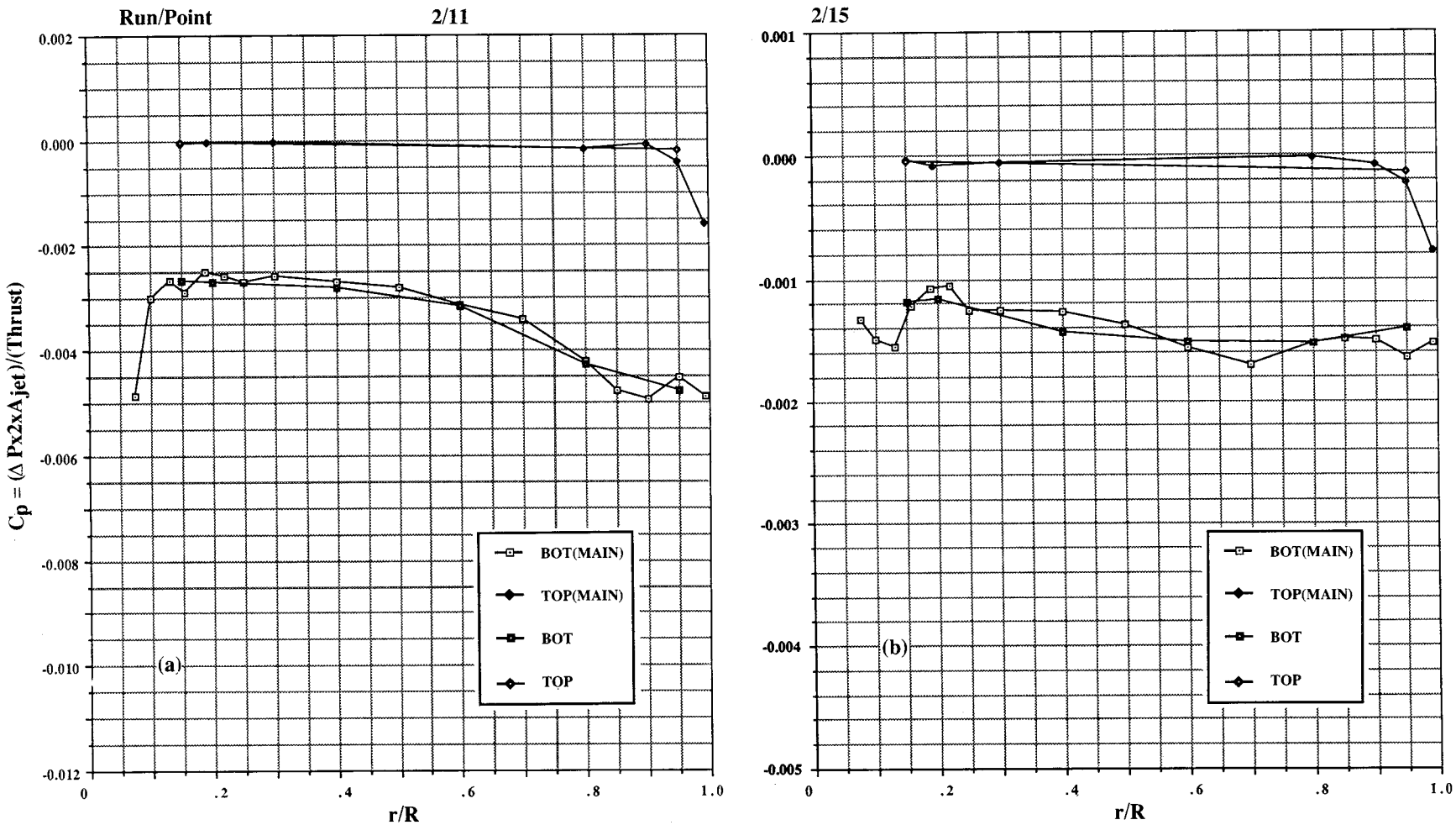

Figure 28. Pressures induced on 20-in. circular plate in ground effect, NPR = 6.0, T = 116 lb, large room. (a) $h/d_e = 3.3$, (b) $h/d_e = 4.9$.

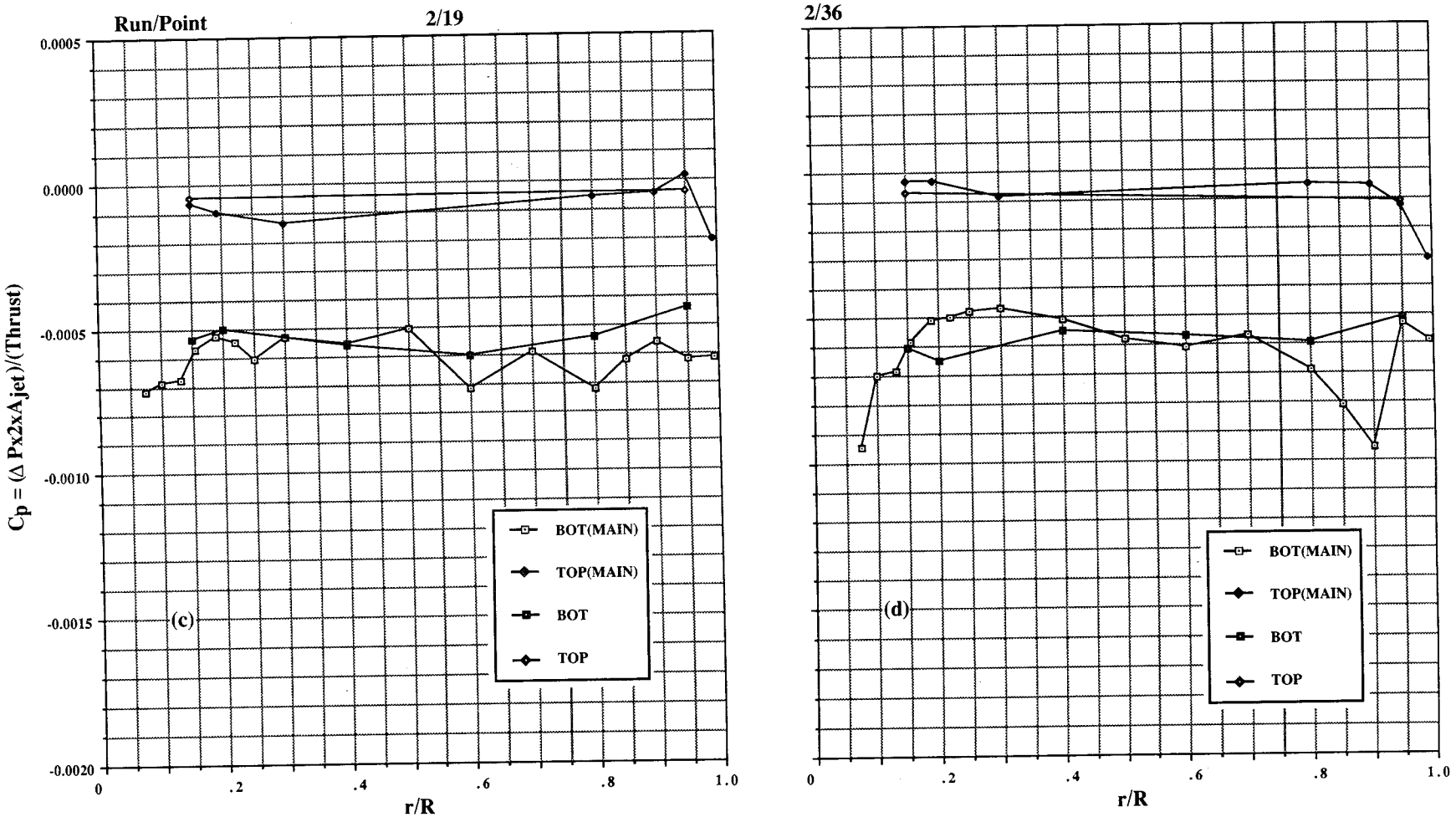

Figure 28. Continued. (c) $h/d_e = 8.1$, (d) $h/d_e = 8.1$ (gap sealed).

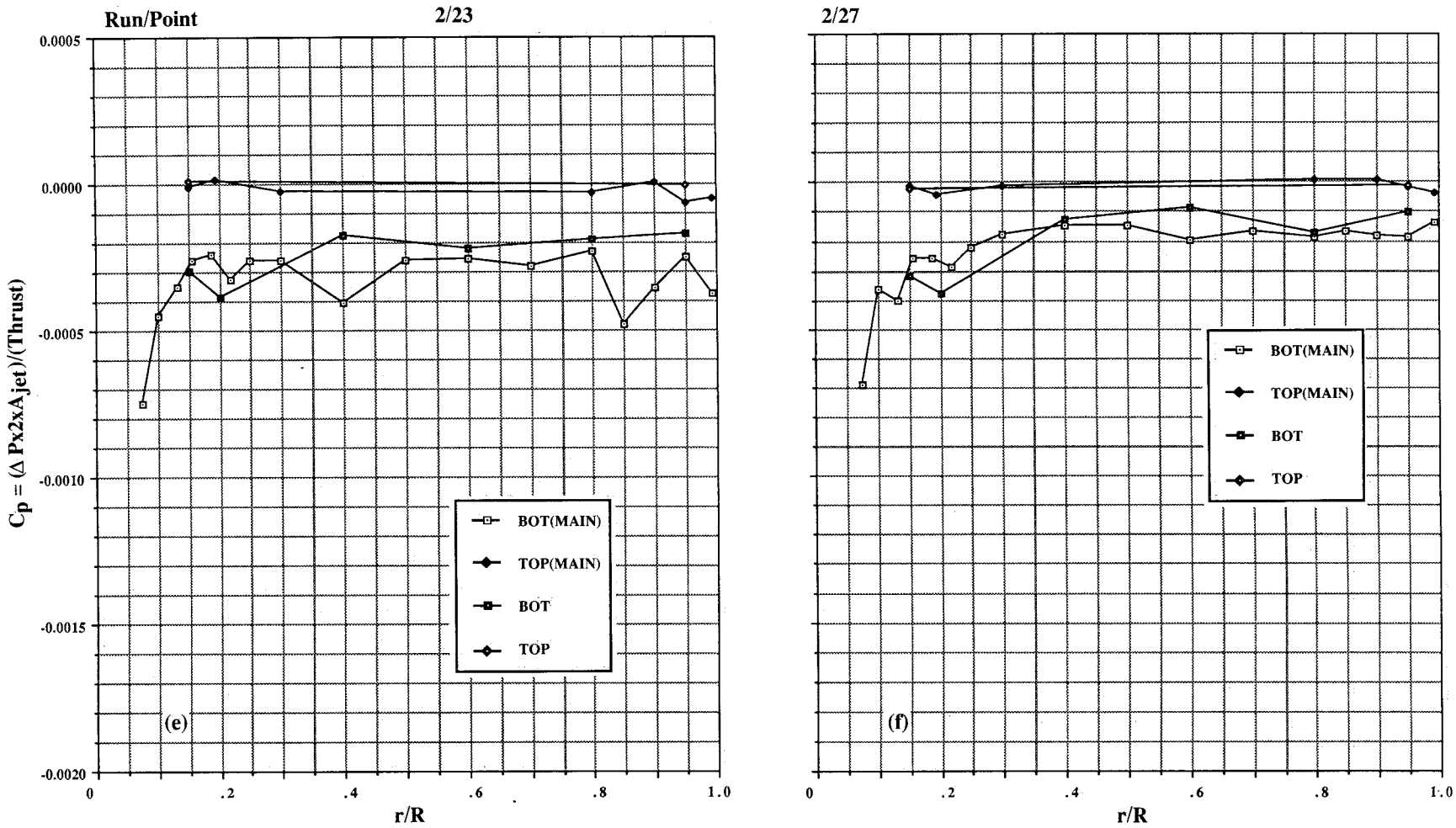

Figure 28. Continued. (e) $h/d_e = 12.2$, (f) $h/d_e = 16.3$.

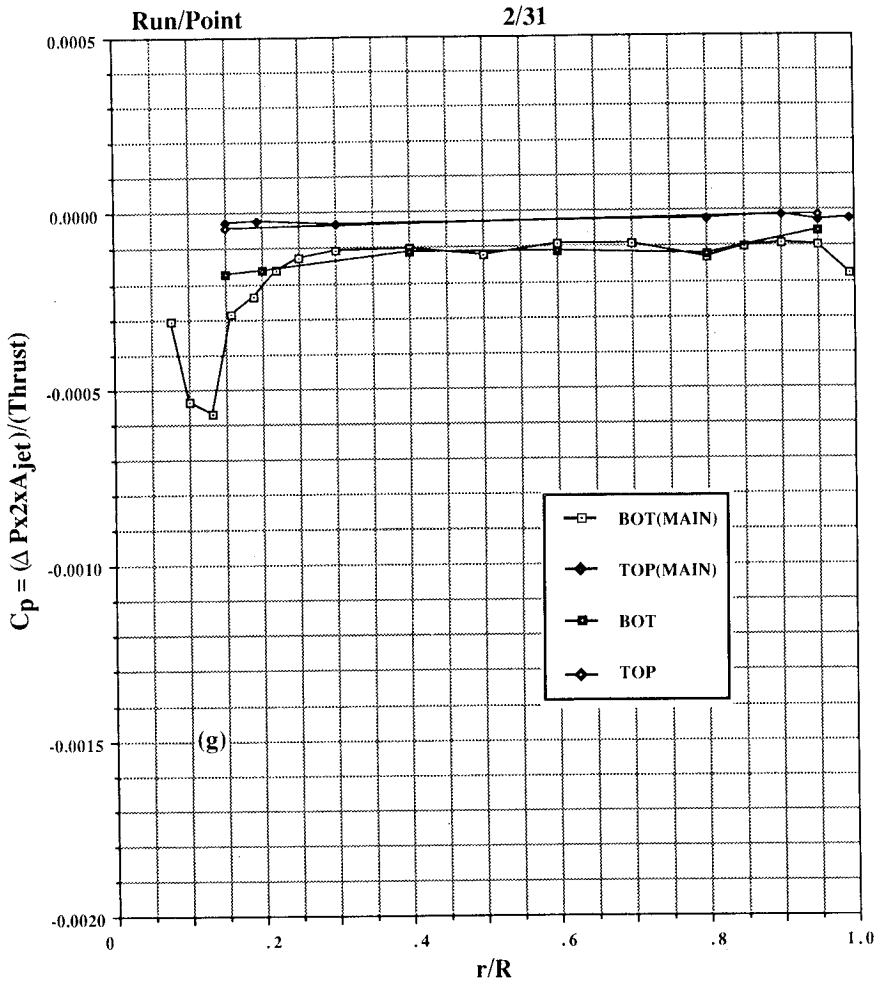

Figure 28. Concluded. (g) $h/d_e = 24.4$.

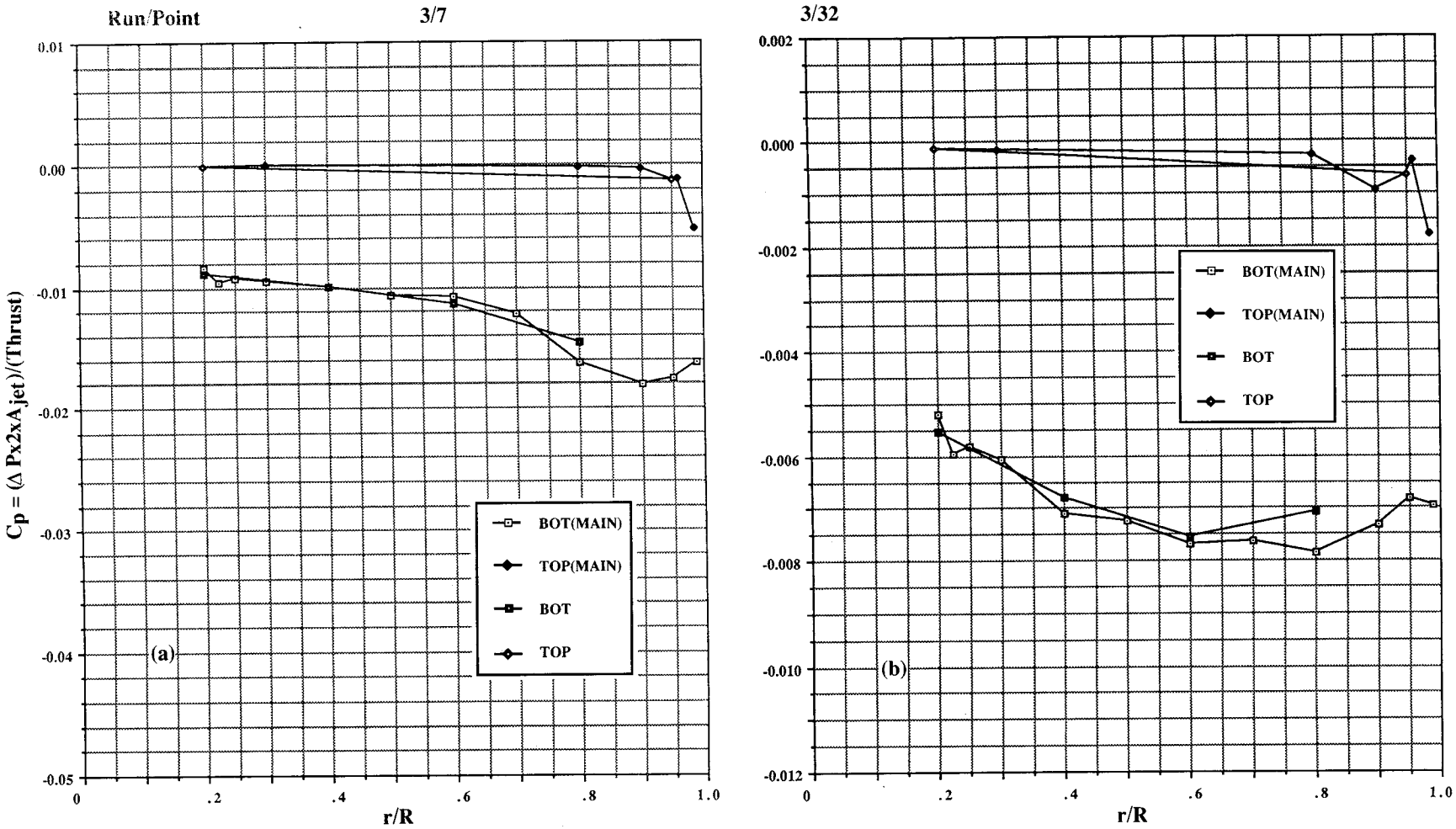

Figure 29. Pressures induced on 10-in. circular plate in ground effect, NPR = 1.5, T = 16 lb, large room. (a) $h/d_e = 1.6$, (b) $h/d_e = 2.4$.

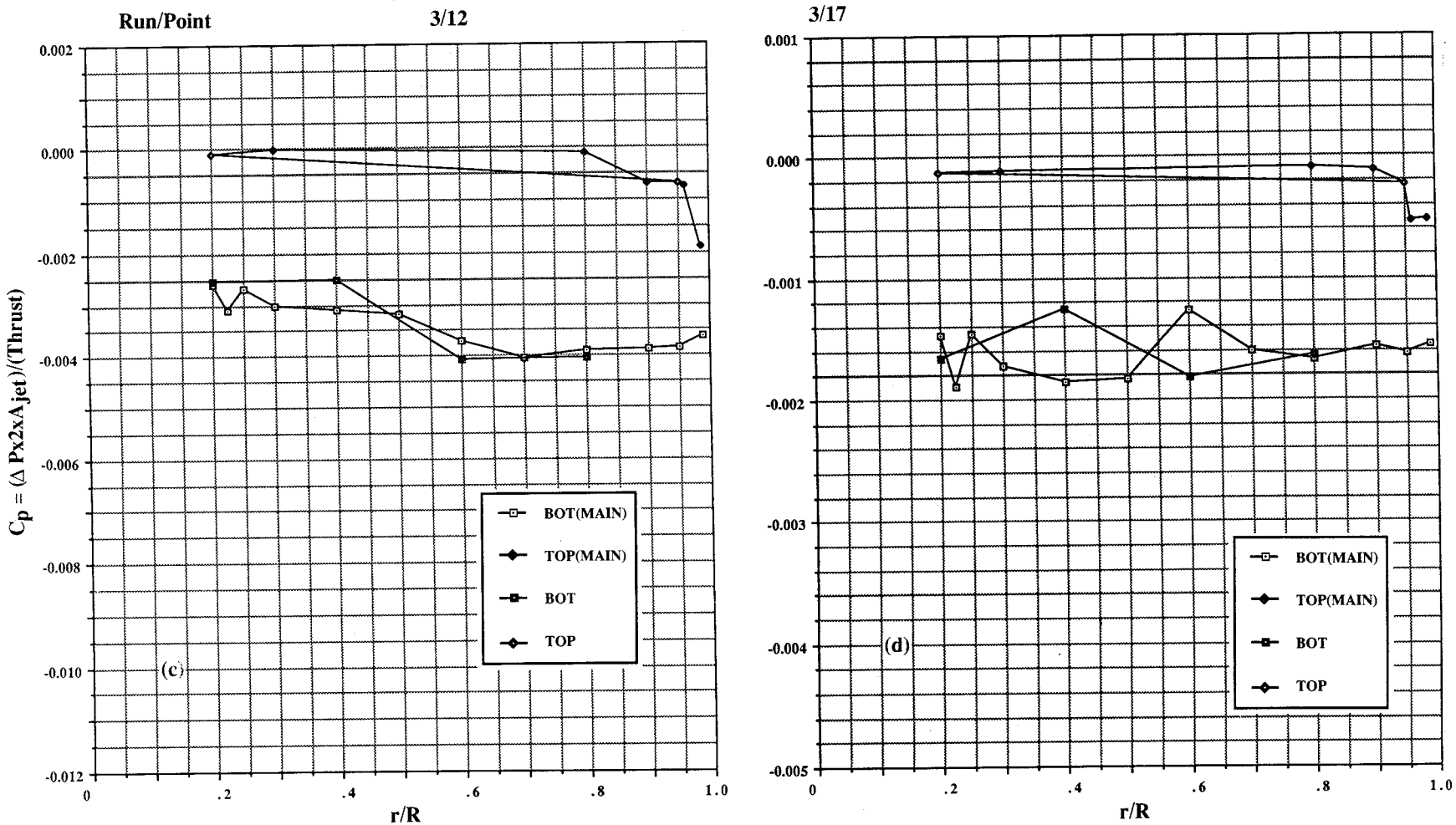

Figure 29. Continued. (c) $h/d_e = 3.3$, (d) $h/d_e = 4.9$.

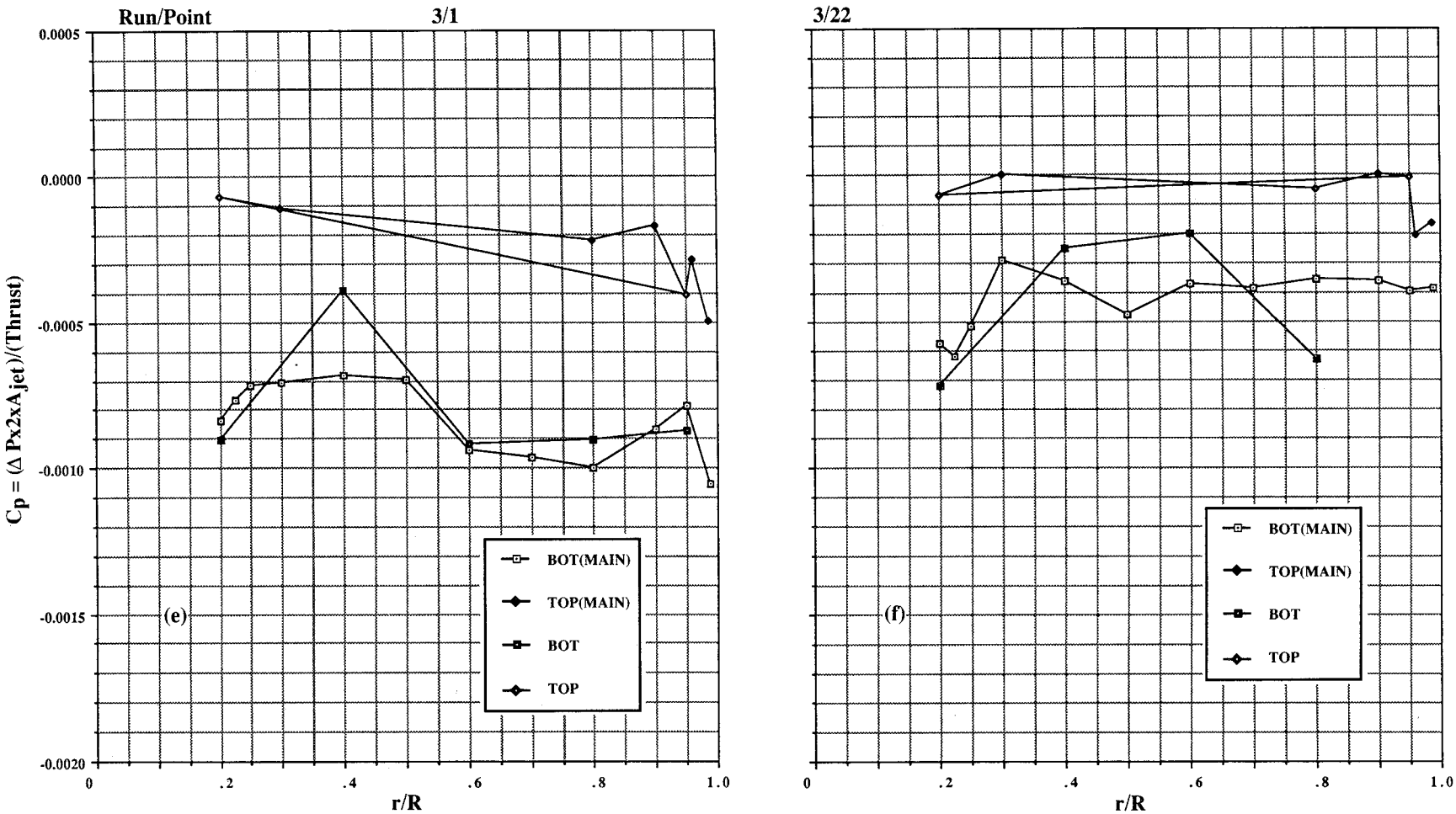

Figure 29. Continued. (e) $h/d_e = 8.1$, (f) $h/d_e = 12.2$.

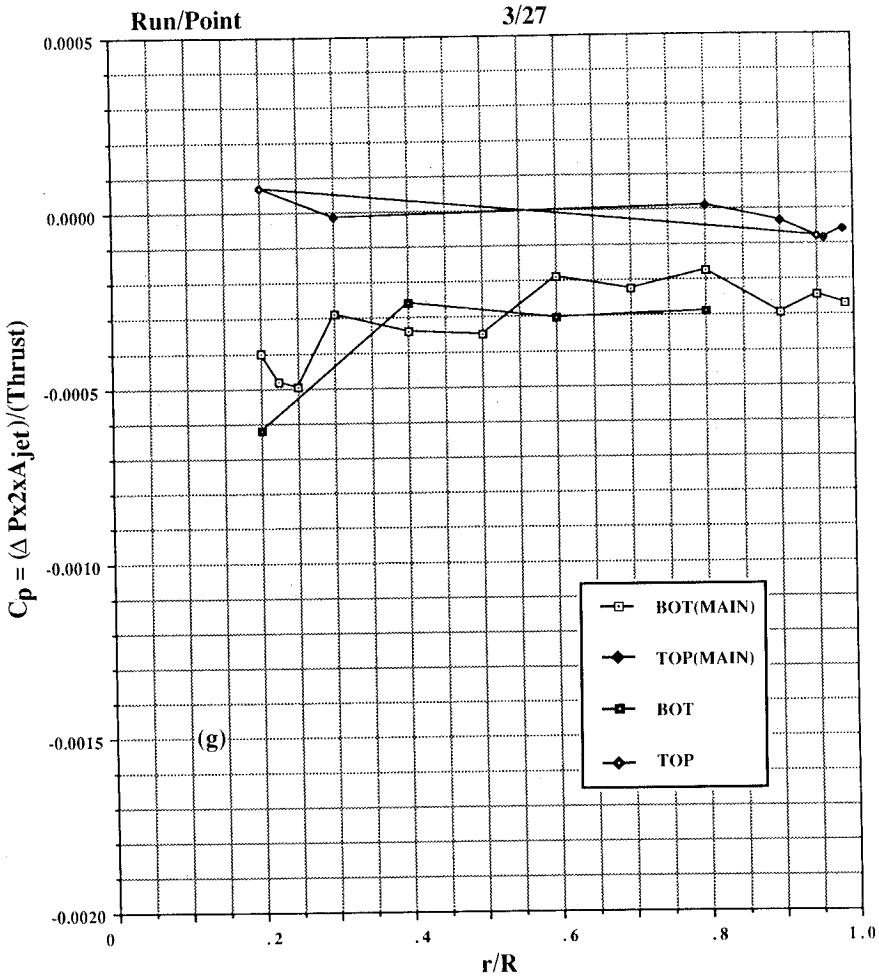

Figure 29. Concluded. (g) $h/d_e = 16.3$.

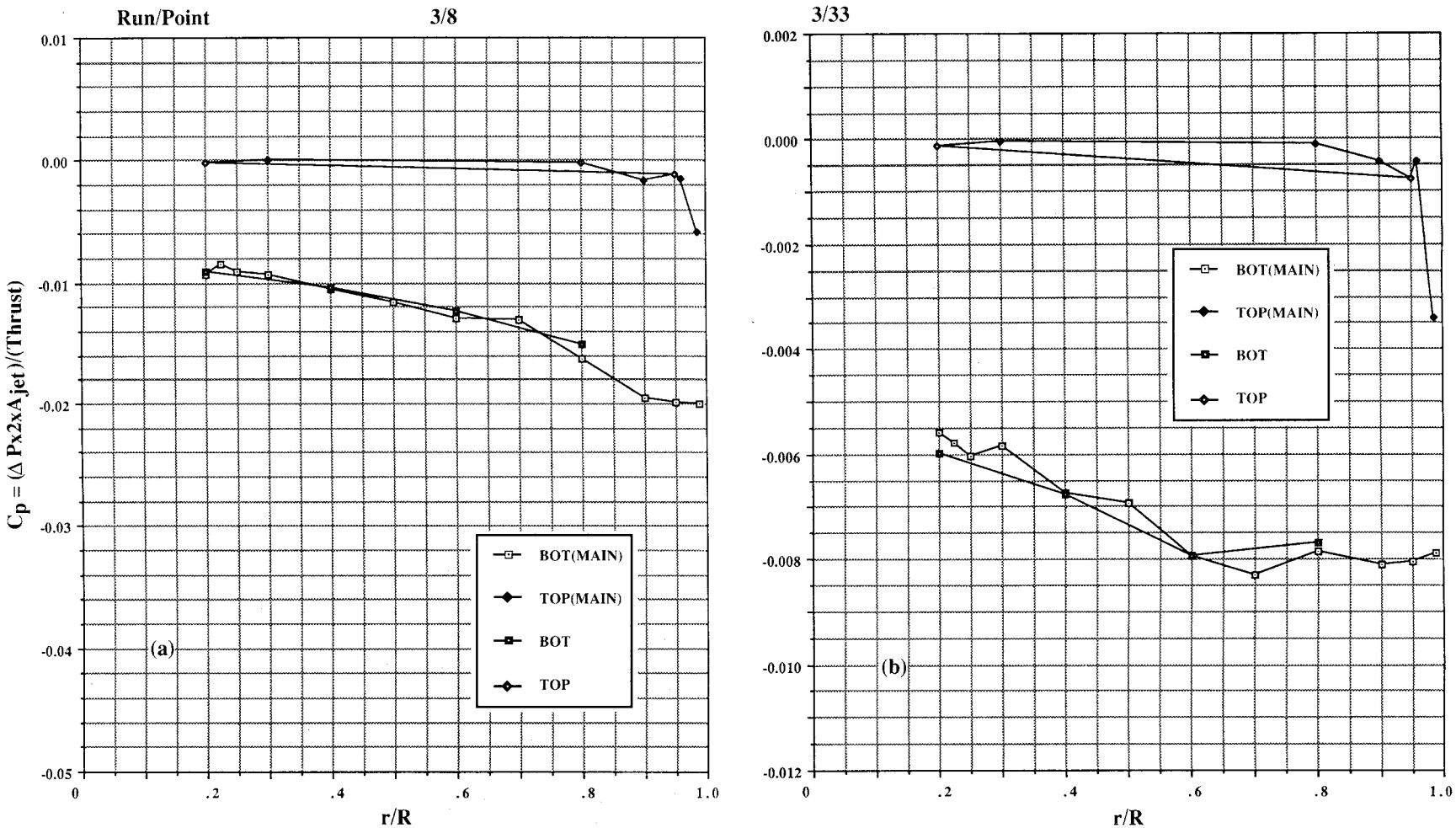

Figure 30. Pressures induced on 10-in. circular plate in ground effect, NPR = 2.0, T = 26 lb, large room. (a) $h/d_e = 1.6$, (b) $h/d_e = 2.4$.

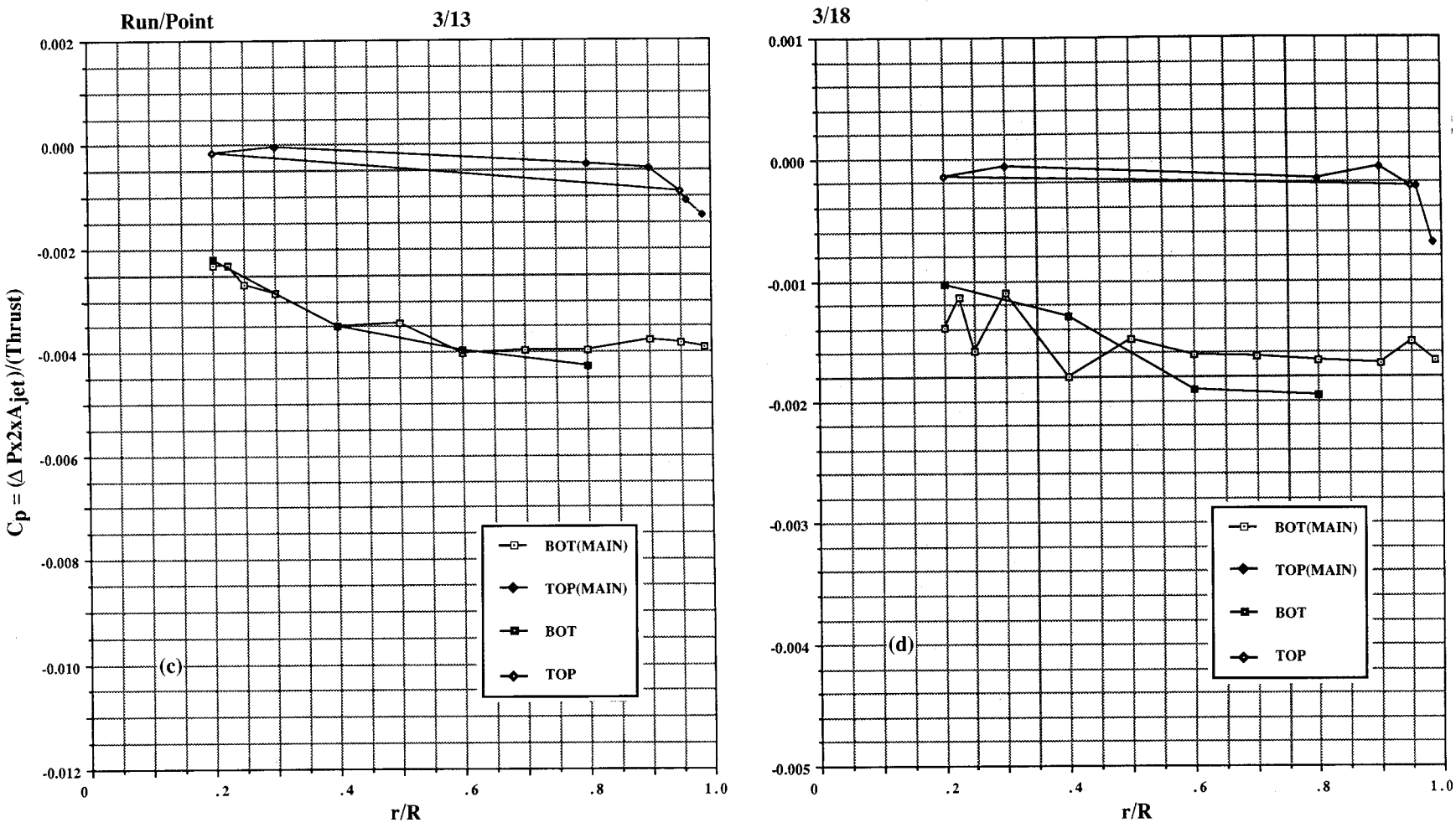

Figure 30. Continued. (c) $h/d_e = 3.3$, (d) $h/d_e = 4.9$.

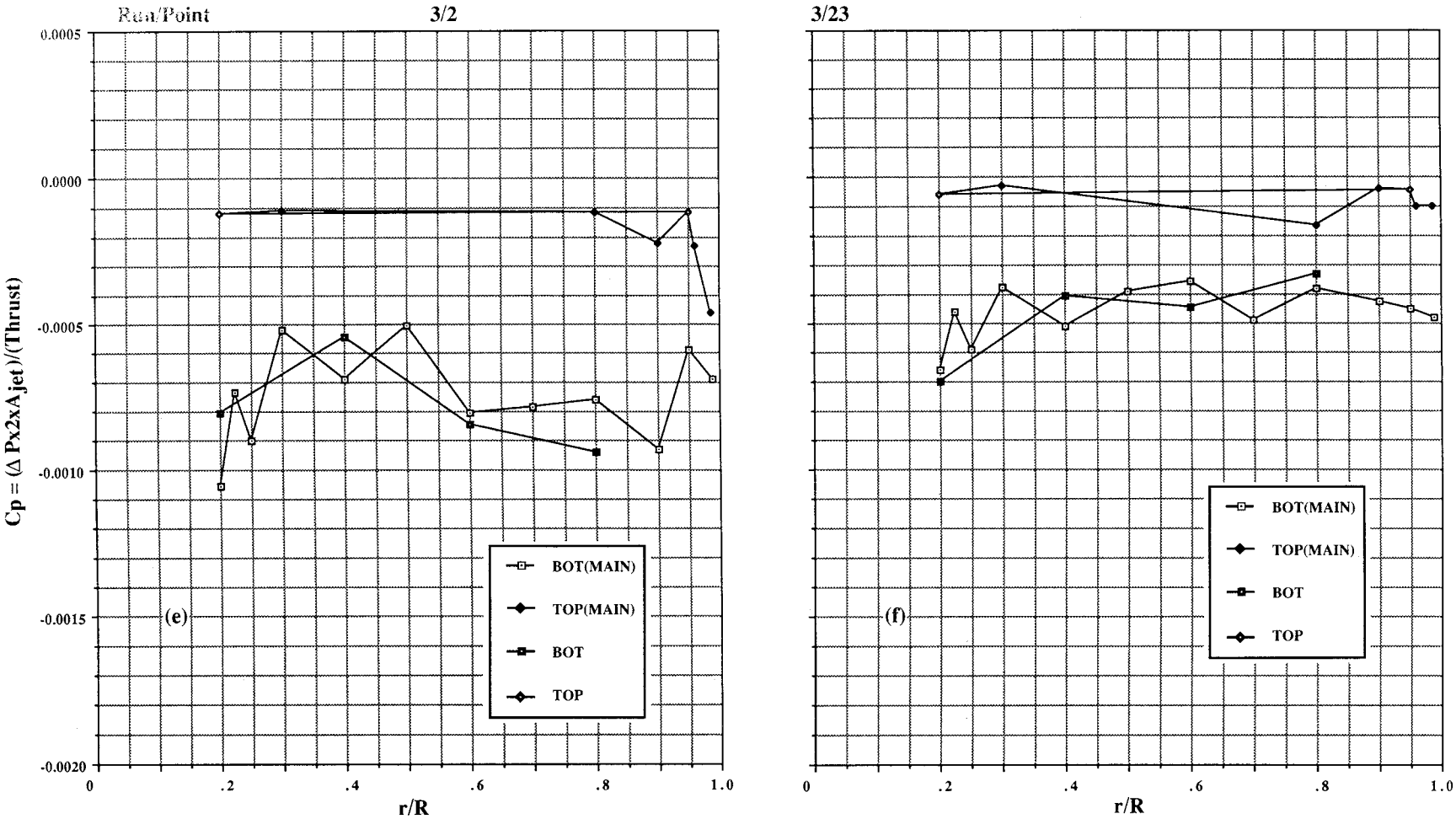

Figure 30. Continued. (e) $h/d_e = 8.1$, (f) $h/d_e = 12.2$.

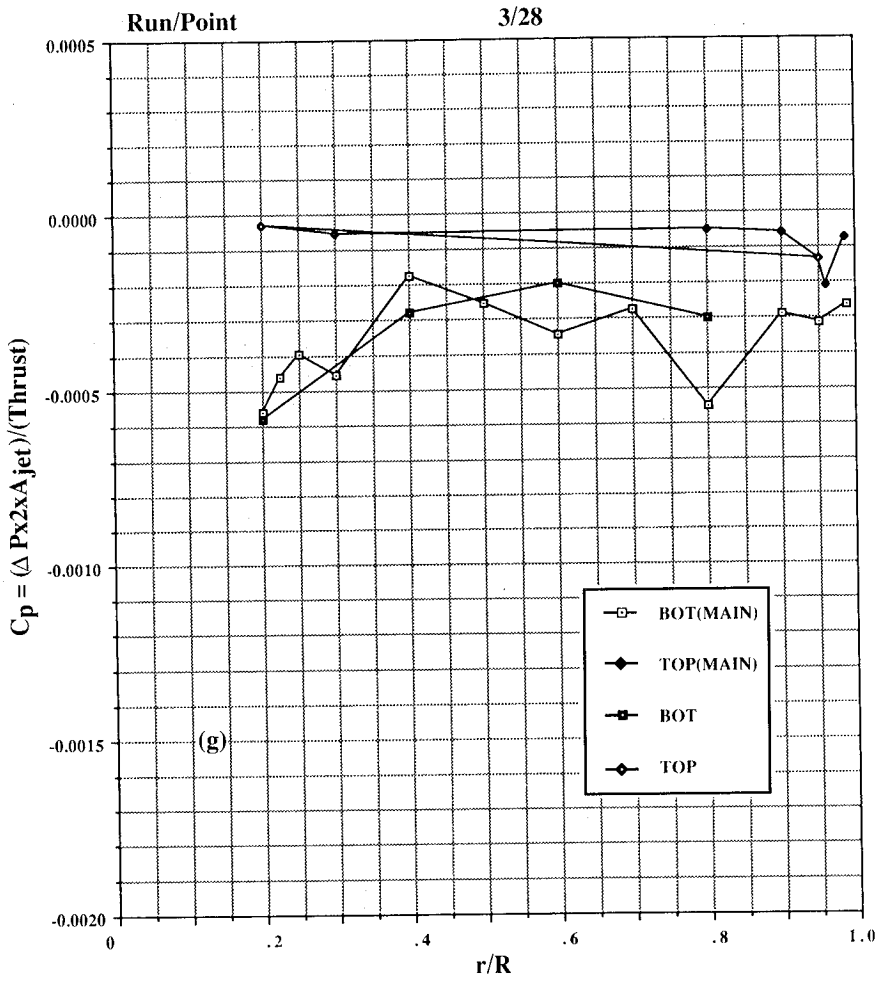

Figure 30. Concluded. (g) $h/d_e = 16.3$.

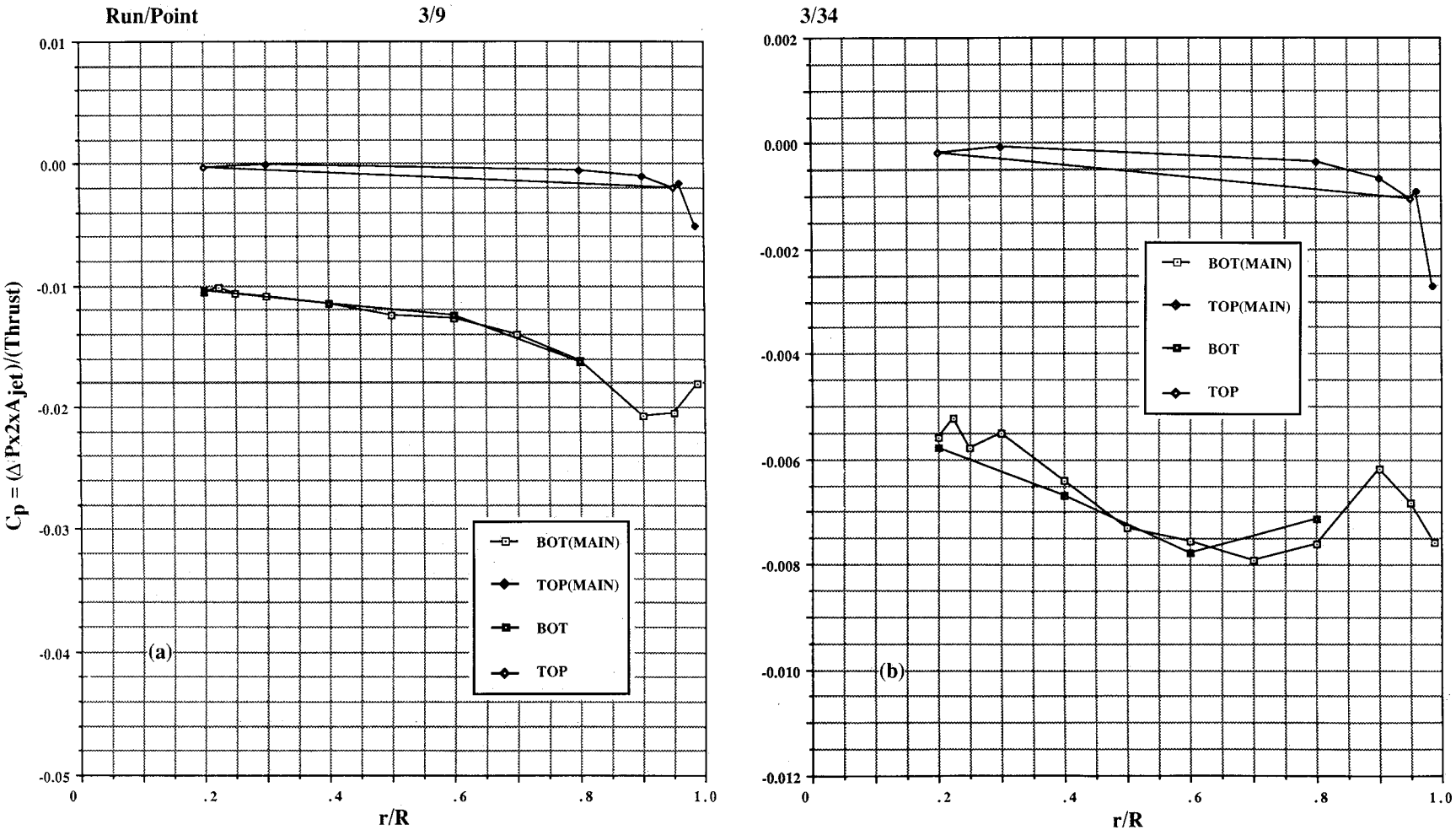

Figure 31. Pressures induced on 10-in. circular plate in ground effect, NPR = 3.0, T = 50 lb, large room. (a) $h/d_e = 1.6$, (b) $h/d_e = 2.4$.

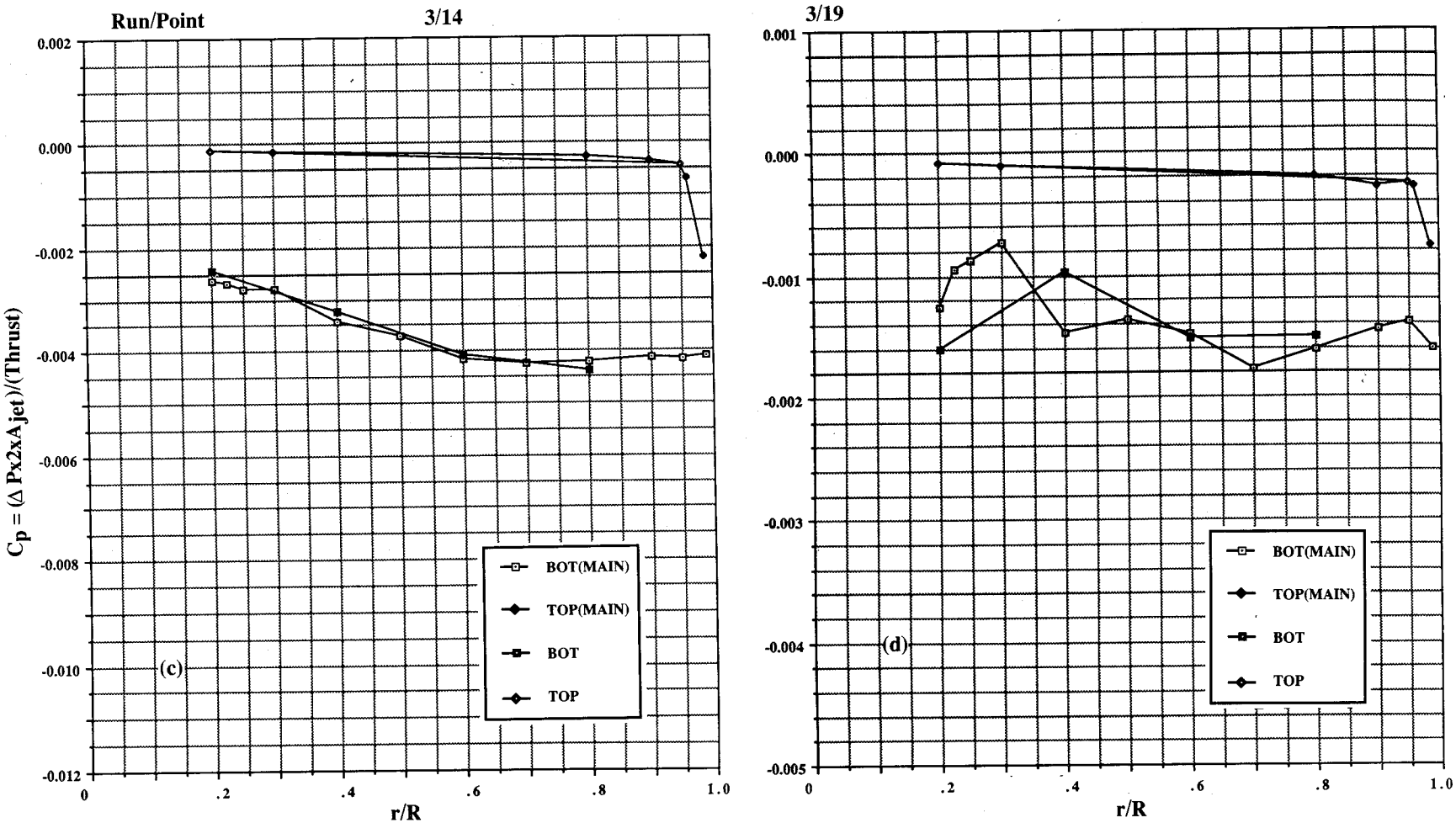

Figure 31. Continued. (c) $h/d_e = 3.3$, (d) $h/d_e = 4.9$.

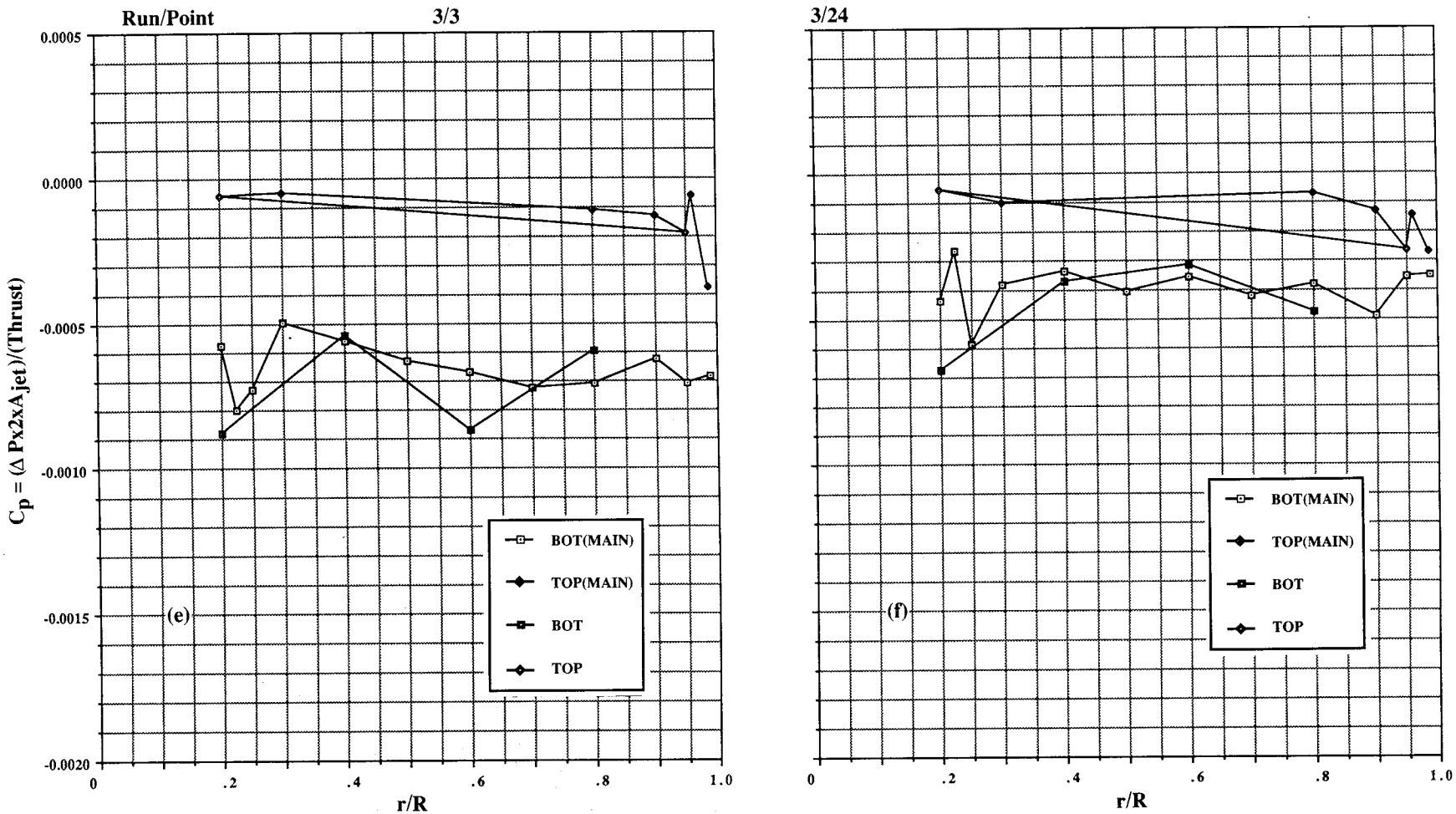

Figure 31. Continued. (e) $h/d_e = 8.1$, (f) $h/d_e = 12.2$.

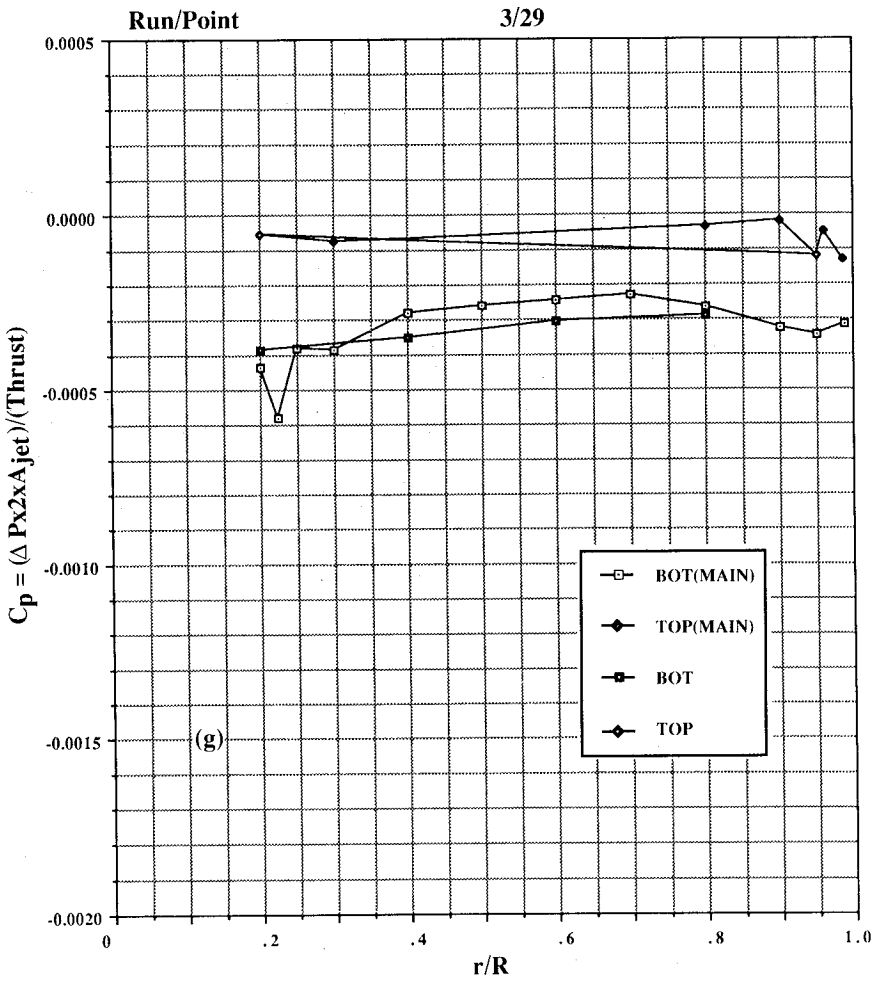

Figure 31. Concluded. (g) $h/d_e = 16.3$.

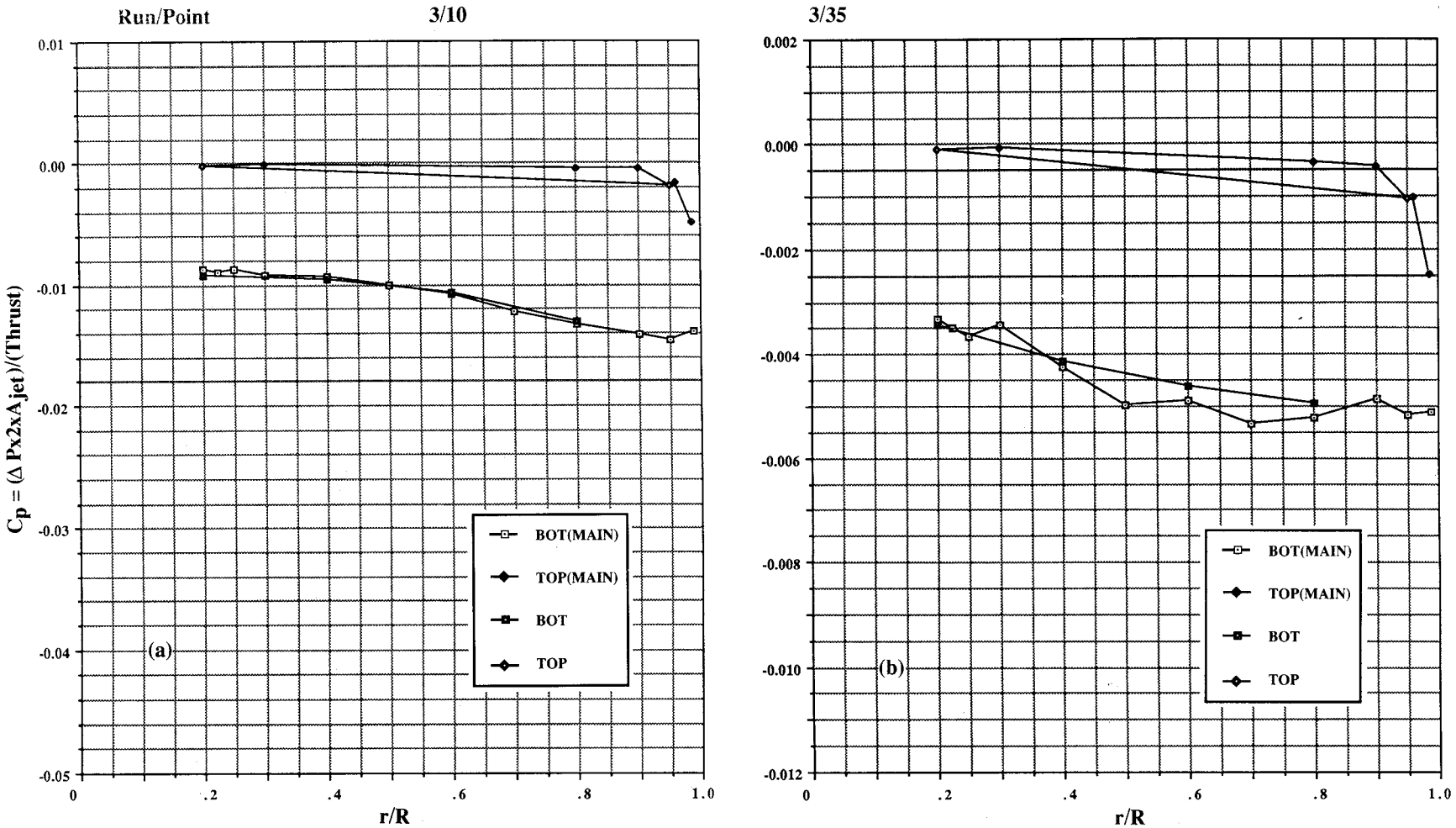

Figure 32. Pressures induced on 10-in. circular plate in ground effect, NPR = 4.0, T = 72 lb, large room. (a) $h/d_e = 1.6$, (b) $h/d_e = 2.4$.

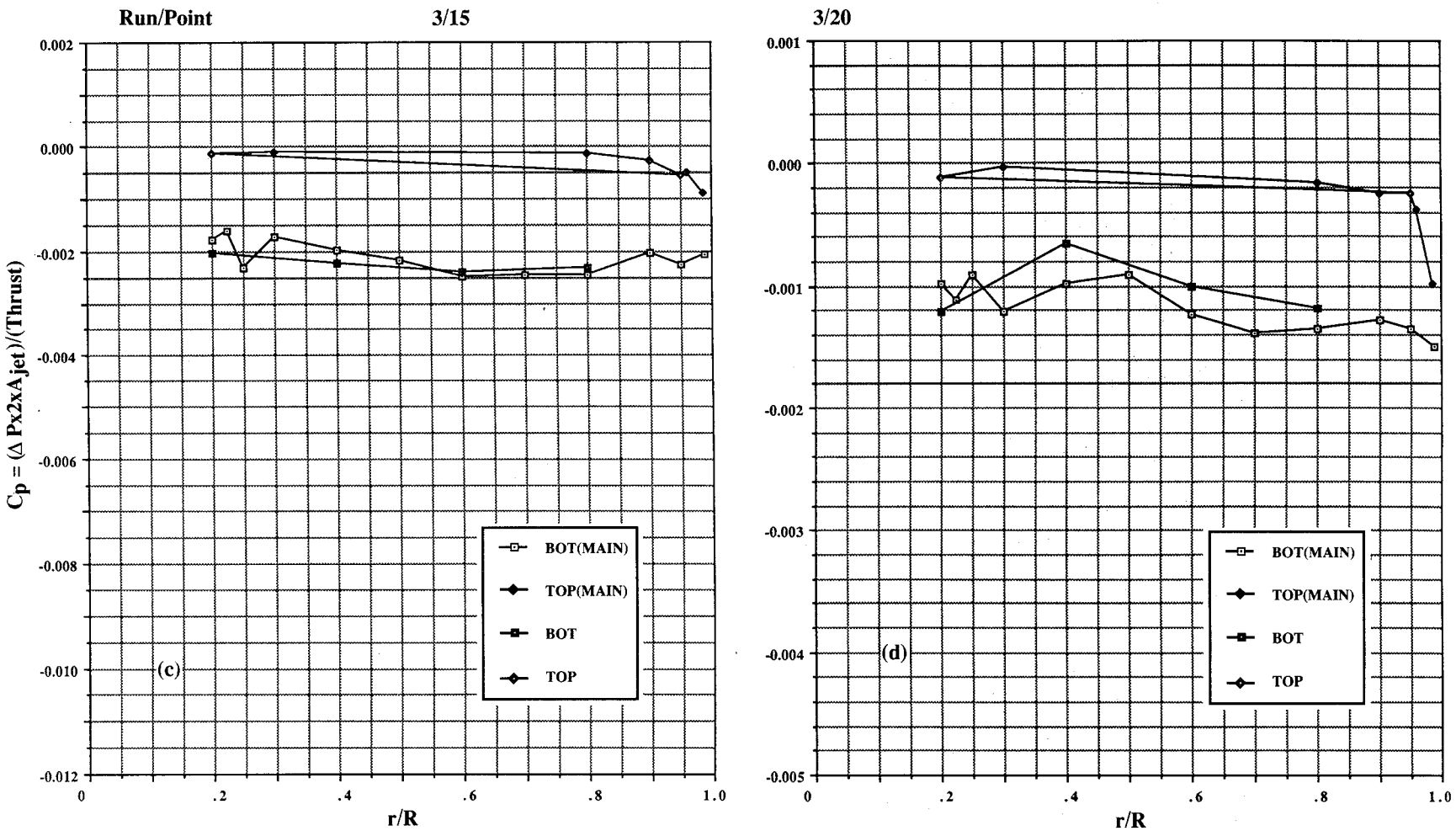

Figure 32. Continued. (c) $h/d_e = 3.3$, (d) $h/d_e = 4.9$.

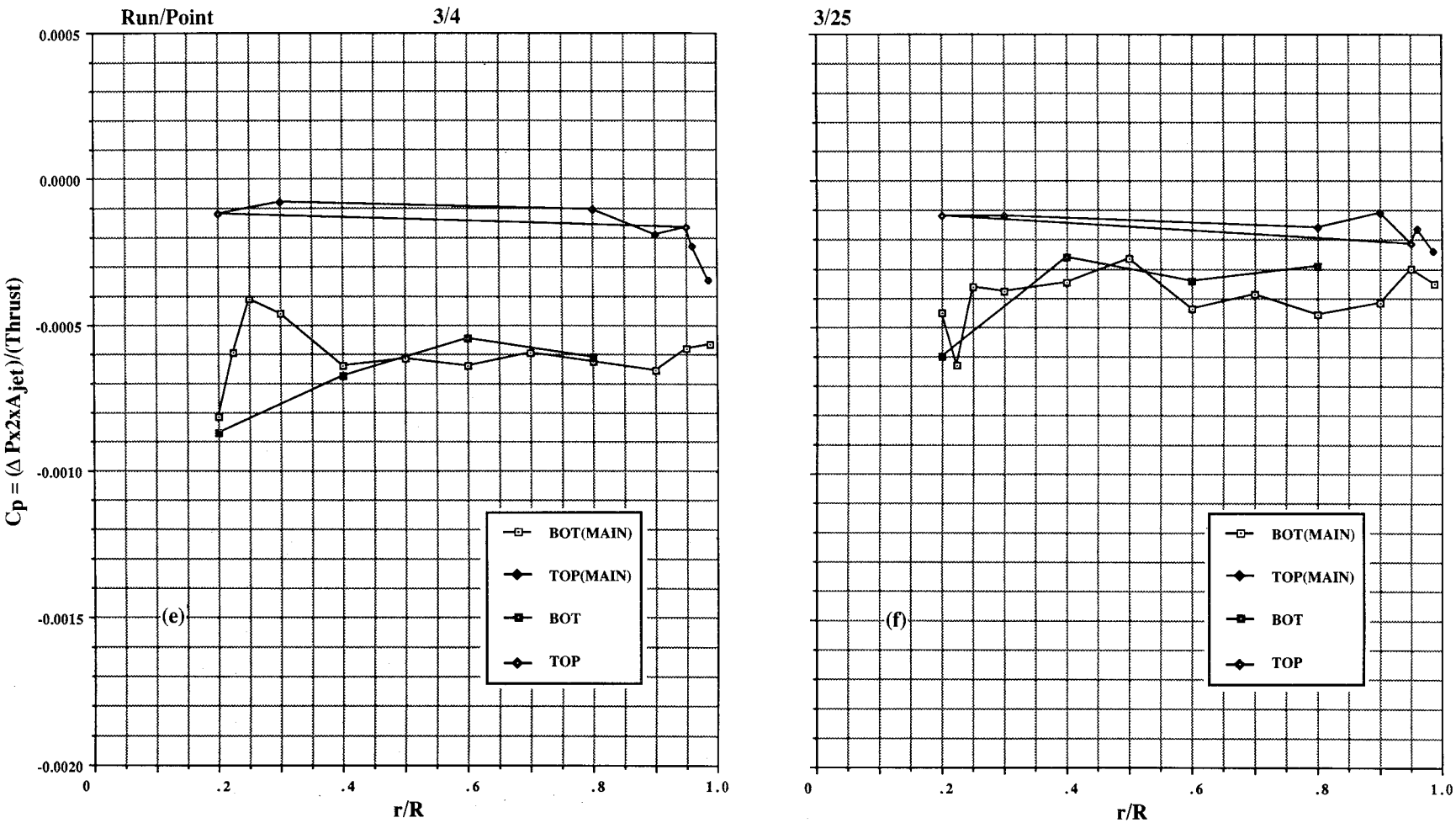

Figure 32. Continued. (e) $h/d_e = 8.1$, (f) $h/d_e = 12.2$.

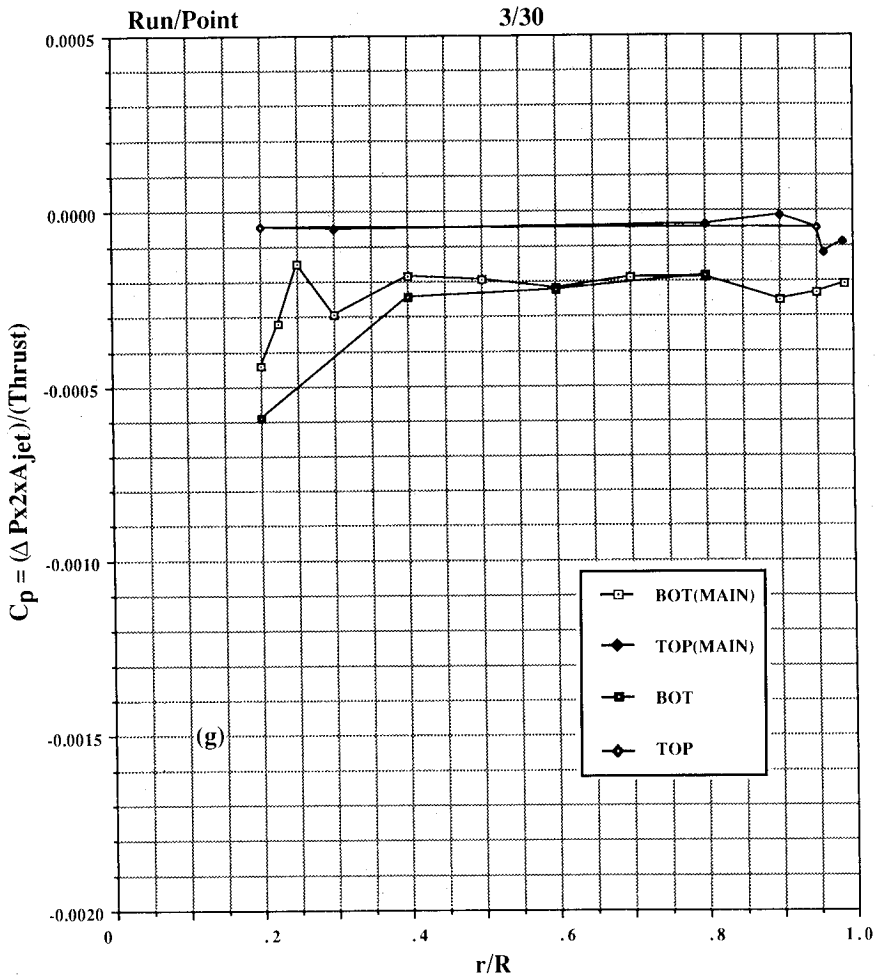

Figure 32. Concluded. (g) $h/d_e = 16.3$.

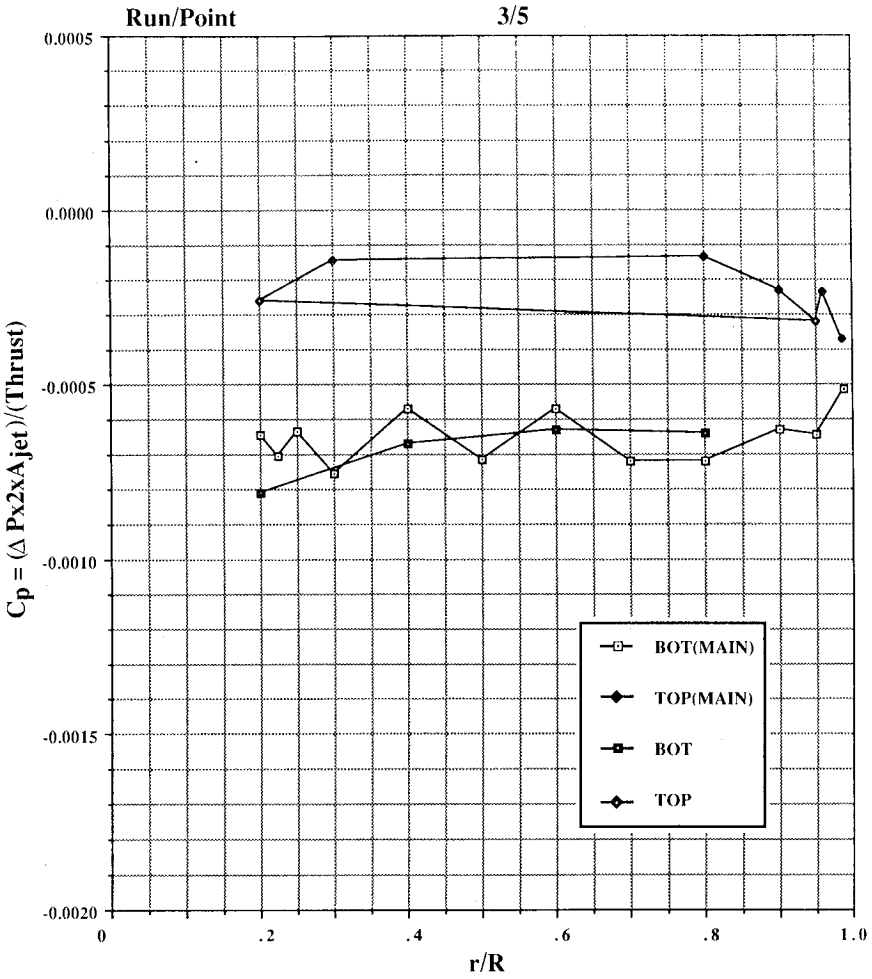

Figure 33. Pressures induced on 10-in. circular plate in ground effect, NPR = 5.0, T = 94 lb, h/d_e = 8.1, large room.

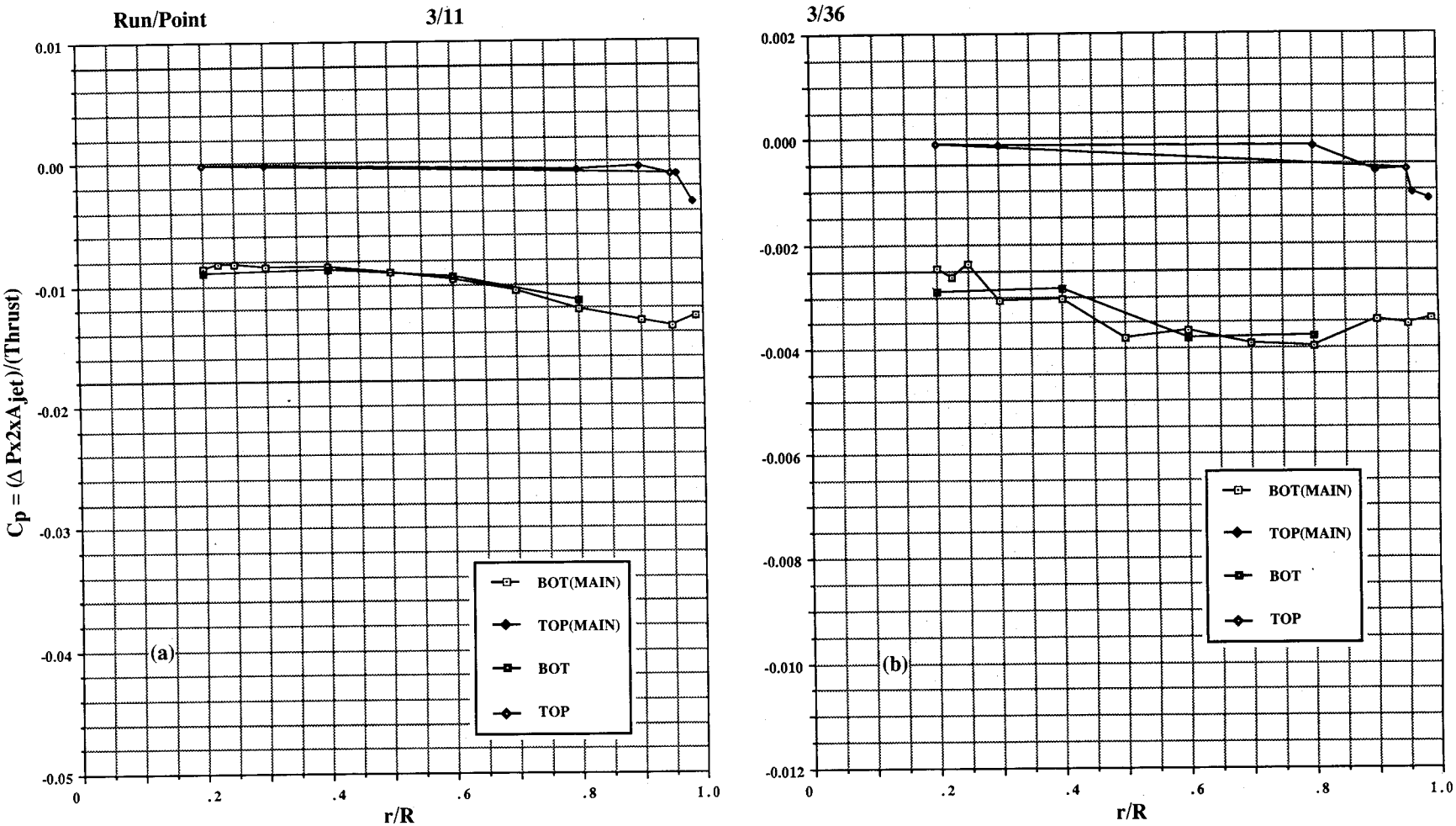

Figure 34. Pressures induced on 10-in. circular plate in ground effect, NPR = 6.0, T = 117 lb, large room. (a) $h/d_e = 1.6$, (b) $h/d_e = 2.4$.

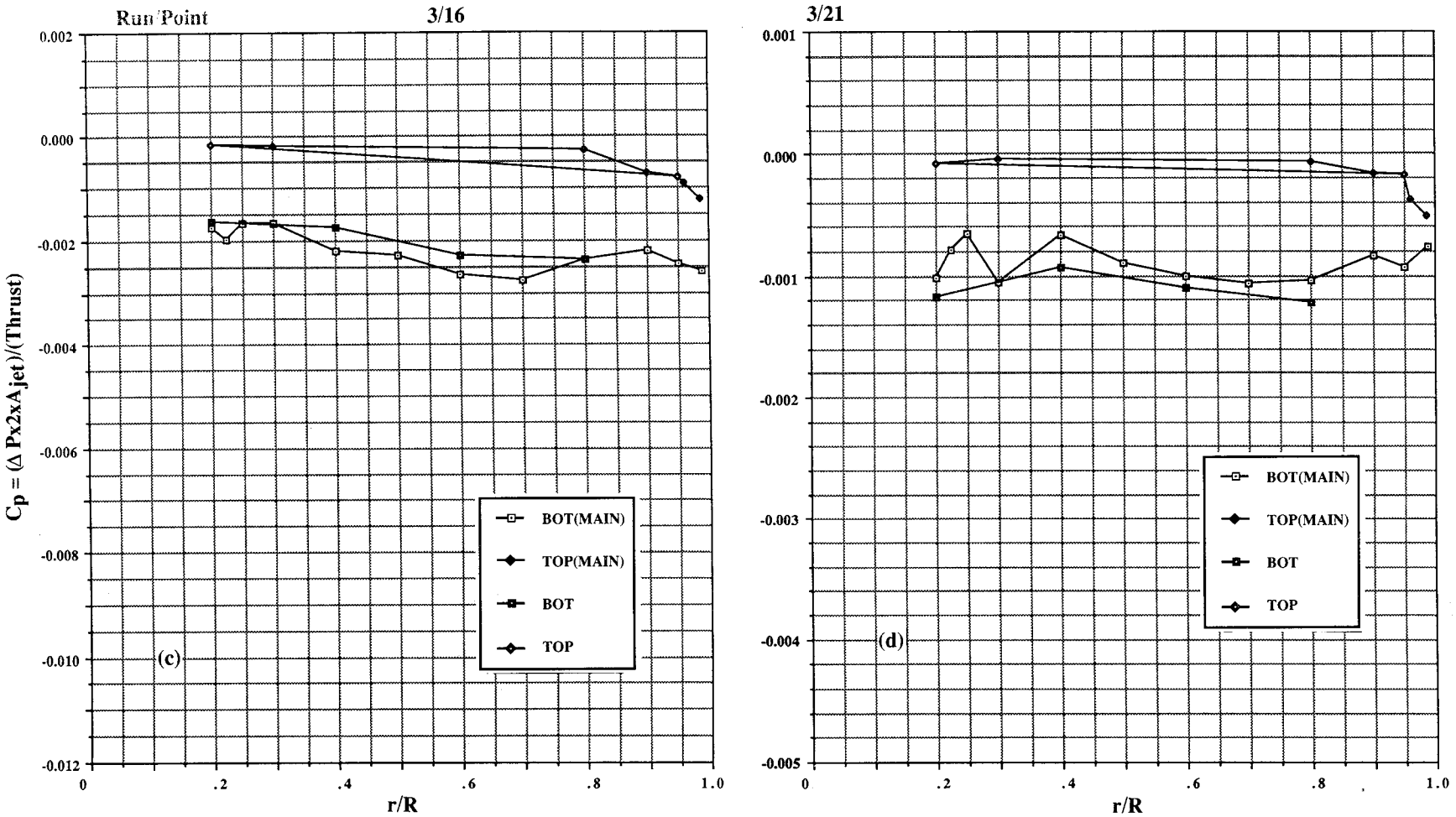

Figure 34. Continued. (c) $h/d_e = 3.3$, (d) $h/d_e = 4.9$.

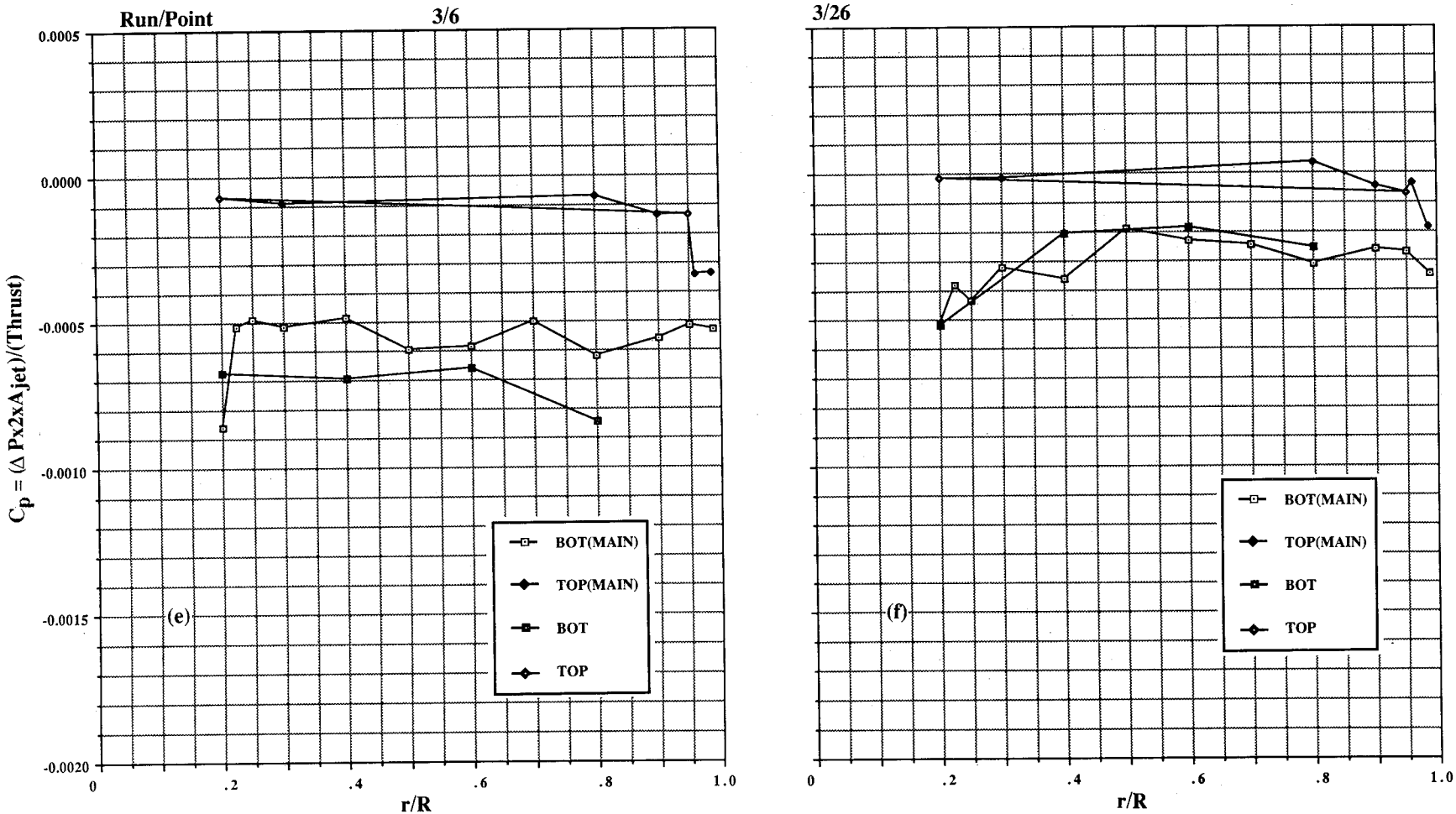

Figure 34. Continued. (e) $h/d_e = 8.1$, (f) $h/d_e = 12.2$.

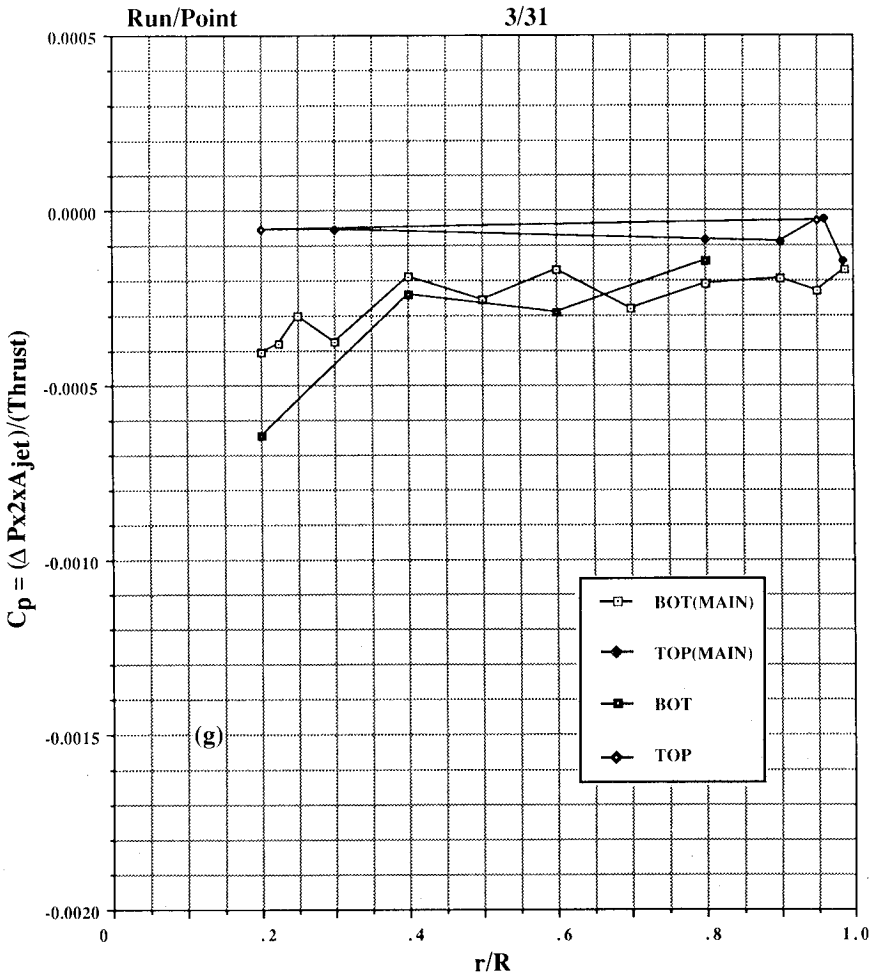

Figure 34. Concluded. (g) $h/d_e = 16.3$.

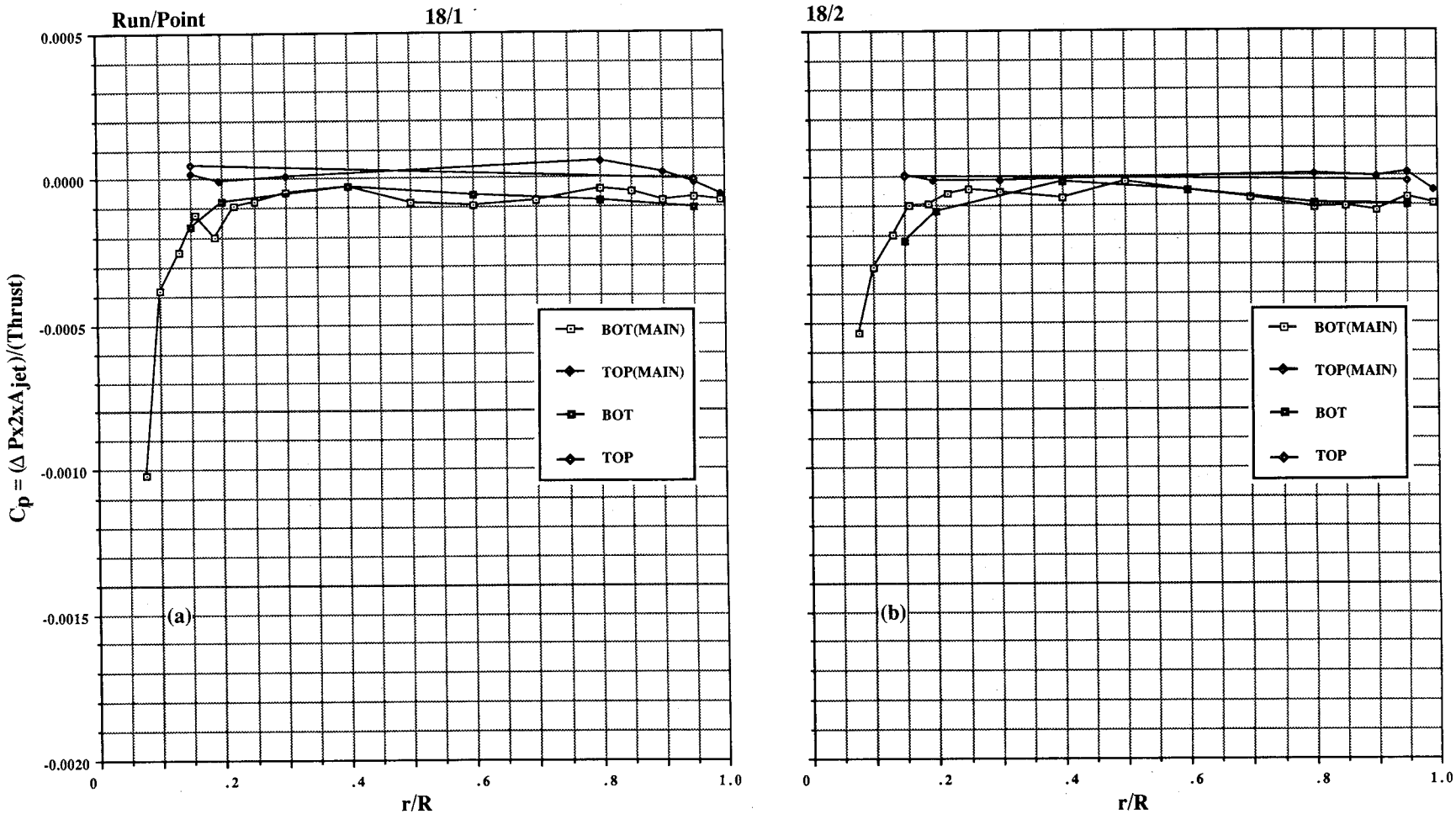

Figure 35. Pressures induced on 20-in. circular plate out of ground effect, test cell. (a) NPR = 1.5, T = 14 lb, (b) NPR = 2.0, T = 26 lb.

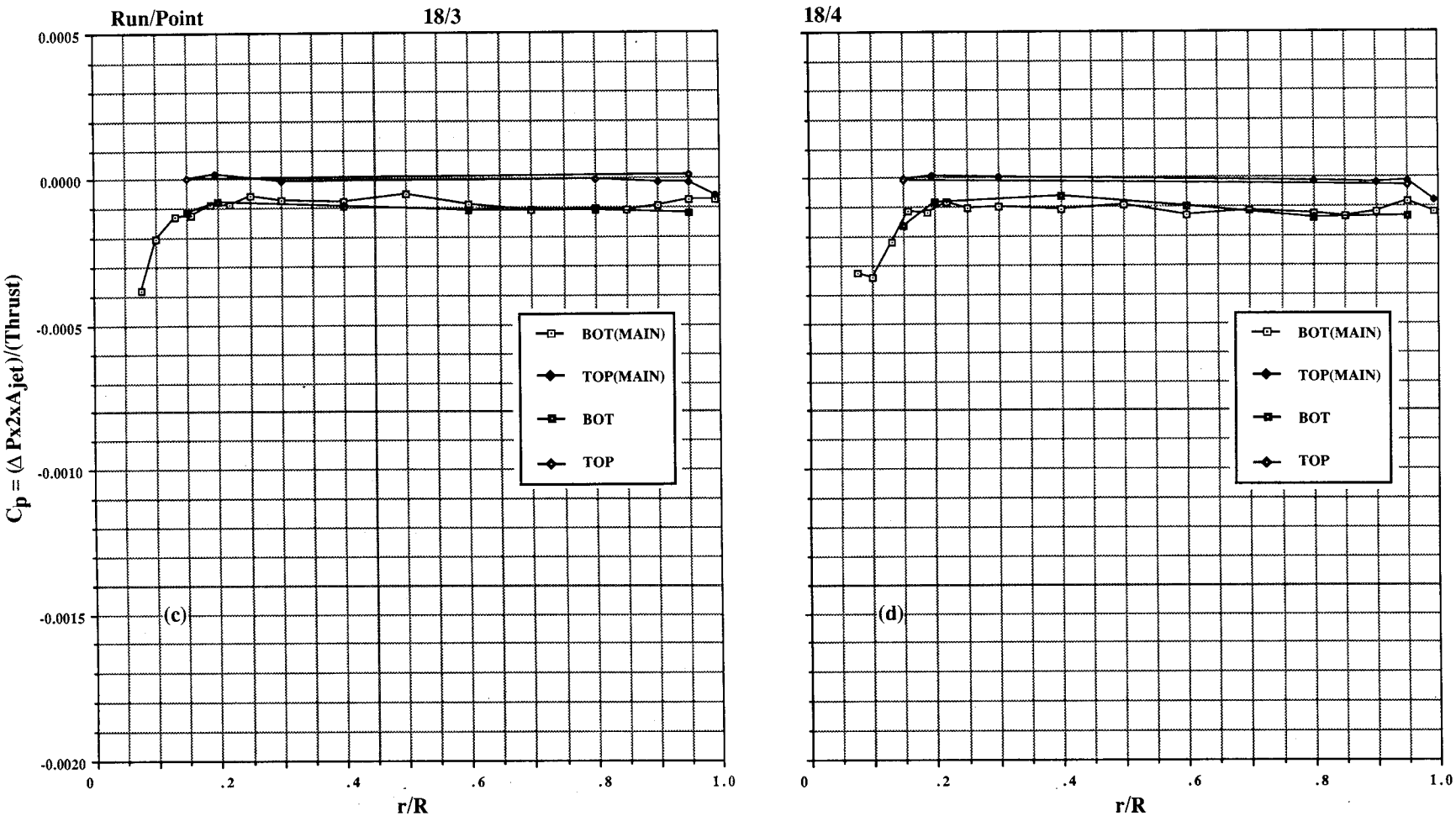

Figure 35. Continued. (c) NPR = 2.5, T = 36 lb, (d) NPR = 3.0, T = 47 lb.

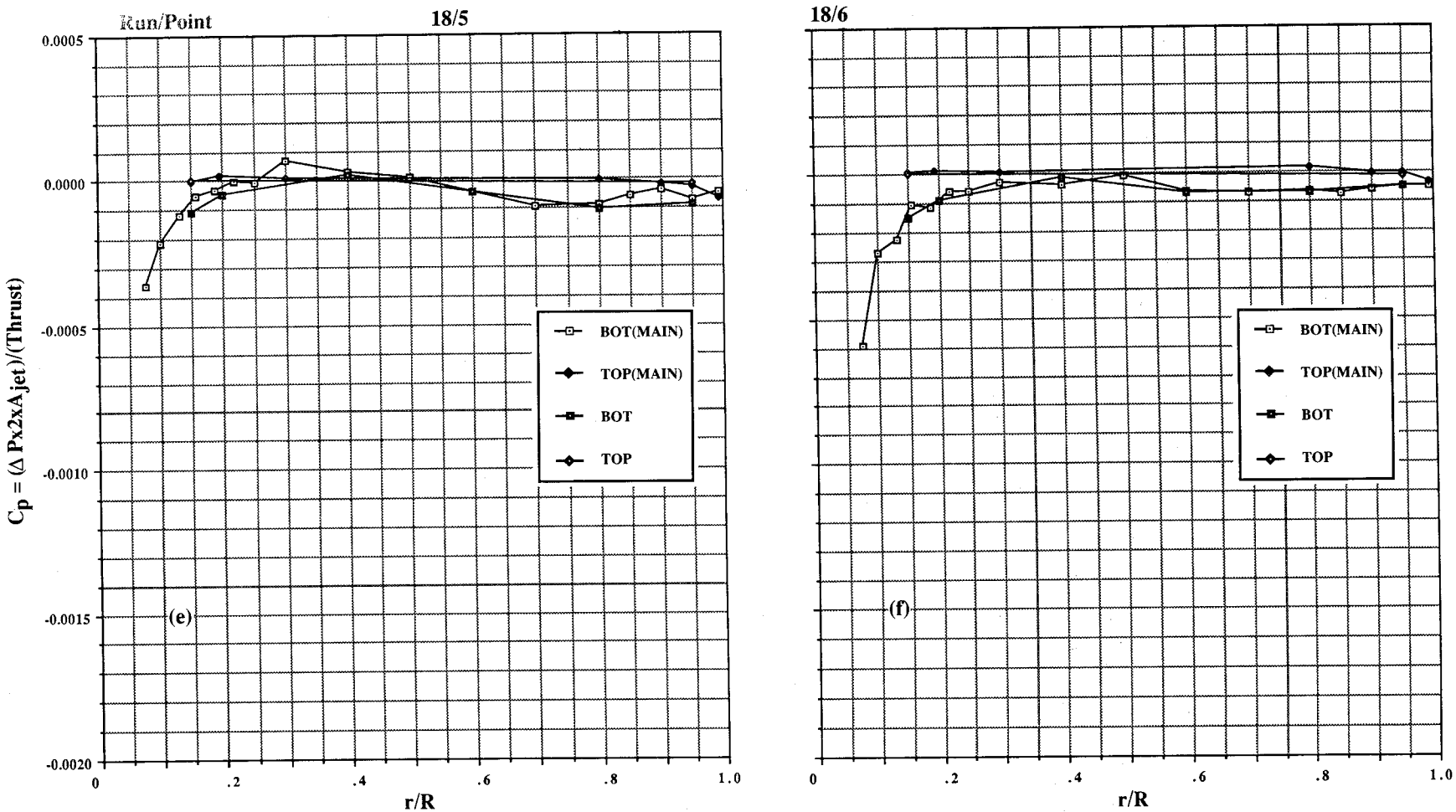

Figure 35. Continued. (e) NPR = 4.0, T = 68 lb, (f) NPR = 5.0, T = 88 lb.

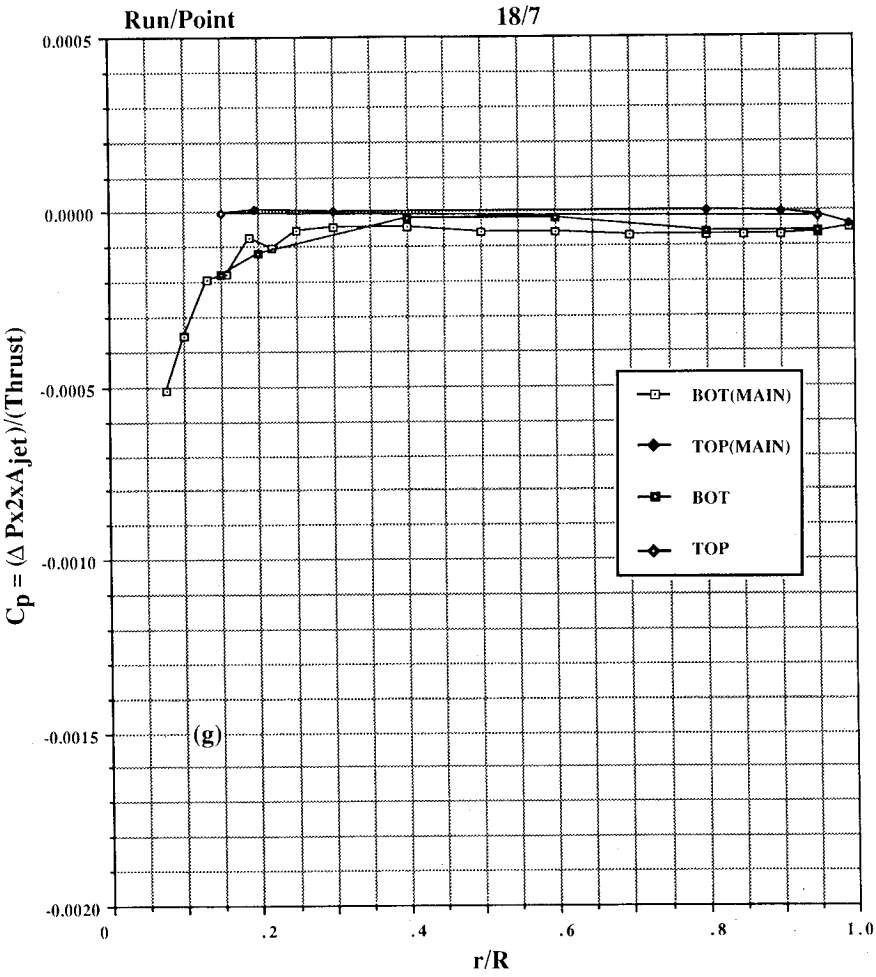

Figure 35. Concluded. (g) NPR = 6.0, T = 109 lb.

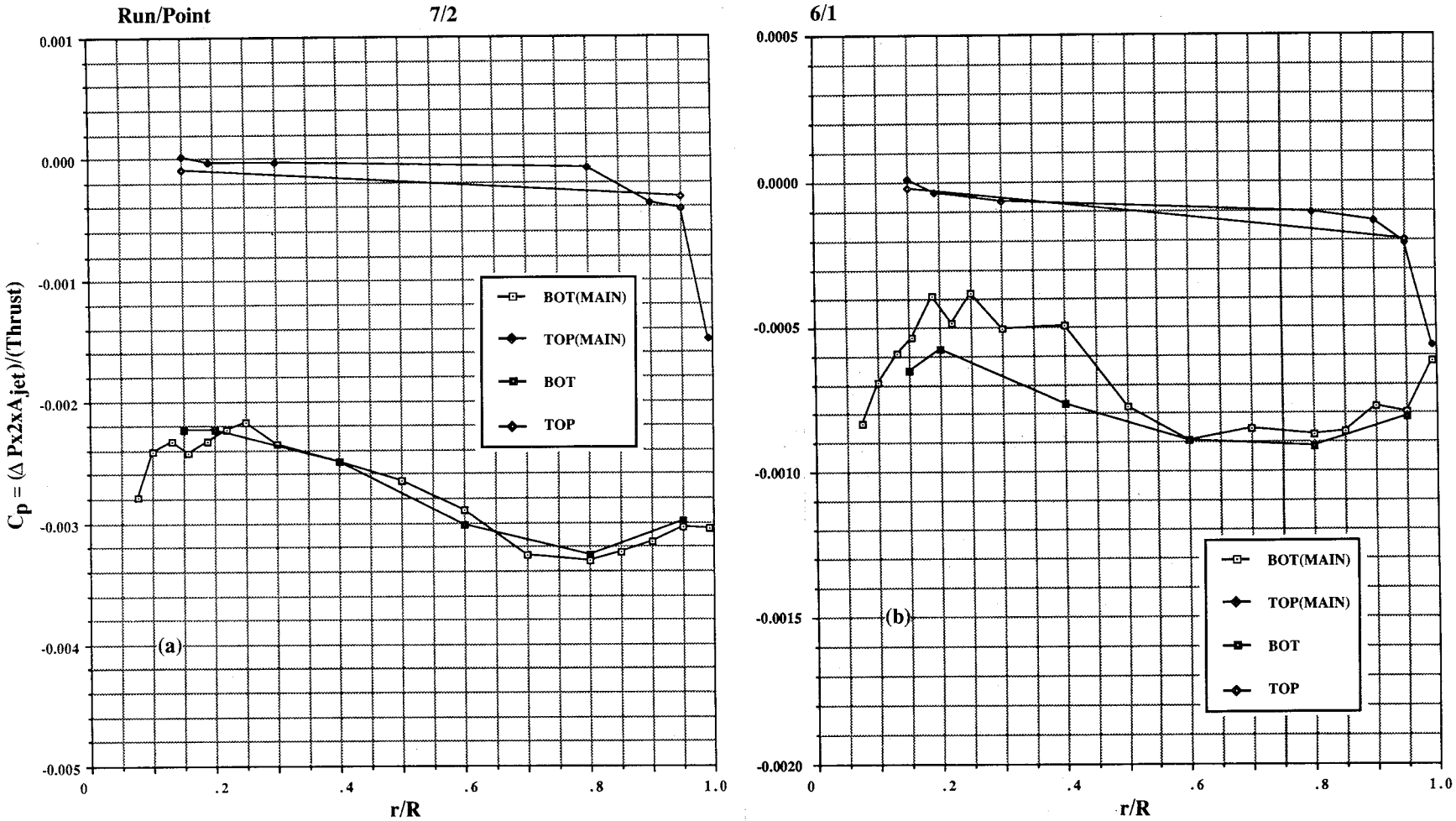

Figure 36. Pressures induced on 20-in. circular plate in ground effect, NPR = 1.5, T = 14 lb, test cell. (a) $h/d_e = 4.1$, (b) $h/d_e = 8.1$.

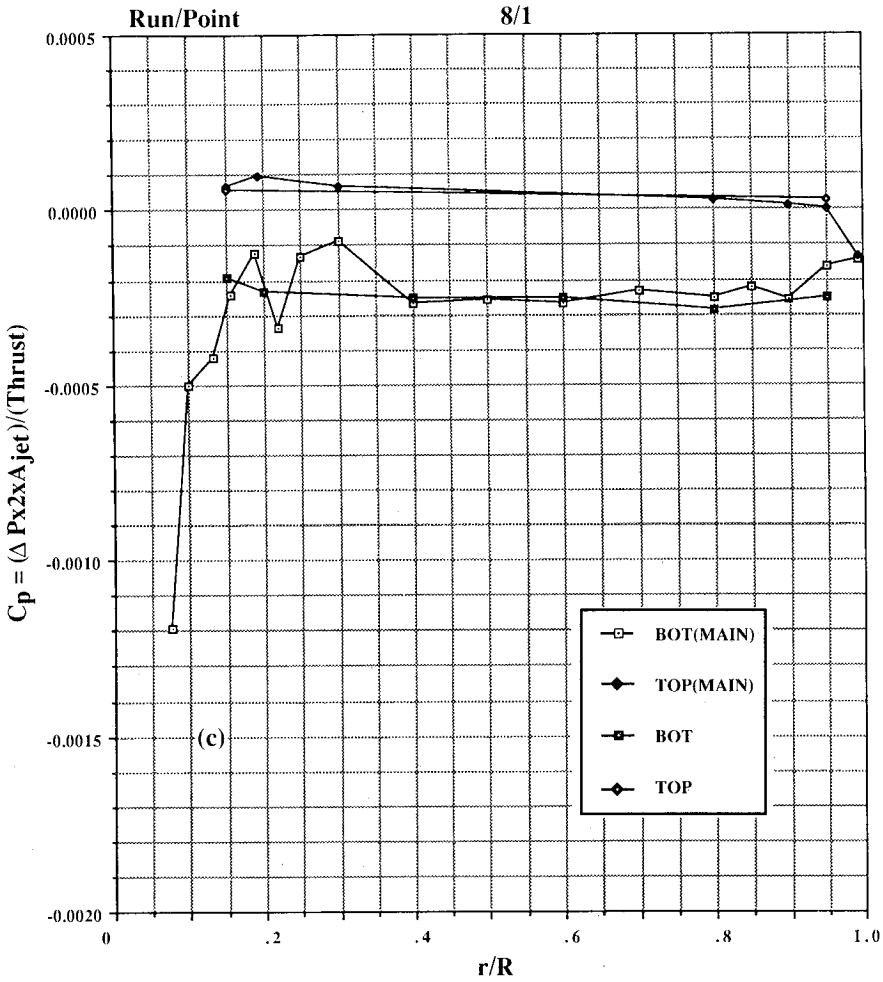

Figure 36. Concluded. (c) $h/d_e = 16.3$.

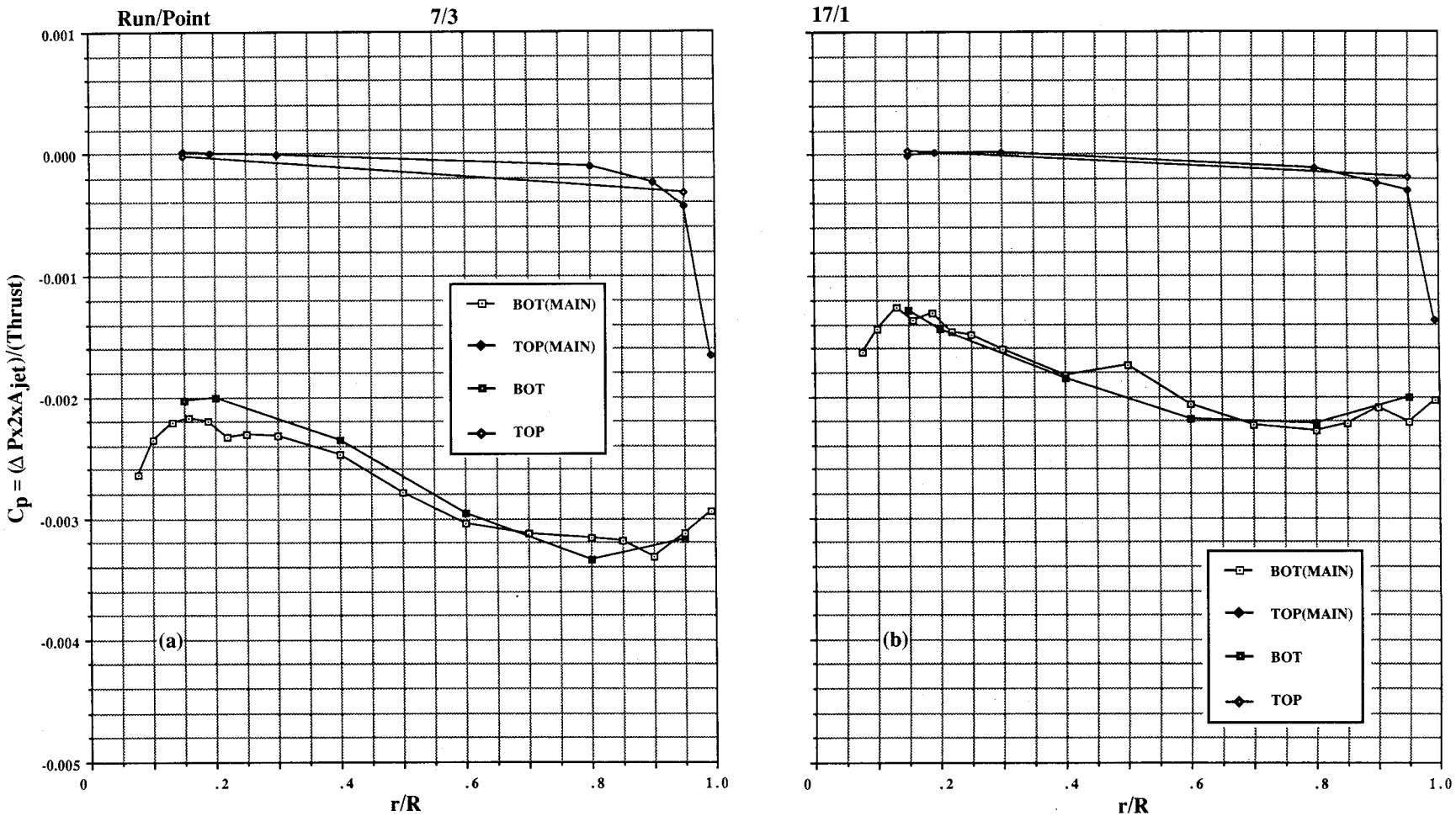

Figure 37. Pressures induced on 20-in. circular plate in ground effect, NPR = 2.0, T = 26 lb, test cell. (a) $h/d_e = 4.1$, (b) $h/d_e = 4.9$.

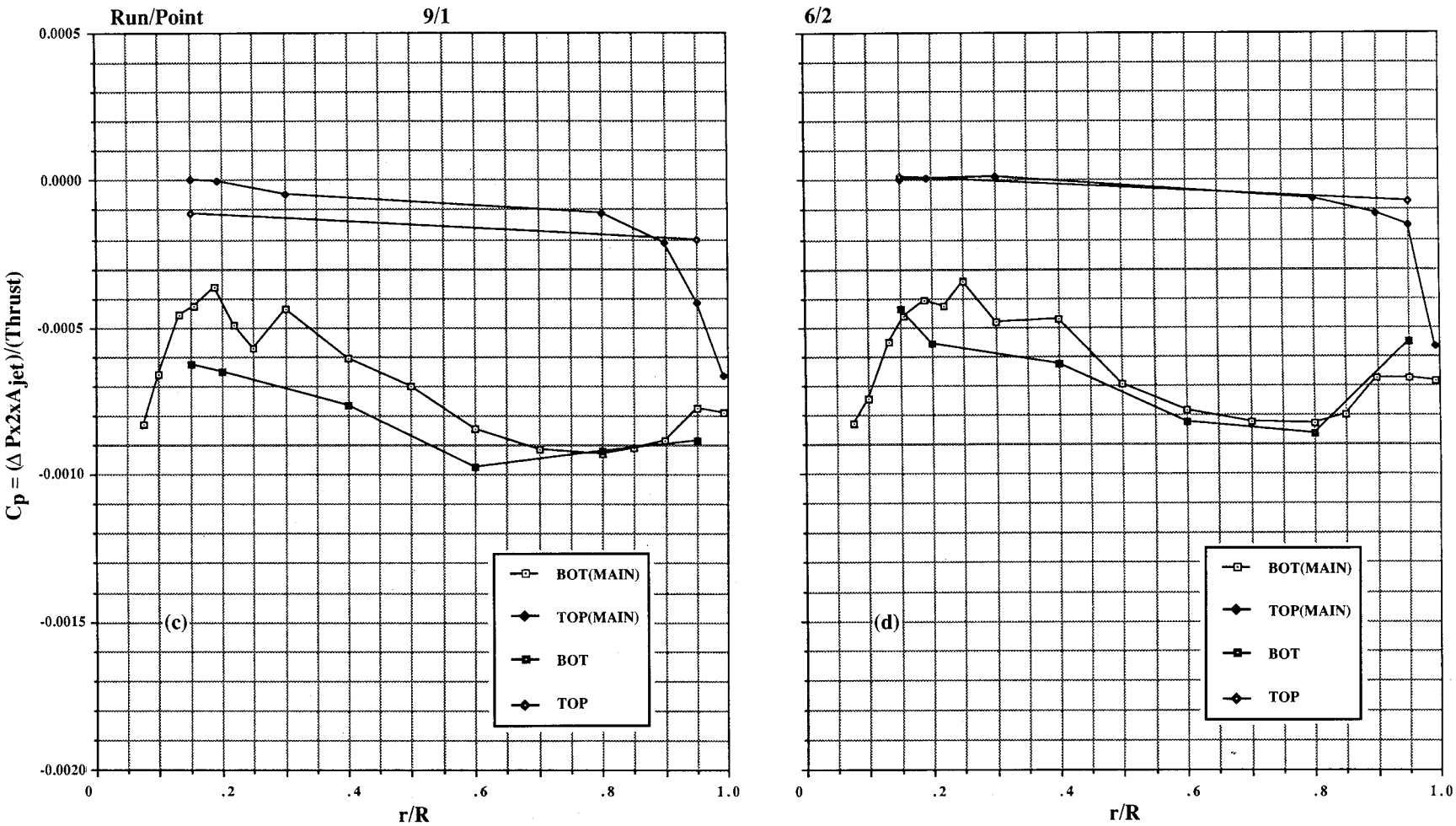

Figure 37. Continued. (c) $h/d_e = 8.1$, (d) $h/d_e = 8.1$ (repeat).

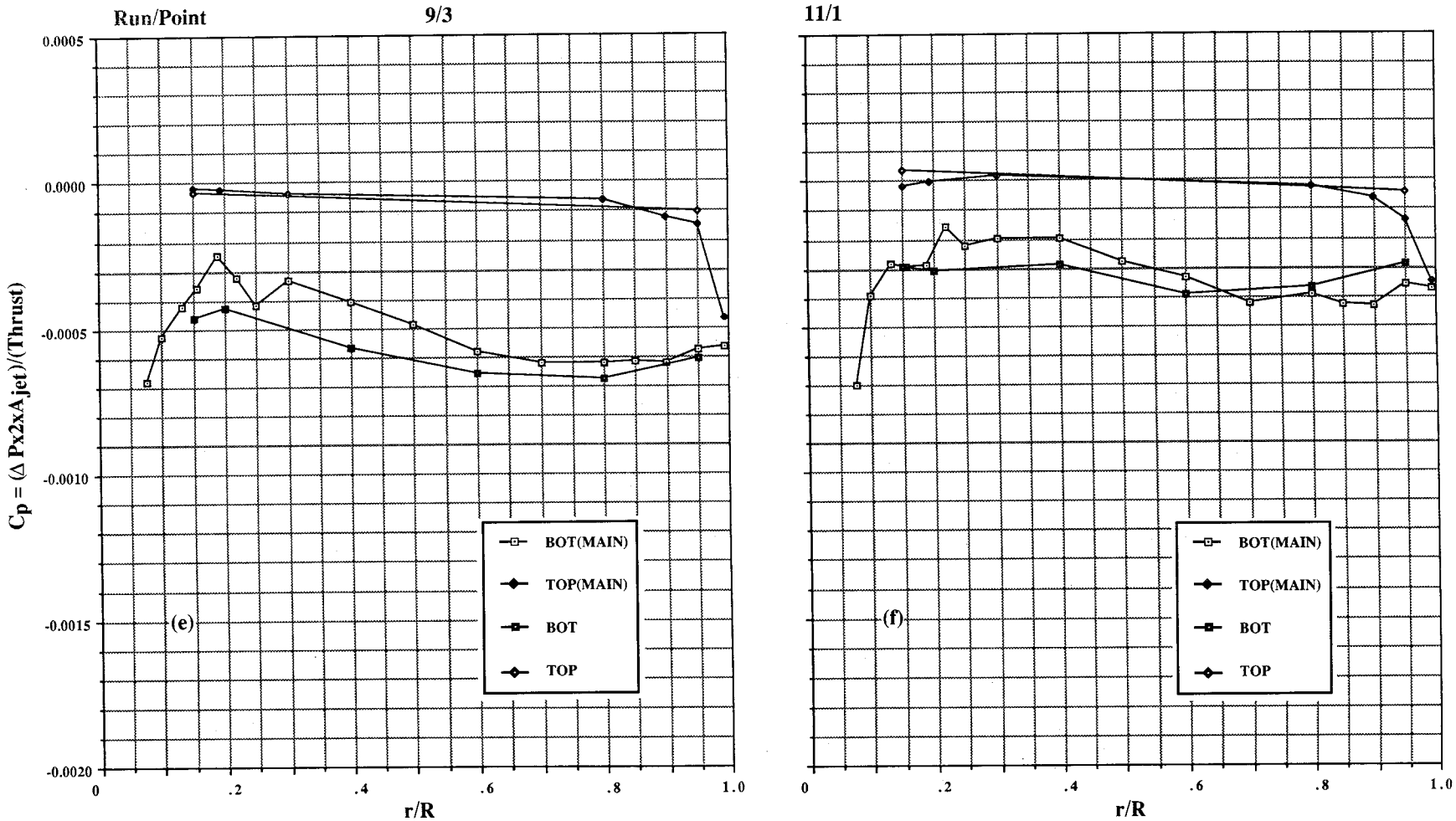

Figure 37. Continued. (e) $h/d_e = 9.8$, (f) $h/d_e = 12.2$.

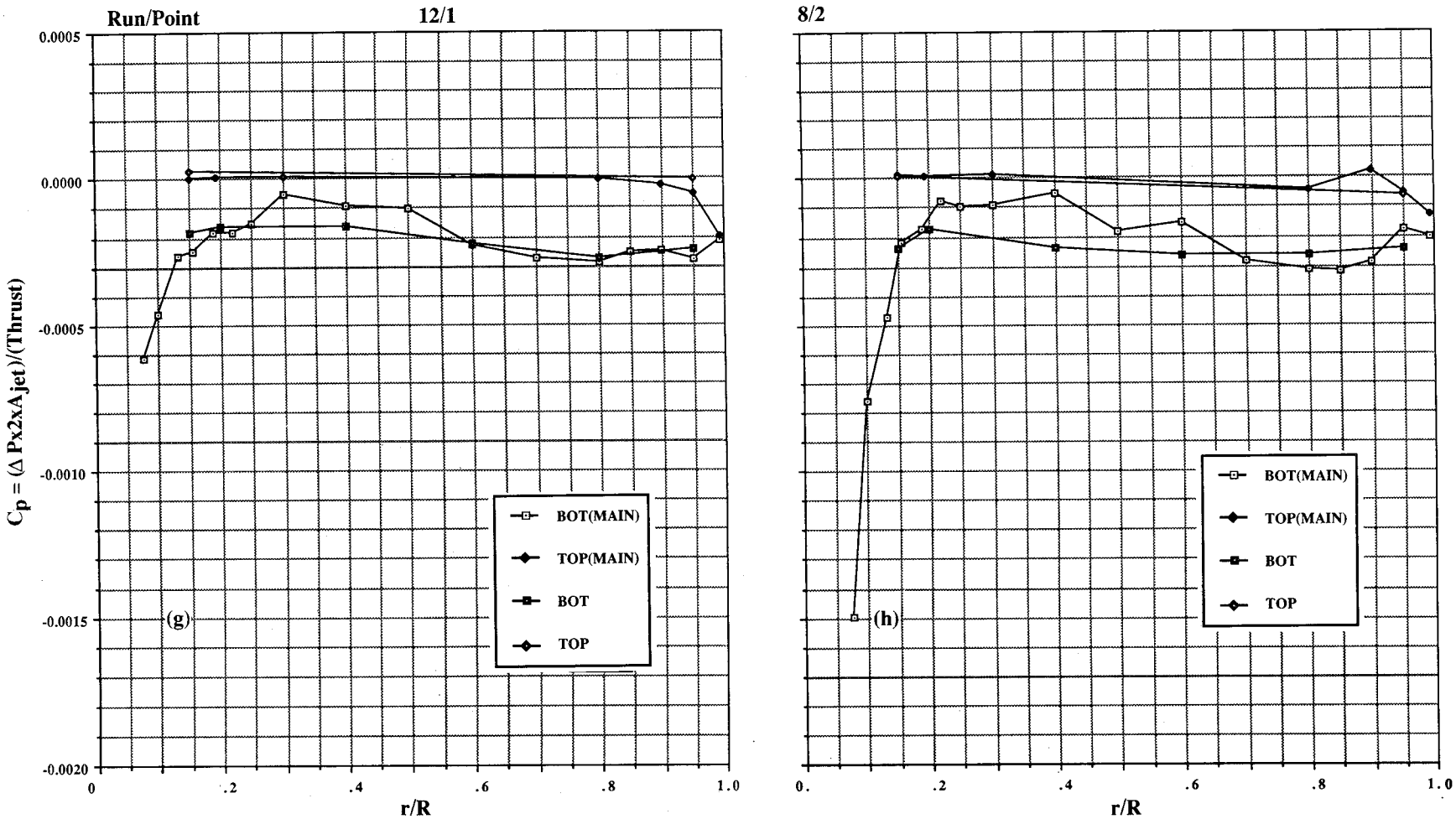

Figure 37. Continued. (g) $h/d_e = 16.3$, (h) $h/d_e = 16.3$ (repeat).

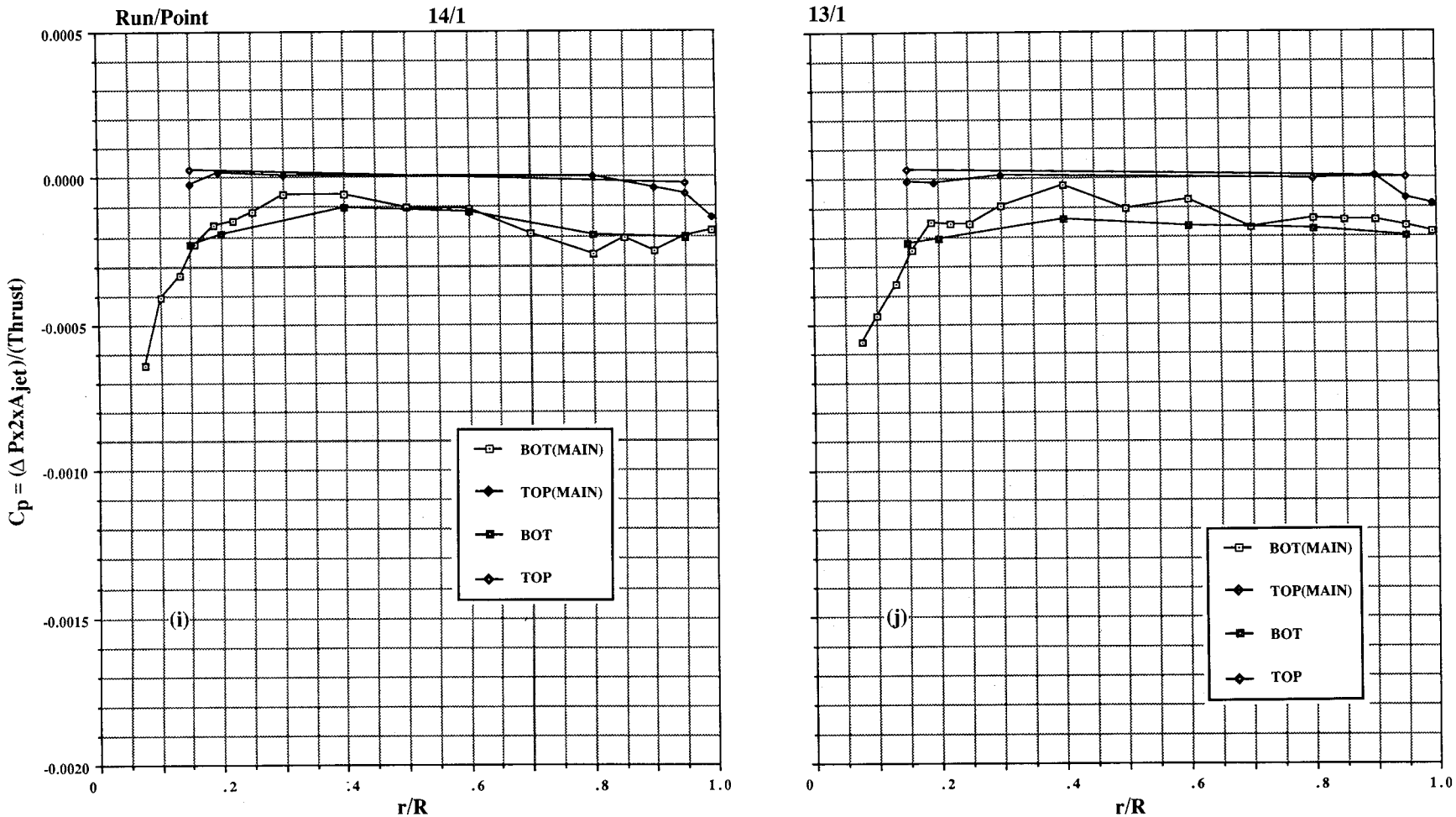

Figure 37. Continued. (i) $h/d_e = 20.4$, (j) $h/d_e = 24.4$.

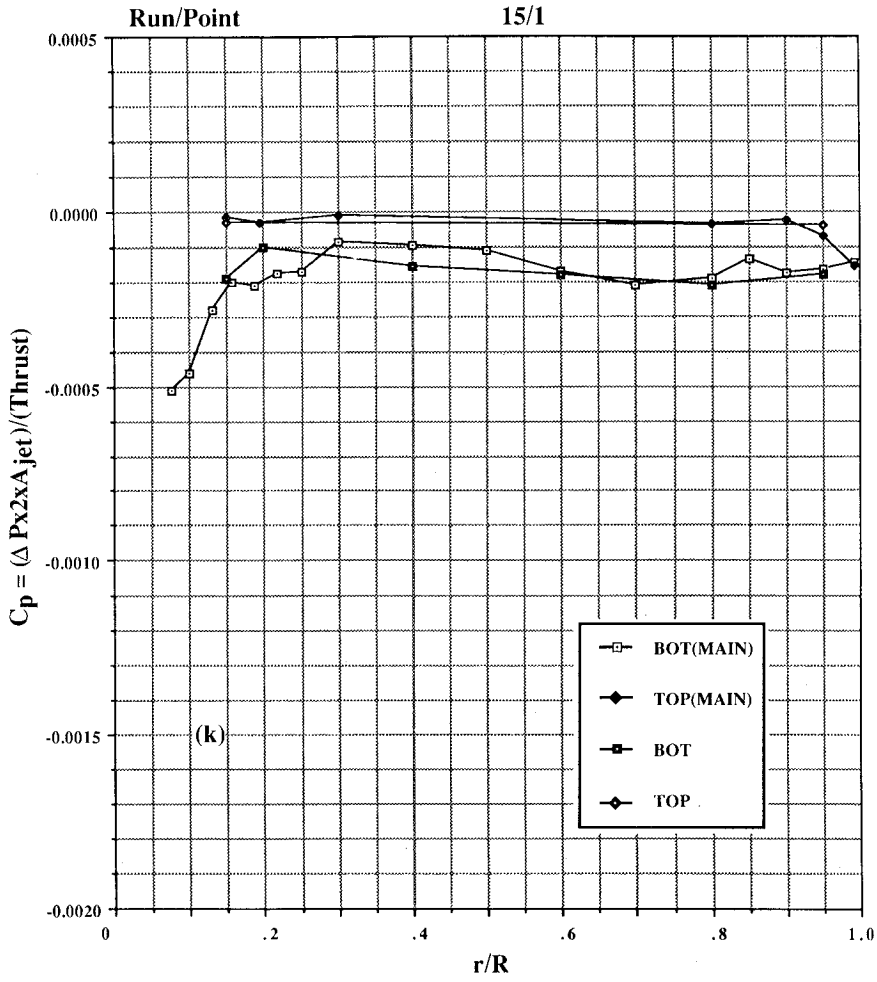

Figure 37. Concluded. (k) $h/d_e = 32.5$.

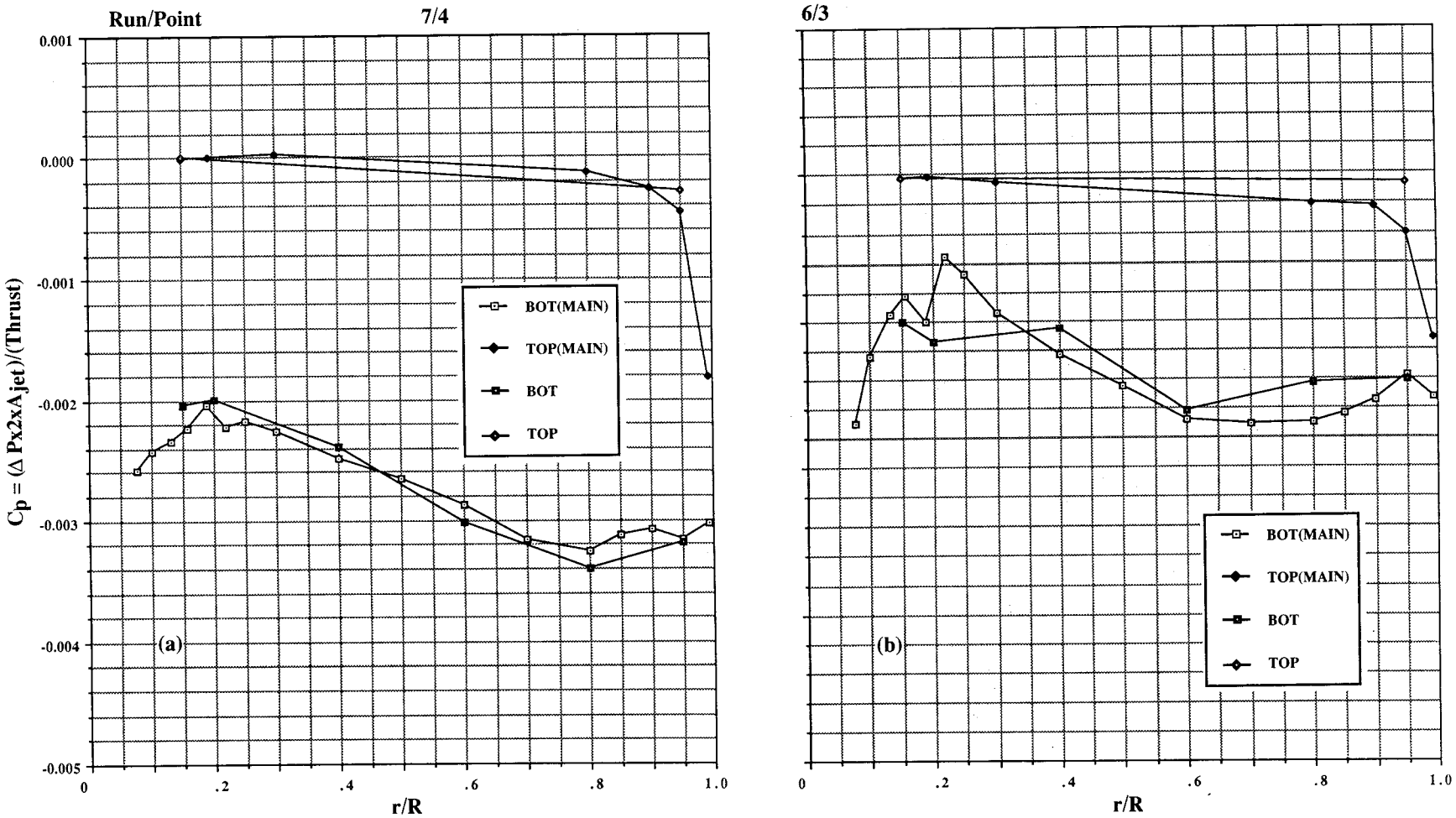

Figure 38. Pressures induced on 20-in. circular plate in ground effect, NPR = 2.5, T = 36 lb, test cell. (a) $h/d_e = 4.1$, (b) $h/d_e = 8.1$.

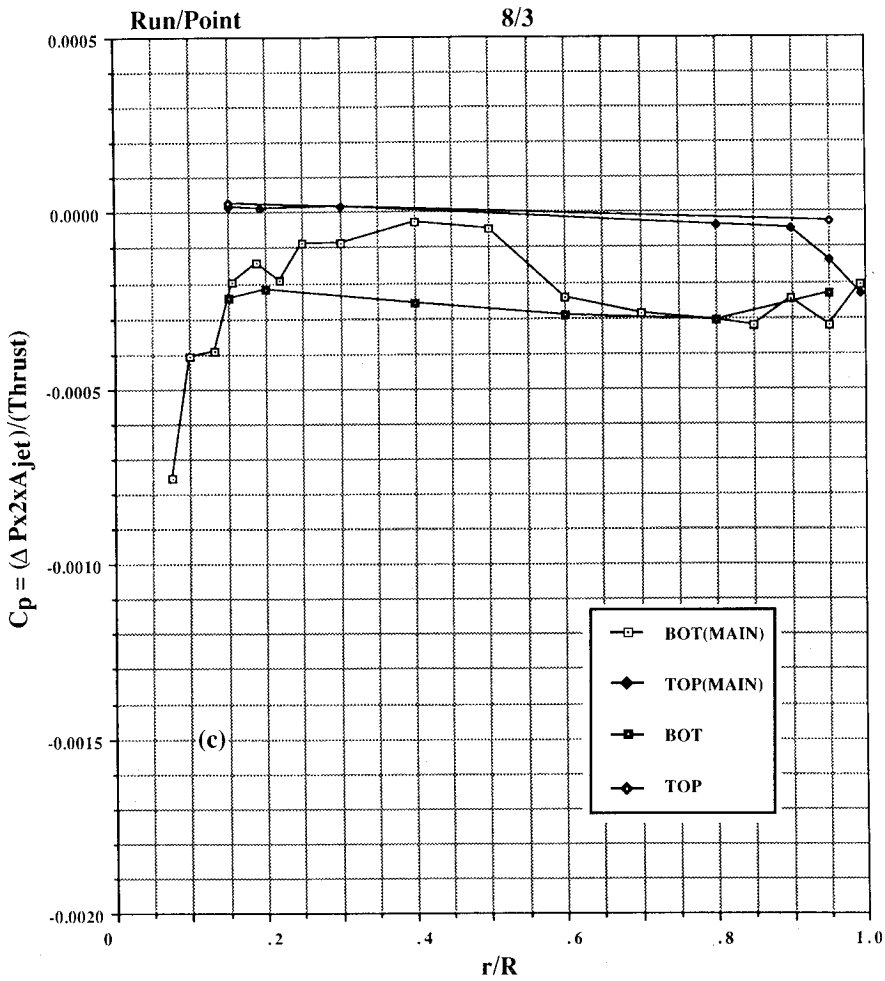

Figure 38. Concluded. (c) $h/d_e = 16.3$.

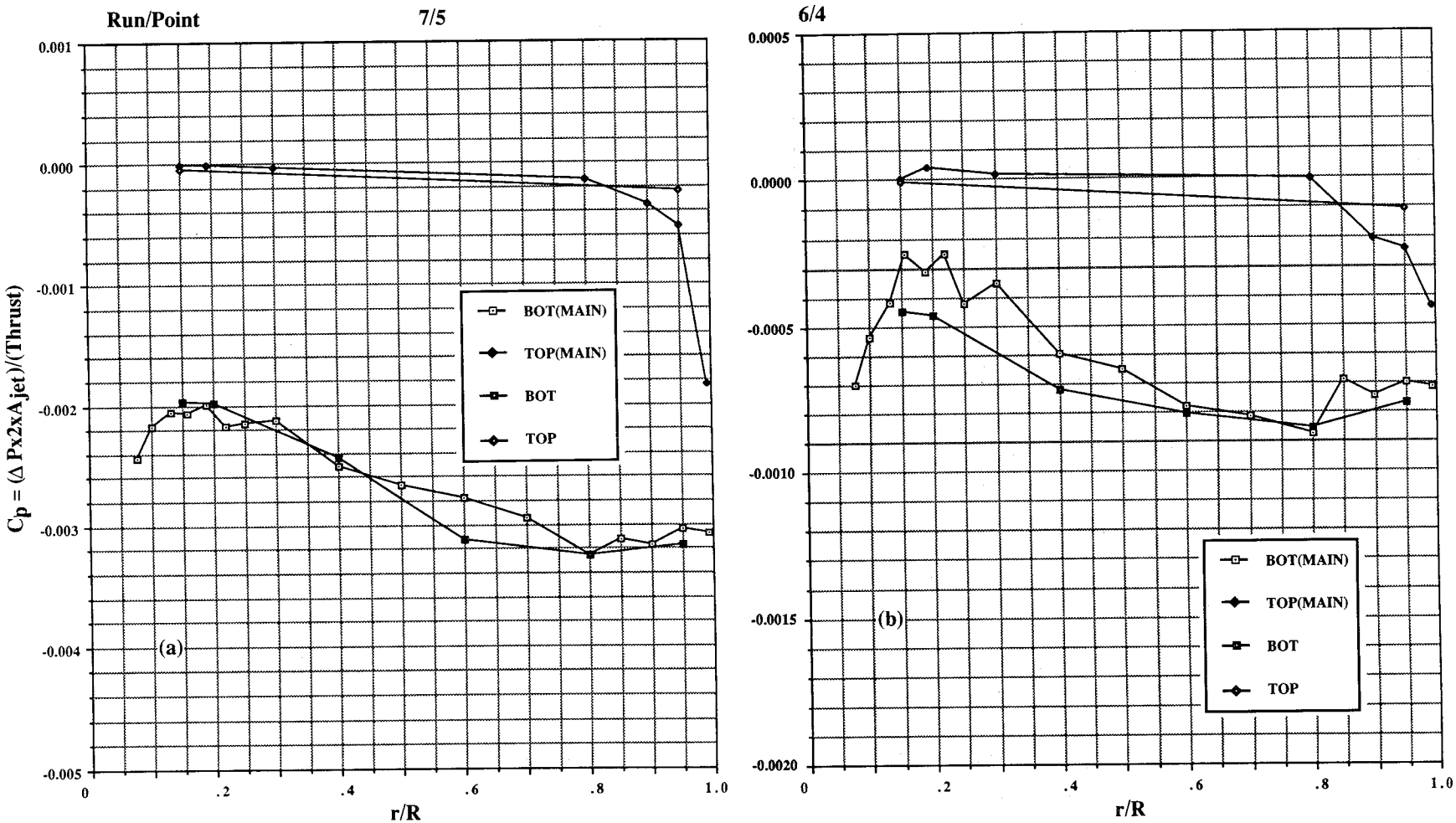

Figure 39. Pressures induced on 20-in. circular plate in ground effect, NPR = 3.0, T = 47 lb, test cell.
(a) $h/d_e = 4.1$, (b) $h/d_e = 8.1$.

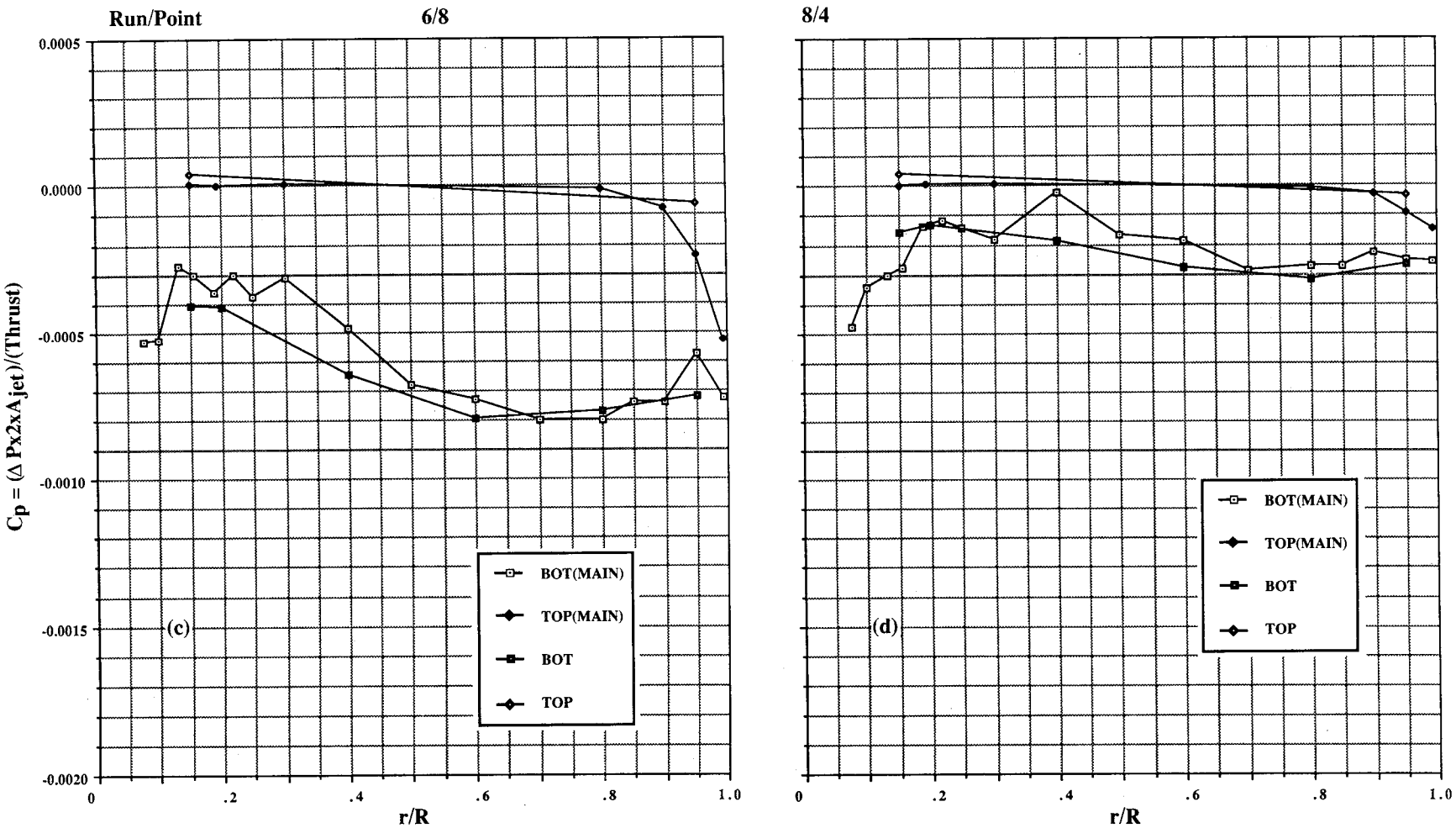

Figure 39. Concluded. (c) $h/d_e = 8.1$ (repeat), (d) $h/d_e = 16.3$.

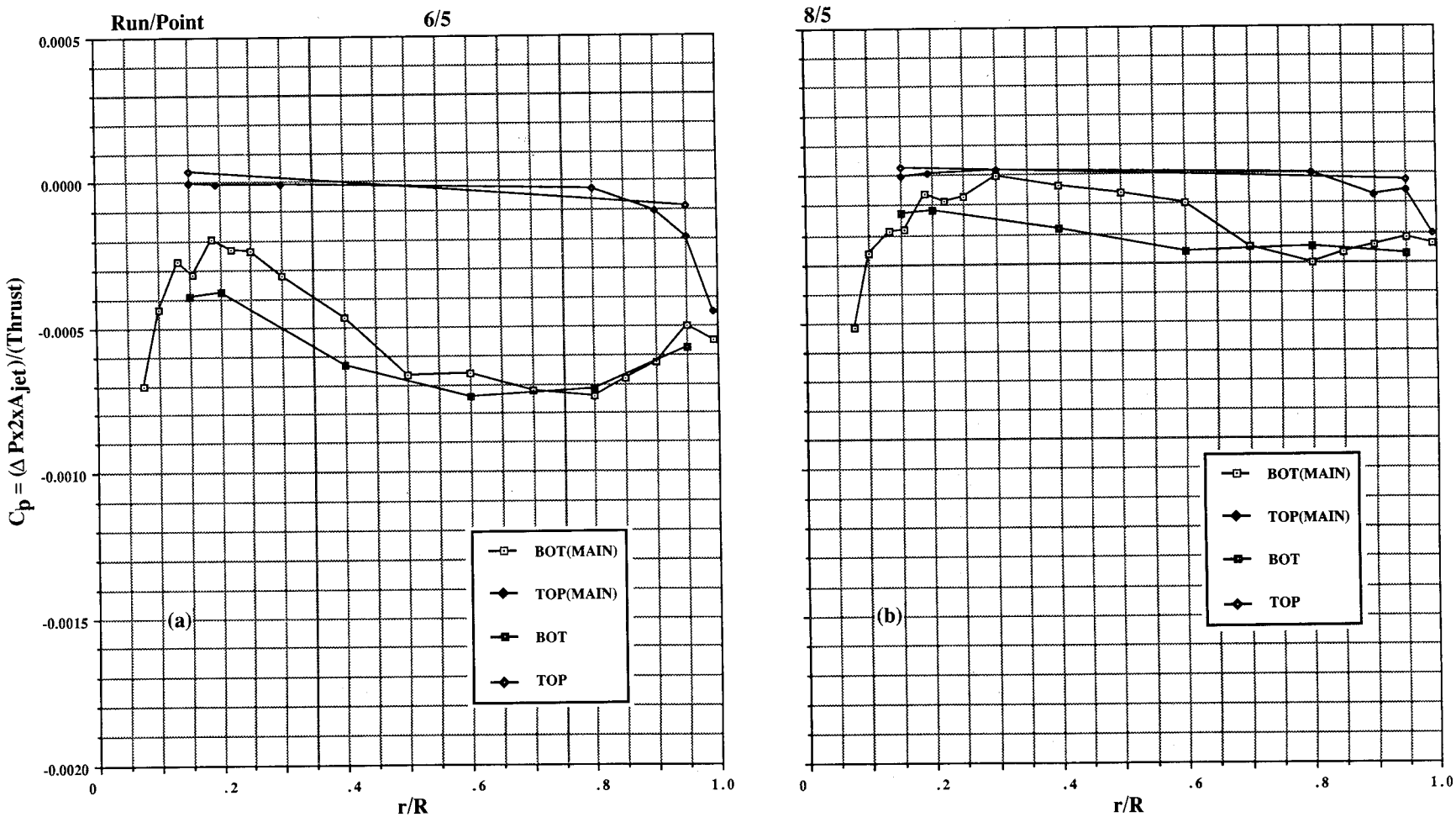

Figure 40. Pressures induced on 20-in. circular plate in ground effect, NPR = 4.0, T = 66 lb, test cell.
(a) $h/d_e = 8.1$, (b) $h/d_e = 16.3$.

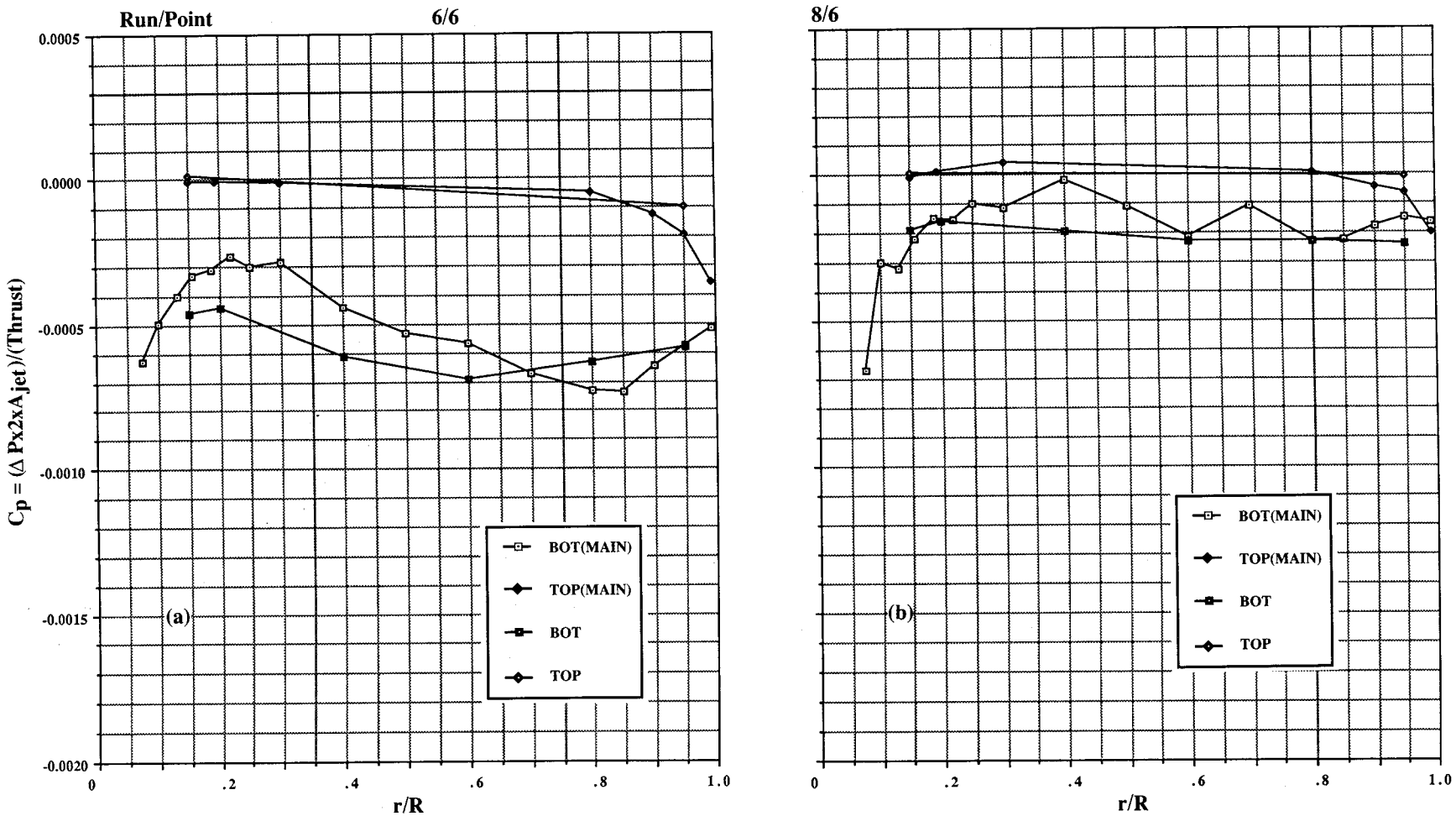

Figure 41. Pressures induced on 20-in. circular plate in ground effect, NPR = 5.0, T = 88 lb, test cell.(a) $h/d_e = 8.1$, (b) $h/d_e = 16.3$.

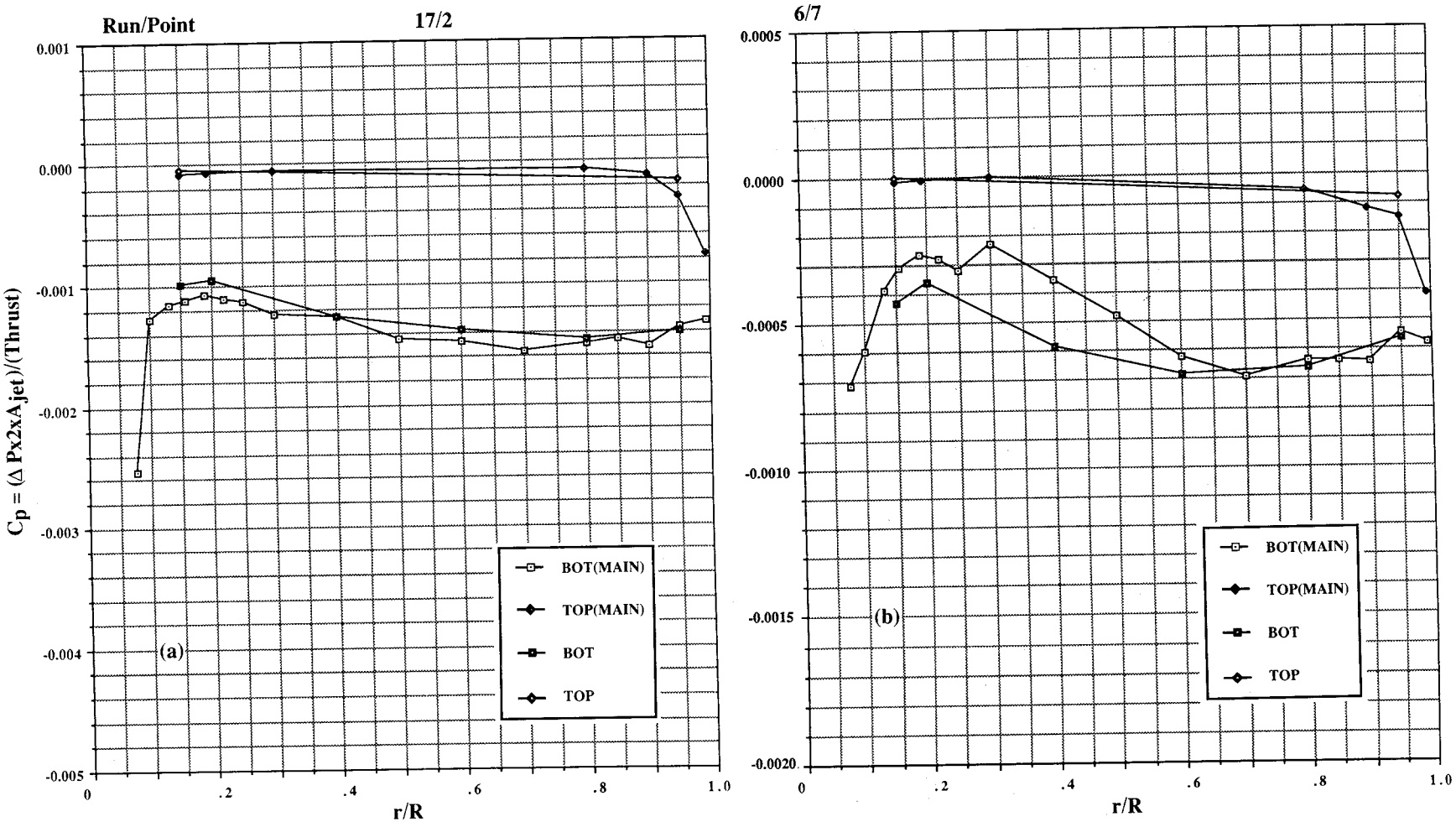

Figure 42. Pressures induced on 20-in. circular plate in ground effect, NPR = 6.0, T = 109 lb, test cell. (a) $h/d_e = 4.9$, (b) $h/d_e = 8.1$.

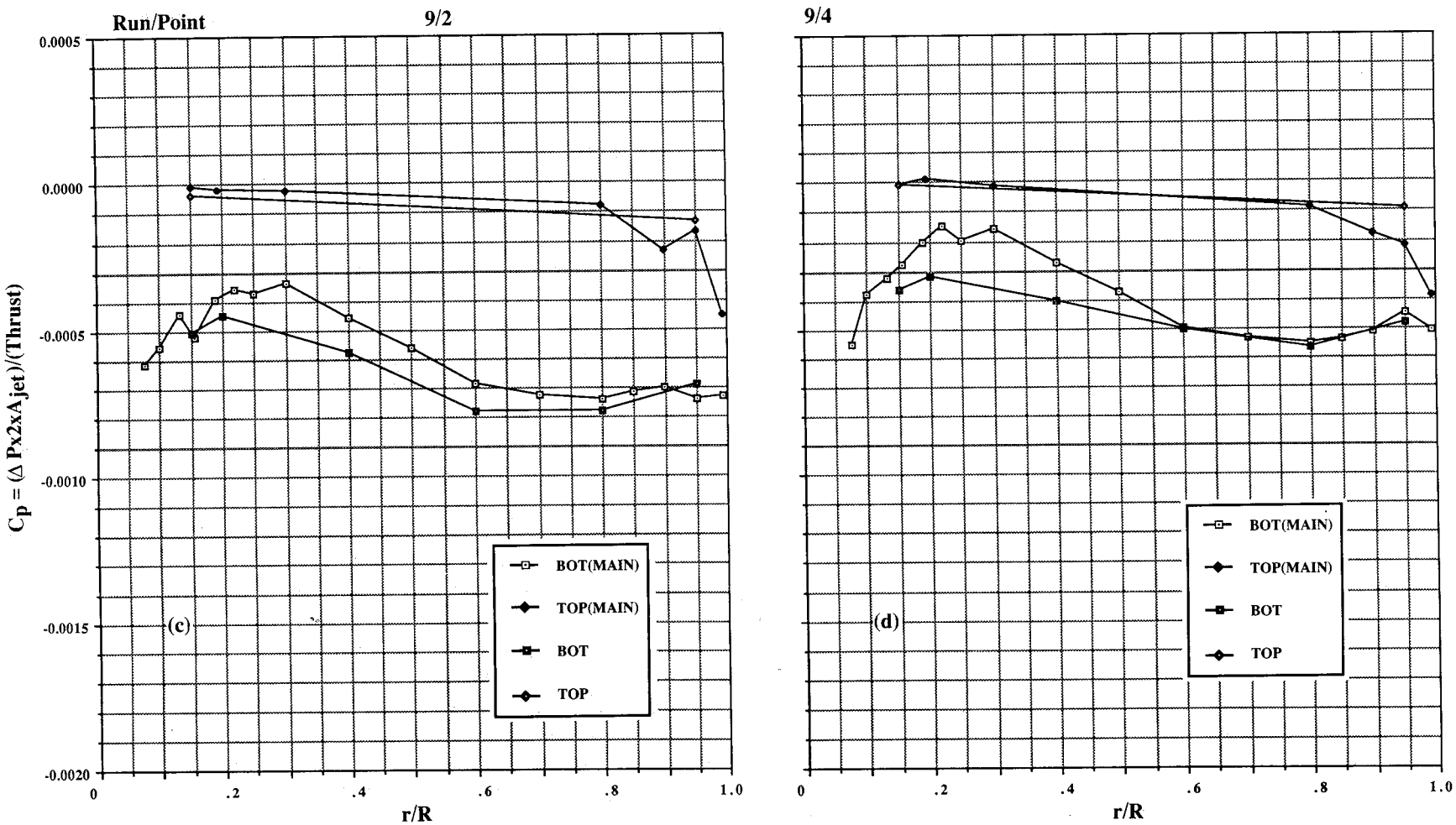

Figure 42. Continued. (c) $h/d_e = 8.1$ (repeat), (d) $h/d_e = 9.8$.

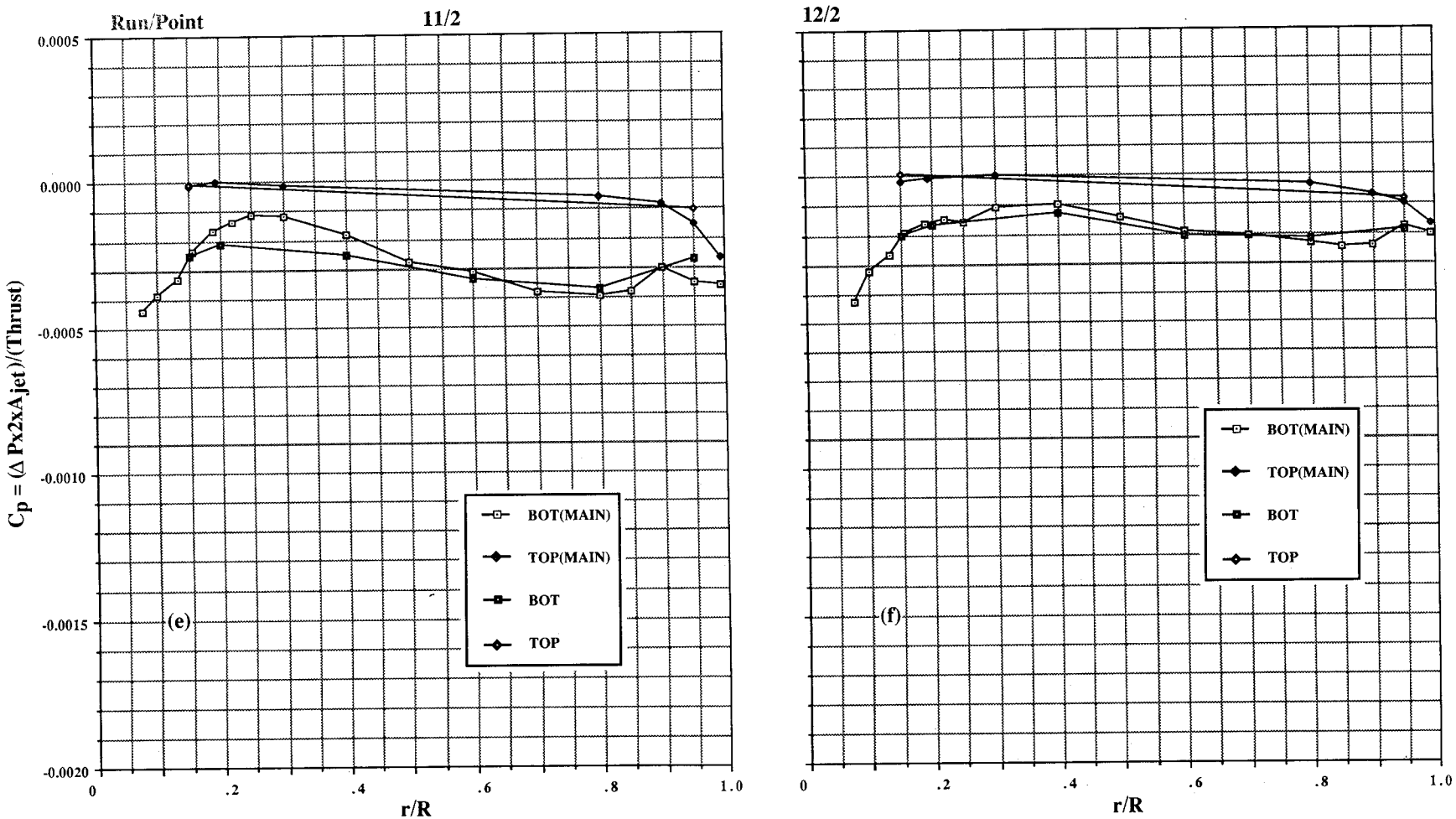

Figure 42. Continued. (e) $h/d_e = 12.2$, (f) $h/d_e = 16.3$.

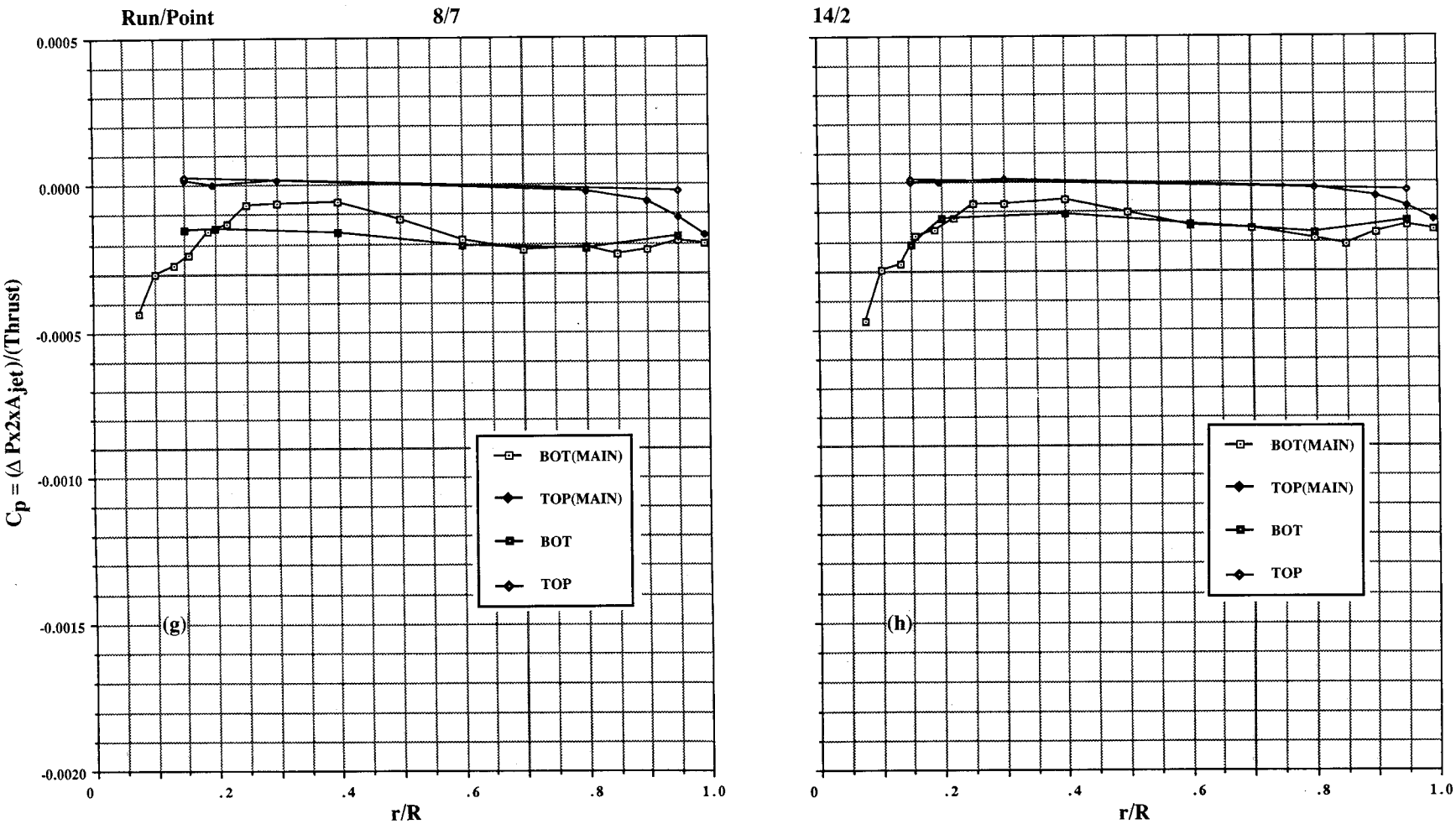

Figure 42. Continued. (g) $h/d_e = 16.3$ (repeat), (h) $h/d_e = 20.3$.

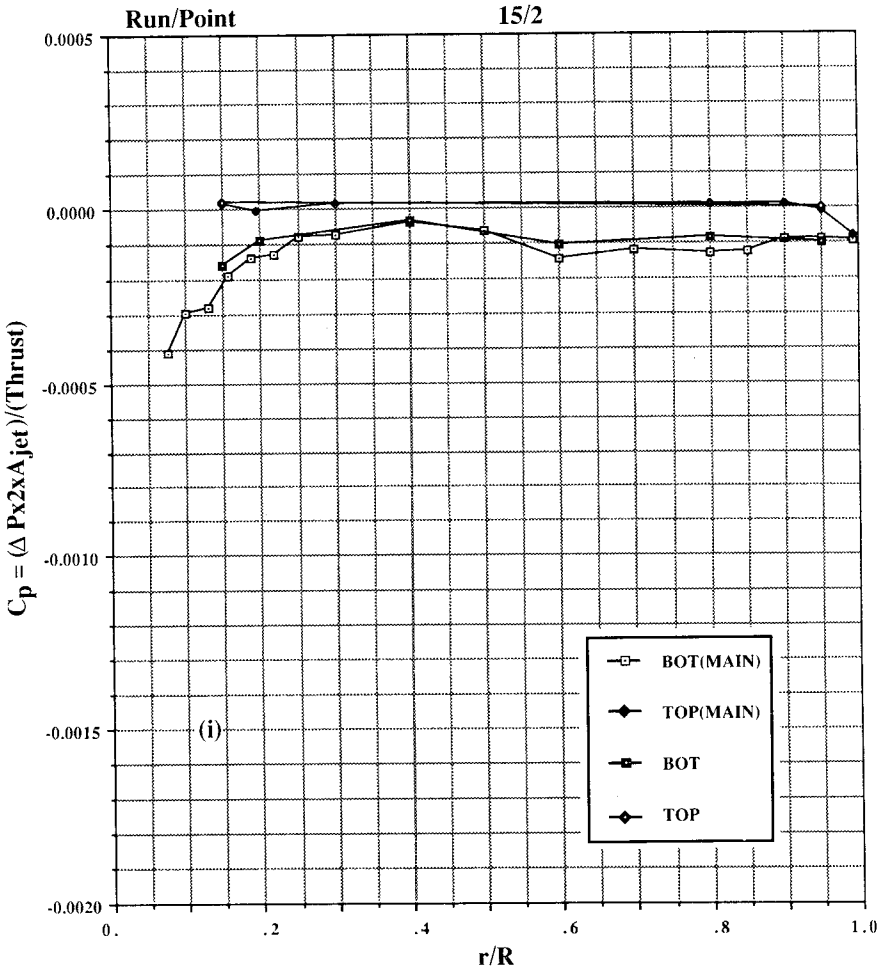

Figure 42. Concluded. (i) $h/d_e = 32.5$.

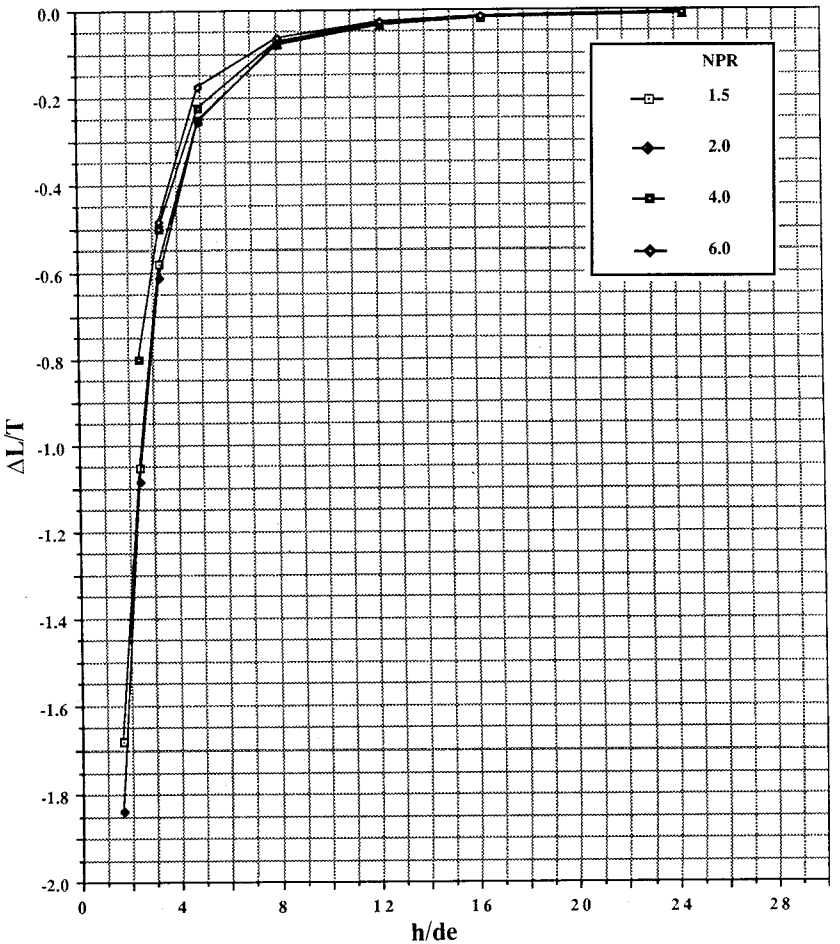

Figure 43. Lift-loss, 20-in. circular plate (Ames), large room.

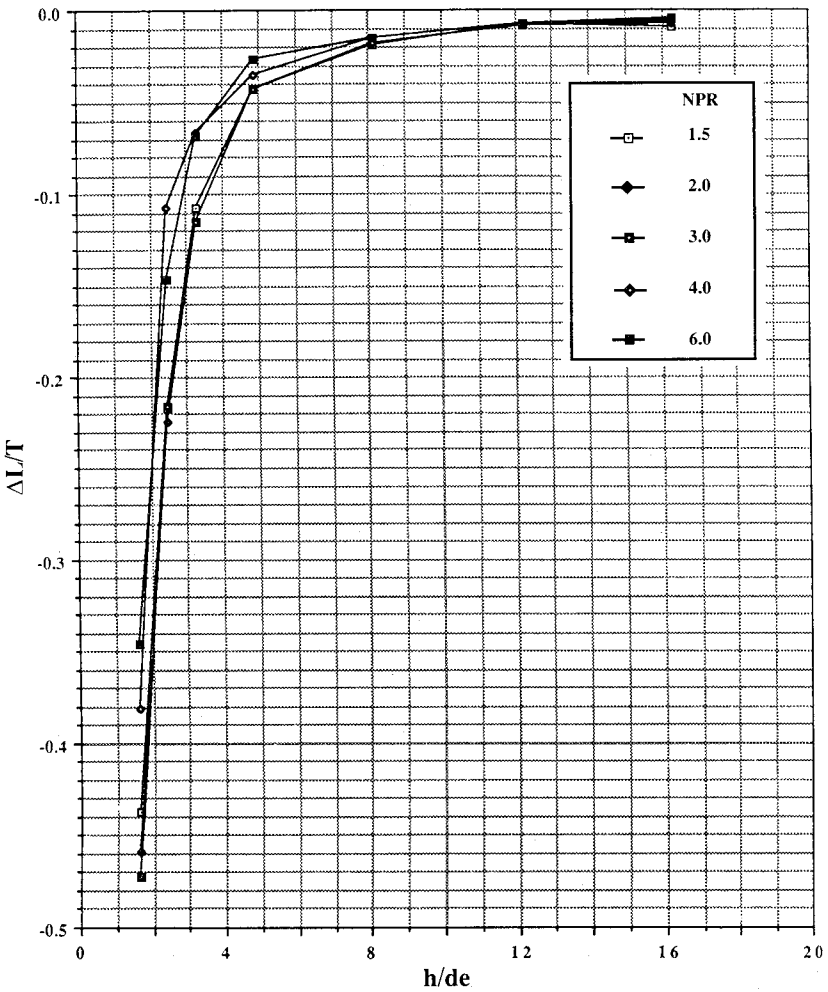

Figure 44. Lift-loss, 10-in. circular plate (Ames), large room.

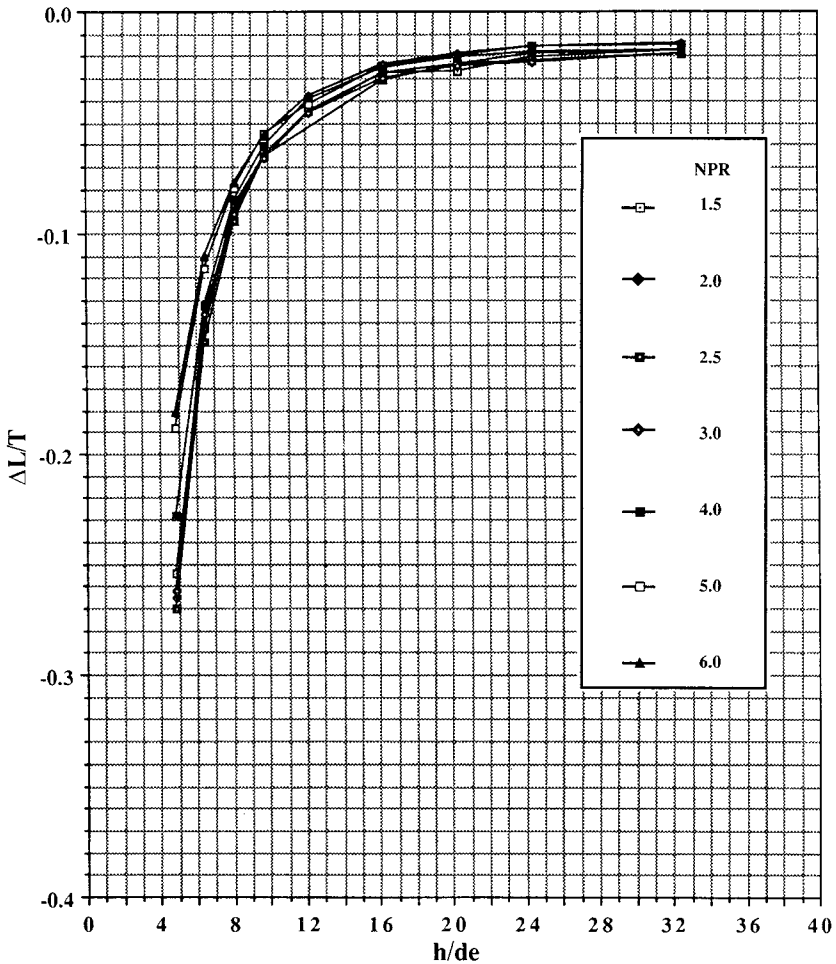

Figure 45. Lift-loss, 20-in. circular plate (Rye), test cell, test cell door half open.

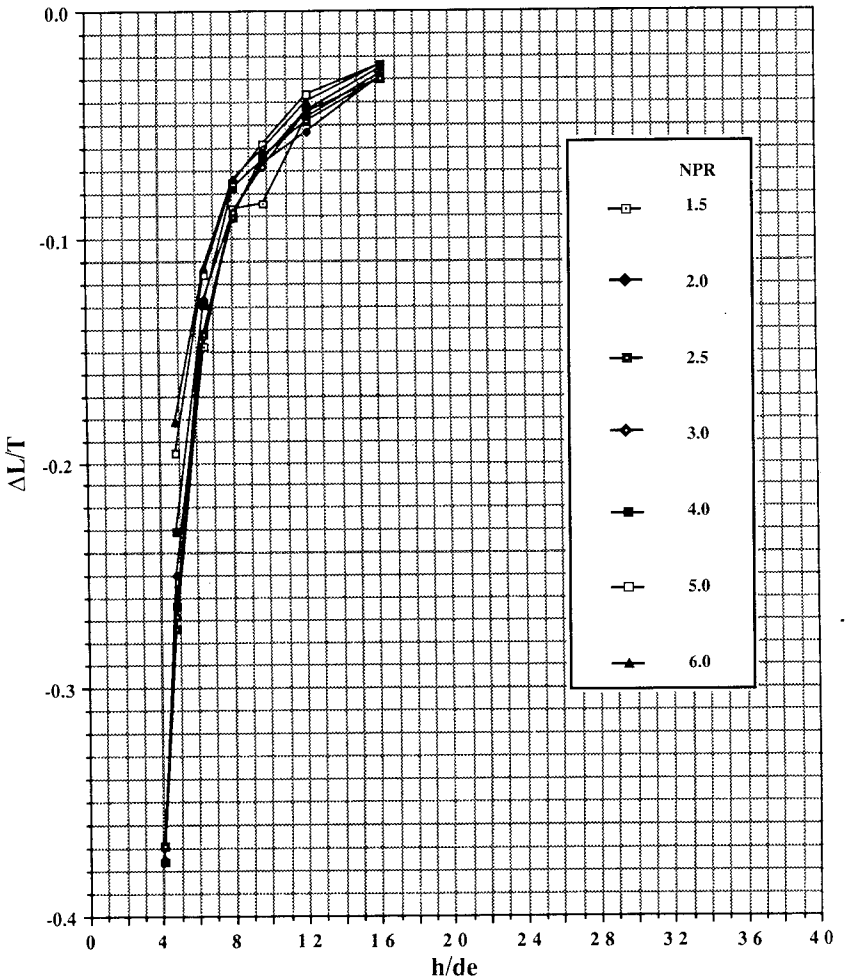

Figure 46. Lift-loss, 20-in. circular plate (Rye), test cell, test cell door full open.

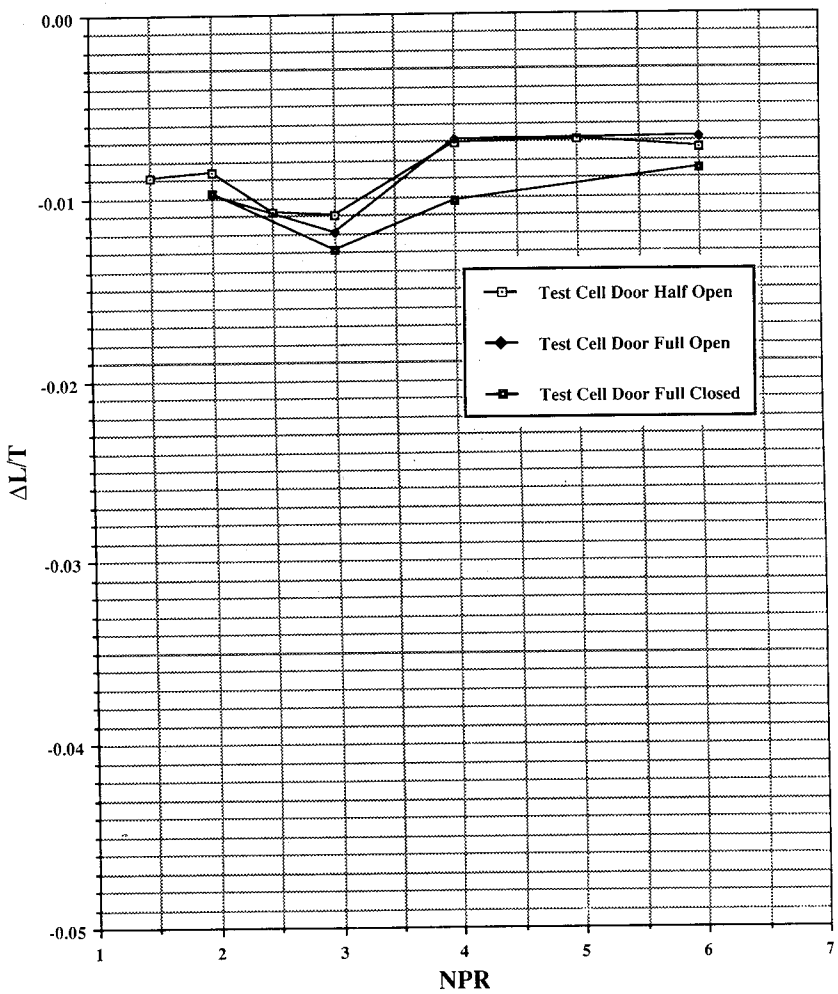

Figure 47. Lift-loss, 20-in. circular plate (OGE), test cell, out of ground effect.

NASA
National Aeronautics and Space Administration

Report Documentation Page

1. Report No.	2. Government Accession No.	3. Recipient's Catalog No.
NASA TM-102816		

4. Title and Subtitle

Forces and Pressures Induced on Circular Plates by a Single Lifting Jet in Ground Effect

5. Report Date

March 1991

6. Performing Organization Code

7. Author(s)

David C. Bellavia, Douglas A. Wardwell, Victor R. Corsiglia, and Richard E. Kuhn*

8. Performing Organization Report No.

A-90142

10. Work Unit No.

505-61-71

9. Performing Organization Name and Address

Ames Research Center
Moffett Field, CA 94035-1000

11. Contract or Grant No.

13. Type of Report and Period Covered

Technical Memorandum

12. Sponsoring Agency Name and Address

National Aeronautics and Space Administration
Washington, DC 20546-0001

14. Sponsoring Agency Code

15. Supplementary Notes

Point of Contact: Douglas A. Wardwell, Ames Research Center, MS 237-3
Moffett Field, CA 94035-1000
(415) 604-6566 or FTS 464-6566

*STO-VL Technology, 16527 Sambroso Place, San Diego, CA 92128

16. Abstract

NASA Ames is conducting a program to develop improved methods for predicting suckdown and hot-gas ingestion on jet V/STOL aircraft when they are in ground effect. As part of that program a data base is being created that provides a systematic variation of parameters so that current empirical prediction procedures can be modified. The first series of tests in this program is complete. This report is one of three that presents the data obtained from tests conducted at Lockheed Aeronautical Systems – Rye Canyon Facility and the High Bay area of the 40- by 80-Foot Wind Tunnel at Ames Research Center. This report specifically deals with suckdown on two circular plates.

17. Key Words (Suggested by Author(s))	18. Distribution Statement
STOVL, V/STOL, Suckdown, Lift loss, Ground effects, Circular plate, Circular disk	Unclassified-Unlimited Subject Category – 02

19. Security Classif. (of this report)	20. Security Classif. (of this page)	21. No. of Pages	22. Price
Unclassified	Unclassified	100	A06

NASA FORM 1626 OCT 86

For sale by the National Technical Information Service, Springfield, Virginia 22161